Università del Piemonte Orientale "Amedeo Avogadro"
Dipartimento di Scienze della Salute

PhD program in Biotechnologies for Human Health
XXVI cycle

EXTRACELLULAR VESICLES: DEVELOPMENT OF ISOLATION METHODS AND ANALYSIS IN ERYTHROID RIBOSOMAL STRESS

PhD thesis of
ROSSELLA CRESCITELLI

Tutor: Prof. Irma Dianzani

By believing passionately something
that still does not exist, we create it.
The nonexistent is whatever
we have not sufficiently desired.

Franz Kafka
(3 July 1883 - 3 June 1924)

SUMMARY

Extracellular vesicles (EVs) are membrane-covered cell fragments released by most cell types, in different physiological and pathophysiological conditions.

Although a definitive categorization has yet to be achieved, EVs can be classified in three classes: apoptotic bodies (ABs), microvesicles/microparticles (MVs/MPs) and exosomes (EXOs). Due to numerous similarities that exist among them the separation is still a challenge so a standardized approach to their isolation and characterization is required.

In the first part of this thesis, we focused on proper separation and characterization of subpopulations of EVs.

First of all we compared a differential centrifugation-based protocol used to isolate ABs and MVs and another protocol used to isolate EXOs after removal of ABs and MVs. EVs from supernatant of three cell lines were characterized focusing on their morphology, RNA profile and surface marker expression. We demonstrated that pellets showed highly different distribution of size, shape and electron density with typical AB, MV and EXO characteristics. Distinct vesicles fractions had clearly different RNA profiles. rRNA was primary detectable in ABs and smaller RNAs without prominent rRNA profiles in EXOs. By contrast, MVs contained little or no RNA except for those collected from TF-1 cells. Moreover, we showed that markers considered typical of EXOs (CD9, CD63 and CD81) were present in all EV types when vesicles were analyzed by flow cytometry using anti-CD63-coated beads.

To further investigate EV subpopulations, we demonstrated that two populations of exosome-like vesicles could be identified with or without using 0.22 μm filter. In particular, just one pellet was collected using filter ("EXOs w/o filter") whereas two different pellets were collected without filter: "additional pellet", at the bottom of the tube and "EXOs w filter", attached to the tube. As well as for ABs, MVs and EXOs, they showed

different RNA profiles with mostly short RNAs in “EXO w filter”, more evident rRNA peaks in “EXOs w/o filter” and prominent RNA peaks in the “additional pellet”. Moreover, loading “EXO w filter” and “additional pellet” on sucrose gradient, RNA profile analysis showed that RNAs in the two pellets have a different distribution. In “EXO w filter”, small RNA was found in lower fractions whereas “additional pellet” showed both rRNA-positive fractions (in upper fractions) and rRNA-negative fractions (in lower fractions). Our results demonstrated that the differences shown in EXO studies could be due not only to a different EXO origin, but also to the different filter used.

Further investigation demonstrated that EV nomenclature is still a problem; authors often investigated the same type of vesicles, but called them in different ways. By loading ABs, MVs, EXOs as well as “EXO w filter” and “additional pellet” on sucrose gradient and looking at RNA profiles, we demonstrated that MV pellet was composed by both rRNA-positive vesicles (in upper fractions) and RNA-negative vesicles (in lower fractions) similar to what observed in “additional pellet”. Fractions obtained from EXO pellet were composed only by rRNA-negative vesicles as observed in fractions from “EXO w filter”.

After the development of EV isolation method, able to reduce the contamination between different EV types, we applied our technical knowledge to investigate EVs in a specific biological process: ribosomal stress, a condition caused by aberrant ribosome biogenesis. Defects of ribosome biogenesis lead to a number of ribosomal diseases. Diamond Blackfan Anemia (DBA) is the first human disorder discovered in this group. Abnormal ribosome biogenesis induces apoptosis in erythroid progenitors so DBA research is limited by the unavailability of the disease cell target. Analysis of EVs shed from erythroid progenitors is useful to overcome this limitation.

First we investigated EV miRNA composition in $CD34^+$ cells after induction of ribosomal stress due to silencing of RPS19 (DBA cell model) and then we evaluated EVs in blood from patients with DBA. miRNAs that were

included in MVs/EXOs released during ribosomal stress ($CD34^+C$) were compared with those identified in their scramble control ($CD34^+S$). Specifically, in MVs C versus MVs S, three miRNA were up-regulated (miR-412, miR-1281, miR-1273f) and eight were down-regulated (miR-153, miR-1248, miR-526b-5p, miR452-5p, miR-105-5p, miR-374a-5p, miR-148a-3p and miR-588). Comparing miRNAs changed in EXOs C versus EXOs S, just one miRNA showed to be up-regulated (miR-643), whereas four miRNAs were down- regulated (miR-654-3p, miR-1276, miR-539-5p and miR-188-3p). Interestingly, two of these miRNAs are involved in cell death i.e. miR-412 and miR-153. miRNA signature in MVs and EXOs released in ribosomal stress has been identified for the first time.

The finding of abnormalities in vesicles shed from cells representing a model for DBA prompted us to explore the diagnostic potential of erythroid vesicles in patients with DBA. MPs were collected from blood of patients with DBA, patients showing a non-DBA haematological disease and healthy controls. Vesicle markers were studied by flow cytometry: CD34, CD71 CD235a (Glycophorin A) and phosphatidylserine (PS). The MP number in specific gates has been calculated. Interestingly, we found that the $CD34+/CD71_{low}$ population was absent in anemic patients with DBA, but was well represented in healthy controls and in patients affected by a non-DBA condition. The receiver operating curve (ROC) analysis showed that MP $CD34+/CD71_{low}$ evaluation had a good diagnostic value for DBA diagnosis. Other MP populations have been identified demonstrating that flow cytometry is able to analyse MP shed from hematopoietic cells at different developmental stage.

TABLE OF CONTENTS

1. Introduction

1.1 Extracellular vesicles (EVs)

Extracellular vesicles (EVs) are membrane-covered cell fragments released by most cell types, in different physiological and pathophysiological conditions (Théry C., 2009), (Mathivanan S J. H., 2010), (Ratajczak J., 2006), (Cocucci E, 2009), (Johnstone RM, 2006).

They can be detected in body fluids including blood, plasma, urine, saliva, amniotic fluid, milk, pleura ascites (Simpson RJ, 2009), (Lässer C A. V., 2011), and contain proteins, lipids and RNA that are representative of host cell (Valadi H, 2007), (Théry C Z. L., 2002), (Mathivanan S L. J., 2010). It is becoming increasingly clear that they have specialized functions and play a key role in intracellular signalling, waste management and coagulation. Consequently, there is a growing interest in the clinical application of EVs. Vesicles can potentially be used for therapy, prognosis and as disease biomarker (van der Pol E B. A., 2012).

The discovery of EV dates back to 1940, thanks to preliminary studies performed with the aim to study the "biological significance of thromboplastic protein of blood" (Chargaff E, 1946). More than twenty years later, this subcellular fraction was identified by electron microscopy and was shown to consist of small vesicles, originating from platelets and termed "platelet dust" (Wolf P., 1967). Ten years later, numerous microvesicles were detected in foetal calf serum (Dalton AJ., 1975). From this preliminary studies, dozen of different names have been used for extracellular vesicles based on their specific function: calcifying matrix vesicles that initiate bone formation (Anderson HC., 1969), tolerosomes that induce immunological tolerance, or their cell origin: dexosomes (dendridic cell-derived exosomes) (Le Pecq JB., 2005), prostasomes (prostate-derived exosomes) (Stegmayr B, 1982), matrix vesicles (vesicles in bone, cartilage and atherosclerotic plaques) (Tanimura A, 1983), synaptic vesicles (vesicles from neurons) (Fischer von Mollard G, 1990). Though a definitive categorization is yet to be achieved (Simpson RJ., 2012), EVs can be classified in three classes based on their size and presumed biogenetic

pathways: apoptotic bodies (ABs), microvesicles (MVs) and exosomes (EXOs) (Kalra H, 2012) (Fig.1).

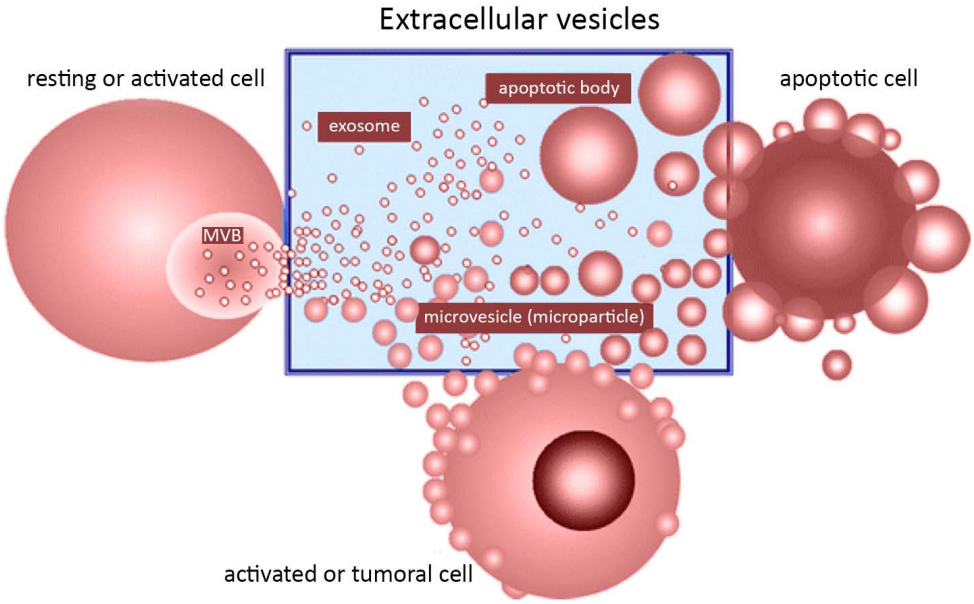

Fig.1: Schematic representation of extracellular vesicles (EVs). Principal populations are shown: apoptotic bodies (ABs), microvesicles (MVs) and exosomes (EXOs). Modified from György B *et al*, 2011.

1.1.1 Apoptotic bodies (ABs)

In 1972, for the first time, the term "apoptotic body" has been used (Kerr JF, 1972), but Horviz R. *et al* conducted the seminal work in apoptosis research studying cell development in Caenorhabditis elegans (Sulston JE, 1977) (Fixsen W, 1985).

These particles have a size between 1-5 μm, similar to the size range of platelets (Hristov M, 2004), a density between 1.16 to 1.29 g/ml, partially overlapping with exosome density and a morphology that is heterogeneous when compared with other vesicles visualized by TEM (van der Pol E B. A., 2012). They are released as blebs from cells undergoing apoptosis. A cell dying by apoptosis goes through several stages: they start with condensation of the nuclear chromatin, followed by membrane blebbing and progress to

disintegration of the cellular content into membrane vesicles termed apoptotic bodies. The clearance of apoptotic bodies by macrophages is mediated by specific interactions between recognition receptors on the phagocytes and the specific changes (such as oxidation of surface molecules) in the composition of the apoptotic cell membrane. These changes create binding sites for Thrombospondin (Tsp) or the complement protein C3b (Akers JC, 2013). (Fig.2)

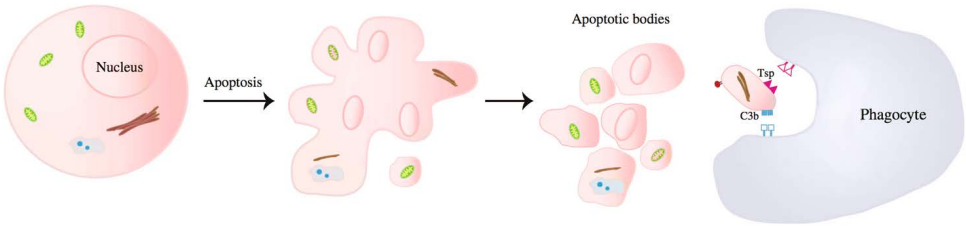

Fig.2: Formation of apoptotic bodies during apoptosis. Modified from Akers JC *et al*, 2013.

Apoptotic cells release two different types of apoptotic vesicles: the first one originates from the plasma membrane and contains DNA and hystones, whereas the other originates from endoplasmic reticulum and does not contain DNA or hystones, but exposes immature glycoepitopes (Bilyy RO, 2012). For studies focused on cells undergoing apoptosis, generally, authors look at the phosphatidylserine expression and DNA fragmentation (Beyer C, 2010). ABs are involved in horizontal transfer of DNA (Holmgren L, 1999) including oncogenes (Bergsmedh A, 2001) and presentation of T cell epitopes (Bellone M, 1997).

1.1.2 Microvesicles (MVs)

They were described for the first time by Chargaff and West in 1946 (Chargaff E, 1946). Twenty years later, Wolf P. isolated a fraction composed by lipid-rich particles obtained by ultracentrifugation from plasma and called them "platelet dust" (Wolf P., 1967).

MVs have a size between 100-1000 nm (Théry C O. M., 2009) overlapping that of bacteria, but there is no consensus on the lower cut-off (Yuana Y, 2011). They are surrounded by phospholipid bilayer and are shed directly from budding of plasma membrane (György B S. T., 2011). They are released during cell stress conditions (van der Pol E B. A., 2012) after activation of cell surface receptors or during apoptosis following intracellular Ca^{2+} increase (Baroni M, 2007), (Kahner BN, 2008). These vesicles are involved in procoagulant function (Leroyer AS, 2008), in the pathogenesis of rheumatoid arthritis (Boilard E, 2010), tumour proinvasive activity (Giusti I, 2008), neoplastic transformation (Antonyak MA, 2011), foetus-mother communication (Pap E, 2008). They are generally characterized by phosphatidylserine but some observations suggest the existence of MVs that are negative for this marker (Connor DE, 2010).

They are isolated using centrifugation-based protocols (Yuana Y, 2011) using a centrifugation force of 10,000-20,000 *g* (Théry C O. M., 2009) or capture-based assays (Sellam J, 2009) followed by flow cytometry (György B M. K., 2011).

Few proteins seem to be ubiquitously expressed; an example is β1 integrin (Dolo V, 1998). MV composition depends on cell of origin. MVs from tumours express metalloproteinases and other proteolytic enzyme (Gutwein P, 2003), (Gasser O, 2003), whereas MVs from platelets express integrins, glycoproteins GPIb, GPIIb-IIIa and P selectin (Del Conde I, 2005), (Cocucci E, 2009). MVs are able to interact with cells that they recognize specifically and transfer receptors, ligands, mRNAs and miRNAs contributing to epigenetic ad proteomic properties of target cells (Fig.3) (Hunter MP, 2008), (György B M. K., 2011).

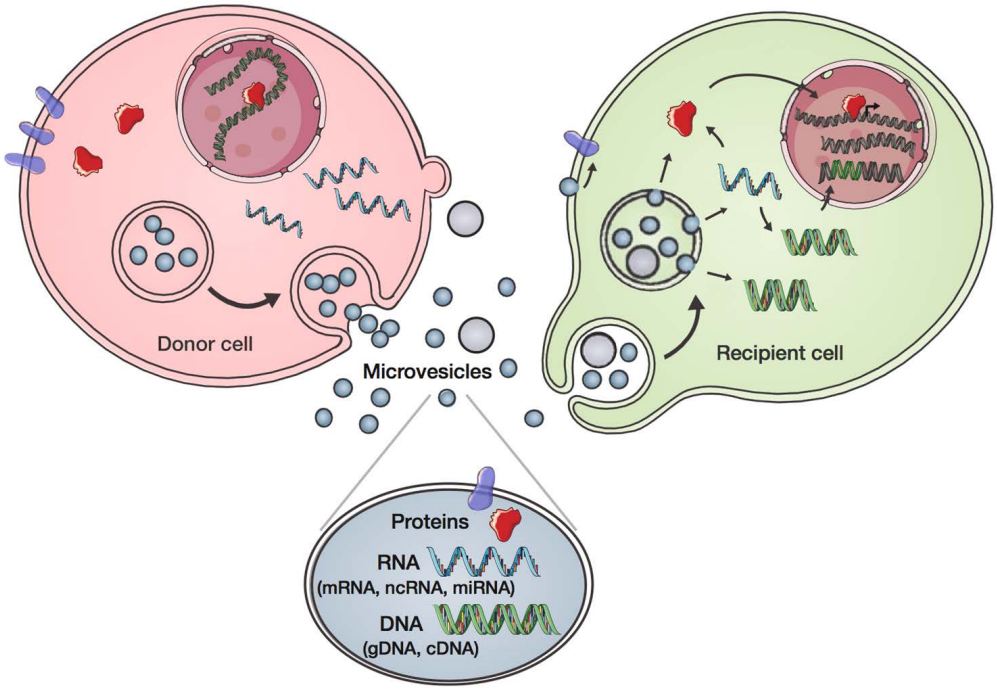

Fig. 3: MV-mediated intercellular communication. Components of donor cells are incorporated into MVs that contain proteins, RNAs and DNA. MVs can be taken up by recipient cells through endocytosis and release their contents after fusing with the endosomal membrane or the plasma membrane. Modified from van der Vos KE *et al*, 2011.

It has been demonstrated that they induce change in the maturation and differentiation of target cells. For example, MVs from neutrophils can impair the maturation of dendritic cells (Eken C, 2008).

They have been through studied in coagulation. Upon exposure to collagen, platelets release MVs coated with tissue factor which binds with its surface ligand (for example P-selectin1) on macrophages (Polgar J, 2005), neutrophils (Pluskota E, 2008) and other platelets.

An increased amount of MVs has been observed in plasma from patients with anti-phospholipid syndrome (Asherson's syndrome) (Ardoin SP, 2007) as well as in inflammatory conditions (Distler JH, 2005).

They have roles in tumours progression and contribute to angiogenic effect through horizontal transfer of mRNAs and miRNAs (Skog J, 2008).

Because of these properties EVs are considered as potentially innovative targets for therapy.

1.1.3 Exosomes (EXOs)

The term "exosome" was first used in 1981 for vesicles with nucleotidase activity that were shed from neoplastic cell lines (Trams EG, 1981). In 1983 Stahl and Johnstone (Harding C, 1983), (Pan BT T. K., 1985) described small vesicles containing transferrin receptor that were released from reticulocytes.

EXOs have a diameter between 50-100 nm and a density that ranges between 1.13 and 1.19 g/ml. They show a phospholipid bilayer structure with a size overlapping that of viruses. They are found in many fluids (urines, blood, ascites, cerebrospinal fluid) (Caby MP, 2005), (Pisitkun T, 2004), (Keller S, 2006), (Vella LJ, 2008).

Differential centrifugations followed by sucrose gradient ultracentrifugations are typically used for EXO isolation (Théry C A. S., 2006). Transmission electron microscopy (TEM), western blot and mass spectroscopy are used for their characterization. Using TEM, the morphology of exosomes has been described as cup-shaped (Johnstone RM A. M., 1987). However, more recent studies have shown that the cup-shaped morphology was an experimental artefact caused by the procedures used to prepare samples (Conde-Vancells J, 2008).

The exosome formation process starts with the invagination of plasma membrane (endocytosis) (Huotari J, 2011). This process can be clathrin-mediated (classical pathway) or clathrin independent, a less studied process compared to the first one (Le Roy C, 2005). Within the cell, endocytic vesicles fuse with early endosomes that mature into late endosomes and then in multivesicular bodies (MVBs). Two types of MVBs are recognized; one is formed in the degradative pathway (i.e. MVBs that fuse with lysosomes) and the other in the exocytosis pathway (i.e. MVBs that fuse with plasma membrane) (Mathivanan S S. R., 2009). Exosomes are formed

by endocytosis of early endosome membrane (Roizin L, 1967). MVB generation and exosome secretion depend on the action of the ESCRT complex, an endosomal complex that is required for transport (Wollert T, 2010) (Fig. 4).

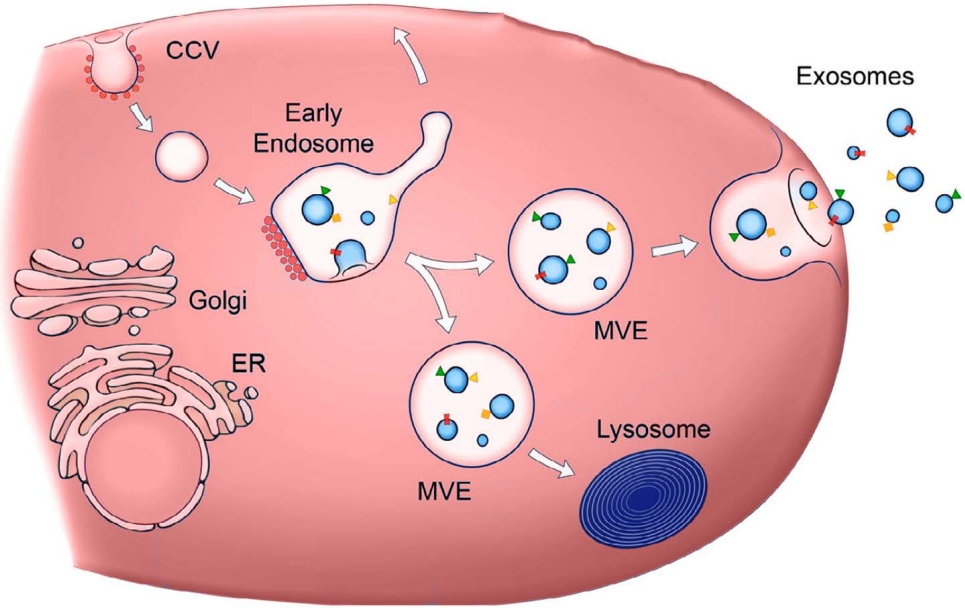

Fig. 4: Schematic description of exosome (EXOs) release. EXOs are represented by small vesicles of different sizes that are formed by budding from early endosomes or MVBs and they are released by fusion with the plasma membrane. Other MVBs fuse with lysosomes. Modified from Raposo G *et al*, 2013.

To date, the most studied and characterized EXOs are those released from immune and tumour cells. They are involved in antigen presentation (Théry C., 2009), (Raposo G N. H., 1996), immunostimulation, tumour growth, metastasis and angiogenesis (van der Pol E B. A., 2012). Thus they can protect tumour cells inhibiting antitumor drug accumulation. They can contribute to multidrug resistance (Ciravolo V, 2012).

They exert their functions in different ways: direct exosome-cell contact, vesicle endocytosis and exosome-cell fusion (Théry C., 2009). As well as microvesicles, they can transfer mRNAs and miRNAs (Valadi H, 2007), but also oncogenic receptors (Al-Nedawi K M. B., 2008) and HIV particles (Izquierdo-Useros N, 2009). By transporting ligands and receptors, they can

drive cell growth and development and thus also modulate the immune system (van der Pol E B. A., 2012). For example, it has been demonstrated that activated T cells and peripheral blood mononuclear cells release EXOs expressing Fas Ligand suggesting that they have a role in cell death during immune regulation (Martínez-Lorenzo MJ, 2004).

Structurally, they are characterized by phosphatidylserine exposure (Chaput N, 2011) and high levels of cholesterol, sphingomyelin, ceramide and lipid rafts (Wubbolts R, 2003), (Simons M, 2009), (Mathivanan S J. H., 2010), (Théry C A. S., 2006). Typical EXO markers are tetraspanins such as CD63, CD81, CD9 and proteins like LAMP1 and TGS101 (Mathivanan S J. H., 2010), (Dignat-George F, 2011) Alix complex, heat shock proteins as well as proteins involved in membrane transport and fusion, like Rab, GTPase, annexin and flottilin (Théry C Z. L., 2002), (Beyer C, 2010), (Bobrie A C. M., 2011), (Record M, 2011).

1.2 Molecular composition of extracellular vesicles

As mentioned in chapter 1.1, the protein composition reflects the origin of the parental cells (Pap E, 2008). EXOs from different cell lines contain endosome-associated proteins such as Rab GTPase, SNARE, Annexin, flotillin. Some of them are involved in multivesicular endosomes biogenesis, such as Alix and Tsg101 (van Niel G, 2006). EVs are enriched in membrane proteins because of their plasma membrane or endosome origin. Tetraspanins are among the most common membrane proteins in all EVs, e.g. CD63, CD81, CD82, CD53 and CD37. They were firstly identified in EXOs from B cells (Escola JM, 1998). EVs are also enriched in proteins associated with lipids raft (such as flotillin) (Théry C R. A.-C., 1999).

EXOs expose different saturated and monosaturated fatty acids as well as cholesterol and sphingomyelin. Little is known about specific proteins and lipid composition of MVs (Raposo G S. W., 2013).

In 2007, Valadi *et al* demonstrated that EVs included both mRNAs and miRNAs. mRNAs from EVs can be translated in protein when inserted in target cells. 1300 mRNAs were found in EXOs from mouse mast cell line, human mast cell line and BMMC (Bone Marrow-derived Mast Cells) (Valadi H, 2007). Extracellular RNA has been found not only in EXOs but also in MVs (Grange C, 2011) and ABs (Zernecke A, 2009). The mRNAs or miRNAs reflect the originating cell profile (Skog J, 2008), (Ratajczak J., 2006). Beyond mRNAs and miRNAs many authors demonstrated that EVs contain other small non coding RNAs such as tRNA fragments, Y RNA, small interfering RNA (Bellingham SA, 2012), (Nolte-'t Hoen EN, 2012) as well as fragments of 28S and 18S rRNA subunits (Jenjaroenpun P, 2013).
The complete protein, lipid and RNA composition of EVs is listed in two online databases: ExoCarta (www.exocarta.org) and EVPedia (www.evpedia.info/).

1.3 Isolation and characterization methods

Extracellular vesicle studies are hampered by lack of a standardized protocol that distinguishes different vesicle types (Onodera T, 2010). Numerous similarities exist among the different EVs; this makes the separation of different subsets a challenge (György B S. T., 2011).
The widely accepted protocol for EXO isolation includes ultracentrifugation followed by sucrose density gradient or cushions (Théry C A. S., 2006). However, a differential centrifugation protocol based on different centrifugations with increased force, is considered the "gold standard" system (Stephen J. Gould, 2013) and useful to separate subpopulations of extracellular vesicles at different steps. The use of a filtration step is debated. There is not a general agreement on the optimal isolation protocol for MVs or ABs.
In general, the isolation procedure includes a first centrifugation step (200-1,500 × *g*) to eliminate cells and cellular debris followed by a stronger

centrifugation (10,000-20,000 × *g*) to eliminate vesicles with a bigger size (100-800 nm generally called MVs). A higher speed centrifugation (100,000 – 200,000 × *g*) is able to pellet EXOs (Mathivanan S J. H., 2010), (Théry C Z. L., 2002), (Théry C A. S., 2006).

To better purify pellets, EVs can be loaded on sucrose gradient or cushions (Théry C A. S., 2006). Other systems include immunoaffinity isolation (employing magnetic beads conjugated with antibodies directed against EV protein markers) (Clayton A C. J., 2001), nanomembrane ultrafiltration concentrator (Cheruvanky A, 2007).

Several companies developed kits to isolate EXOs or to distinguish different EV subpopulations. The most used kits are ExoQuick™ from System Biosciences and "Total Exosome Isolation" from Invitrogen. Moreover Bioo Scientific Company developed the ExoMir™ Plus kit that uses filters with pores of different diameters and allows to directly isolate RNA from cells, ABs, MVs and EXOs, without centrifugation steps.

However, it is important to state that, since vesicles are heterogeneous, there is no system able to accurately separate a specific type. The isolation efficiency depends on the shape and viscosity of solution, as well as on temperature, centrifugation time and the rotor type used for the centrifugation (van der Pol E B. A., 2012). Furthermore, isolation methods are based on size, sedimentation, density, and surface molecules, but there is no consensus about these specific characteristics for each subpopulation of extracellular vesicles. For example MV density is unknown, and there is no agreement on specific EXO markers that are able to distinguish EXOs from MVs (Théry C., 2009).

For these reasons there is a need to develop a standardized method to distinguish EV types (Tauro BJ, 2012), (Yamada T, 2012), (Taylor DD Z. W.-T., 2011).

Because of all these limits, a combination of different methods has been suggested. Due to their small size, it is not possible to use optical methods to visualize EXOs as well as MVs and ABs. They can only be directly visualized by electron microscopy (TEM). To date, TEM is considered the

gold standard for vesicles size determination, but the procedures used to obtain the pellet (centrifugation, dehydration, fixation) could alter EV morphology (György B S. T., 2011). Electron microscopy is the only method that shows the presence of different subpopulations of extracellular vesicles (Lässer C E. M., 2012). Thanks to other techniques such as Cryo-EM (Tatischeff I, 2012), scanning electron microscopy (Sokolova V, 2011) and atomic force microscopy (György B M. K., 2011), nowadays researchers consider the cup-shaped EXO morphology, a TEM artefact due to fixation process (Théry C A. S., 2006). A very innovative method is Raman tweezers microspectroscopy (RTM) that provides an EXO global composition without using any exogenous label (Tatischeff I, 2012).

Western blot and flow cytometry have also been used. The use of Western blot is limited because no EV-specific protein marker is known. Commonly, CD63, Tsg101 and Alix are used to identify EXOs. The absence of proteins such as calnexin (from endoplasmic reticulum) is used as a negative control because it indicates no contamination by EVs from endoplasmic reticulum (Théry C A. S., 2006), (Lässer C E. M., 2012).

Probably the most used technique is flow cytometry. It is very useful for high-throughput EV quantification and multiparameters characterization (van der Vlist EJ, 2012), but many flow cytometers are not able to analyse EVs due to their lower detection limit of 300-500 nm (Freyssinet JM, 2010) (Lacroix R., 2010). Often, to overcome this limit, authors bind EXOs to antibody-coated beads before flow cytometry. The antibody choice depends on EXO origins but antibodies able to recognize EXO common markers are often used (i.e. anti-CD63) (Lässer C E. M., 2012).

Other very innovative systems are dynamic light scatter (DLS) and nanoparticle tracking analysis (NTA). They allow EV size determination through Brownian motion (van der Vlist EJ, 2012), (Tatischeff I, 2012), (Sokolova V, 2011). Even if several authors have favourably valuated these new techniques (van der Pol E H. A., 2010), (Filipe V, 2010), others feel that quantification of an EV pool of heterogeneous size is not precise and

only few parameters can be analysed at the same time (van der Vlist EJ, 2012).

There is an increased interest to analyse RNAs in subpopulations of extracellular vesicles because the EXO RNA differs from cellular RNA and probably, from that included in EVs. This characteristic may allow to distinguish different EV subpopulations and to evaluate contamination from different vesicles in a specific pellet. Using capillary electrophoresis, cells show two prominent RNA peaks corresponding to 18S and 28S rRNA subunits whereas EXOs lack prominent ribosomal RNA peaks and are enriched by smaller RNAs (Valadi H, 2007) (Lässer C, 2013).

1.4 Extracellular vesicles: medical implications and therapeutic/diagnostic potential

It is clear that EVs have metabolic effects on their target cells. This property supports their relevance in human disease (Anderson HC, 2010).

Their involvement has been shown in ostheoarthritis (Ali SY, 1983), gastric ulcers and bacterial infection (Nowotny A, 1982), (Bhatnagar S, 2007), (Ismail S, 2003), (Kuehn MJ, 2005), atherosclerosis (Tanimura A, 1983), (Hsu HH, 1999), thromboembolic conditions (Chironi GN, 2009), (Cocucci E, 2009), hypertension (Daniel L, 2008) and cancer (Peinado H, 2012), (Taylor DD G.-T. C., 2011), (Zhu W X. W., 2006), (Zhu W H. L., 2012).

In atherosclerosis, Hsu *et al* demonstrated that macrophages and intimal smooth muscle cells release MVs (Tanimura A, 1983), (Hsu HH, 1999). Rautou *et al* showed that vesicles from atherosclerotic plaques are able to transfer ICAM-1 to endothelial cells. This process induces phosphorylation of extracellular signal regulated kinase 1/2 and supports a role of EVs in atherosclerotic plaque progression (Rautou PE, 2011).

Another well known MV role involves promotion of normal and pathological blood coagulation (Chironi GN, 2009), (Pásztói M, 2009). On their surface, MVs from platelets expose platelet-derived tissue factor and

von Willebrand's factor, the major coagulation initiator (Dvorak HF, 1981). Therefore, EVs represent a surface in the assembly of the complexes involved in the coagulation cascade (Lentz BR., 2003).

MVs have been involved also in thrombotic thrombocytopenic purpura, a disease characterized by thrombi formation in the microcirculation. MVs have procoagulant activity and induce microthrombi formation (Galli M, 1996). It is not surprising that the MV number is increased in plasma from patients with this disease (Galli M, 1996).

An increased amount of MVs is documented also in plasma from patients with chronic renal disease (Faure V, 2006).

EVs role in cancer has been thoroughly studied. Tumour cells are able to constitutively release all types of EV subpopulations (György B S. T., 2011). These EVs are involved in many tumour aspects such as tumour cell survival, growth, host invasion and metastasis. Moreover, they are able to evade host immunity (Valenti R, 2007). Thanks to their capability to transport and release proteases (Ginestra A, 1998), they promote tissue invasion. Local blood coagulation induced by EVs favours tumour cells adhesion to vessels (Dvorak HF, 1981). Tumour growth is supported by MVs expressing epithelial growth factor (Al-Nedawi K M. B., 2009) and tissue factors (Osterud B, 2003). The role of EVs has been studied in glioblastoma (Skog J, 2008), melanoma (Hood JL, 2009) and lung cancer. EXOs from lung cancer are enriched in specific miRNAs such as miR27, miR29, miR21 that are Toll like receptors agonists and are able to increase the inflammatory response. This process induces tumour growth and metastasis (Fabbri M, 2012).

Taverna *et al* demonstrated that EXOs from chronic myelogenous leukemia cells induce angiogenesis (Taverna S, 2012). Umezu *at al* studied the ability of exosomal miR-92 from chronic myelogenous leukemia (K562) to induce cell migration and tube formation in human umbilical vein endothelial cells (HUVECs) (Umezu T, 2013).

The investigation of EV role in disease not only can be useful to better understand pathophysiology of diseases, but it also may open new perspectives for both diagnosis and therapy.

Because of EXO specific tropism and their ability to transfer cargo to recipient cells, many researchers focused on EXO (and EVs in general) potential in therapies. EXOs are well tolerated by human body and have a long half-life in circulation (Lai RC, 2013). They can also overcome the blood-brain barrier (van den Goor JM, 2007). These characteristics give them a delivery potential for drugs and genes. For example, Sun *et al* have been able to load an anti-inflammatory drug (curcumin) in EXOs. They demonstrated that encapsulation of curcumin into exosomes increases its solubility, stability, and bioavailability (Sun D, 2010).

Many studies dealt with genetic material delivery using EXOs: Ohno *et al* demonstrated that EXOs are able to release the anti tumour miR-let-7a to breast cancer cells that express EGFR (Ohno S, 2013).

Other therapeutic EV applications derive from their ability to induce immune response against tumour. Maheveni *et al* demonstrated the ability of EXOs from melanoma and glioma cells to induce immune response and improve mice survival (Mahaweni NM, 2013). Other research groups used EXOs to treat malaria (Martin-Jaular L, 2011) or AIDS patients (Nanjundappa RH, 2011). Two clinical trials are ongoing (Escudier B, 2005), (Morse MA, 2005).

However, many challenges need to be dealt with, in particular the best technique to load EVs with drugs and how to target the cargo (Borges FT, 2013).

EVs are also considered potential biomarkers for disease diagnosis. Because EV protein marker and nucleic acid content reflects the nature and state of their parental cells, EVs are considered a precious source of information (Corrado C, 2013). For example Noerholm *et al* demonstrated that serum microvesicle RNA from patients with glioblastoma multiforme has significantly down-regulated levels of RNAs coding for ribosome

production, compared to normal healthy controls (Noerholm M, 2012). An increase of claudin-containig EXOs in blood is associated with ovaric cancer (Li J S.-B. C.-T., 2009). A mutant transcript of EGFR has been observed in plasma EXOs from glioblastoma patients (Skog J, 2008).
All these possible applications require improvement in isolation and detection methods.

1.5 Extracellular vesicles from blood samples

Different subpopulations of extracellular vesicles have been reported in blood. Sometimes authors refer to blood EVs as microparticles (MPs) or cellular membrane microparticles. This term is not fully descriptive, but is often used (Freyssinet LM., 2003).
Many studies documented the MP number variation in different pathologies and support their use in diagnostics. It is clear that MP release is a well controlled biological process. It has been demonstrated that platelets vesiculate in response to shear stress (Miyazaki Y, 1996) and storage (Bode AP, 1991). Combes *et al* demonstrated that a dramatic increase of MPs from platelets was observed when TNF-α promoting proapoptotic pathway was induced (Hamilton KK, 1990).

1.5.1 Pre-analytical challenges

Aiming to use MP analysis in diagnosis, pre-analytic variables need to be considered.
Pre-analytic factors have not been extensively studied in literature. The MP release, especially from erythrocytes and platelets, is strongly sensitive to environmental factors. For this reason, all steps, from blood collection until analysis, need to be standardized. The variables that need to be considered are: the diameter of needle used for sample collection, way of collection (vacutainer, syringe, tube) and type of anticoagulant, storage temperature,

freeze-thaw cycles and analytic protocol (Simak J, 2006), (György B S. T., 2011). Simak and Gelderman suggested that time between collection and isolation should be as short as possible. In that period, blood should be maintained at room temperature with gentle agitation (Simak J, 2006). Rubin *et al* demonstrated that erythrocyte EV concentration changes depending on agitation, storage time and temperature (Rubin O, 2010). Moreover, the number of Annexin V-positive MPs increases after several freeze-thaw steps in platelet-rich plasma (Connor DE, 2010).

A crucial step in the centrifugation is represented by platelet depletion. MP lost and the induction of MP release from platelets and erythrocytes could depend on centrifugation protocol (Simak J, 2006).

Shah *et al* demonstrated that just two centrifugation steps yield a high number of MPs as compared with a three steps centrifugation protocol. On the other hand, needle diameter does not seem to affect MP number.

Citrate is generally used as anticoagulant. However, Shah *et al* showed that high levels of platelet- and erythrocyte-derived MPs were detected using heparin and Phe-Pro-Arg-chloromethylketone as anticoagulants as compared to citric acid-sodium citrate dextrose and sodium citrate (Shah MD, 2008).

It is not often possible to process samples immediately after collection. Storage could create artefacts. Shah *et al* demonstrated a reduced number of MPs that are positive for AnnexinV/tissue factor after storage. On the other hand, the storage at -70 °C of platelet-free plasma for a couple of weeks does not influence MP analysis. A quick cycle of freeze-thaw is suggested because the prolonged incubation of samples at 37 °C could lead to deterioration of MPs and antigen loss (Shah MD, 2008).

Generally, each laboratory develops its own assay to study MPs but different protocols of extraction, antibodies, and their clones have a dramatic impact on the results of MP analysis. Standardized procedures need to be implemented.

1.5.2 Methods of EV analysis in blood

A lot of different methodological approaches have been used to analyse MPs from blood. Two methods are mostly used: 1) microparticle affinity assay and 2) flow cytometry.

The first one is an ELISA assay based on antibodies able to recognize MP specific protein markers. A particular affinity assay uses Annexin V in presence of Ca^{2+} to recognize only MPs that are positive to phosphatidylserine (Simak J, 2006). This is a robust method, easy to use in the clinical setting and allows the analysis of a high number of samples at low cost. However, it does not allow MP quantification. Only "quality" information is obtained, no information about size and granularity. Furthermore, the MP positivity to phosphatidylserine is under discussion. Although it has been used as a typical MP marker, recent studies suggest the presence of Annexin V-negative MPs. Connor *et al* demonstrated that more than 80% of platelet-derived MPs in blood are Annexin V-negative (Connor DE, 2010).

Flow cytometry (FACS) is the most common used approach to MP analysis, although the commonly used instruments cannot analyse MPs with a size less than 300-500 nm (Freyssinet JM, 2010). It allows the rapid analysis of a large number of MPs and provides information about size and granularity. Using labelled antibodies to recognize specific MP antigens, it can distinguish MPs shed from different cellular populations (Shah MD, 2008). However, results should be interpreted carefully. György *et al* demonstrated that during MP flow cytometry acquisition, immune complexes are formed and may be detected. Furthermore, when indirect labelling is used, they showed that primary and secondary antibodies form immunocomplexes detected in the MP gate and may hamper interpretation. To avoid immunocomplex formation these authors suggest to use direct immunolabelling (György B M. K., 2011).

The use of FACS needs instrument calibration before MP analysis. Size beads of different diameters may be used to evaluate MP size (Simak J,

2006). Fluorescent beads of standardized size are produced by different companies (Becton Dickinson, Sigma, BioCytex). Generally, three bead diameters are used and MP gate is chosen accordingly (Robert S, 2009).
FACS allows quantification of MPs that are positive for specific protein markers. Two methods are generally used: 1) the flow rate method is based on the number of MPs detected in a settled time (Nantakomol D, 2008); the analysis of biological samples with different viscosities is unfeasible (Orozco AF, 2010); 2) TruCount™ tubes (Becton Dickinson) contain a lyophilized pellet that dissolves during sample preparation releasing a known number of fluorescent beads, that allow calculation of the absolute MP number.
The TruCount™ tubes major benefit is that the amount of labelled-beads is not introduced by the operator, eliminating a possible technical error. The absolute MP number is calculated from the number of events in MP and TruCount™ bead gate, total number of TruCount™ beads in the tube and the volume where the sample and beads have been re-suspended (Shet AS, 2003), (Jayachandran M, 2009). It is the most thorough system to analyse the absolute MP number. On the other hand, it could be expensive depending on the sample number (Orozco AF, 2010). Flow cytometry is the best candidate to be considered as the "gold standard" for MP analysis (Gelderman MP, 2008).

1.6 Erythropoiesis and erythroid progenitor markers

The hematopoietic system ensures the production of the different cell types that compose the human blood. The continuous blood cell production is guaranteed by pluripotent stem cells (HSC) that are progressively committed to multipotent progenitors and evolve to committed progenitors (Testa U., 2004).
In particular, erythropoiesis is a multistep process that leads HSC to differentiate in erythrocytes, cells specialized for oxygen transport.

The first step is the differentiation of HSC in hematopoietic progenitors named CFU-GEMM. Subsequently, they evolve to committed erythroid progenitors, i.e. erythroid burst-forming units (BFU-e) and erythroid colony-forming units (CFU-e). Then erythroid precursors with a characteristic morphology are formed. The first identifiable erythroid precursor is the proerythroblast, a cell characterized by a large nucleus, basophilic nucleoli and cytoplasm. Through several cell divisions they evolve first to the basophilic erythroblast, then to the polychromatophilic erythroblast and to the orthocromatic erythroblast. During these steps size is reduced, chromatin is condensed and sensitivity to erythropoietin (EPO) appears because EPO receptors are expressed (Testa U., 2004). Finally, the orthocromatic erythroblast loses its nucleus and becomes a reticulocyte, a non-nucleated cell with remnants of Golgi and endoplasmatic reticulum compartments.

After a brief stay in bone marrow (R1), it passes through the endothelial wall of marrow sinuses and reaches blood circulation (R2) (Videl M., 2010). Here it becomes an erythrocyte, a biconcave disk without nucleus and organelles that contains mostly haemoglobin.

Erythroid differentiation is based on a well regulated transcriptional process which result in the different expression of specific antigens (Santos PM, 2011). These antigens can be used to identify differentiation stages and to distinguish the different committed precursors. FACS analysis allows to evaluate many antigens at the same time (Fig. 5).

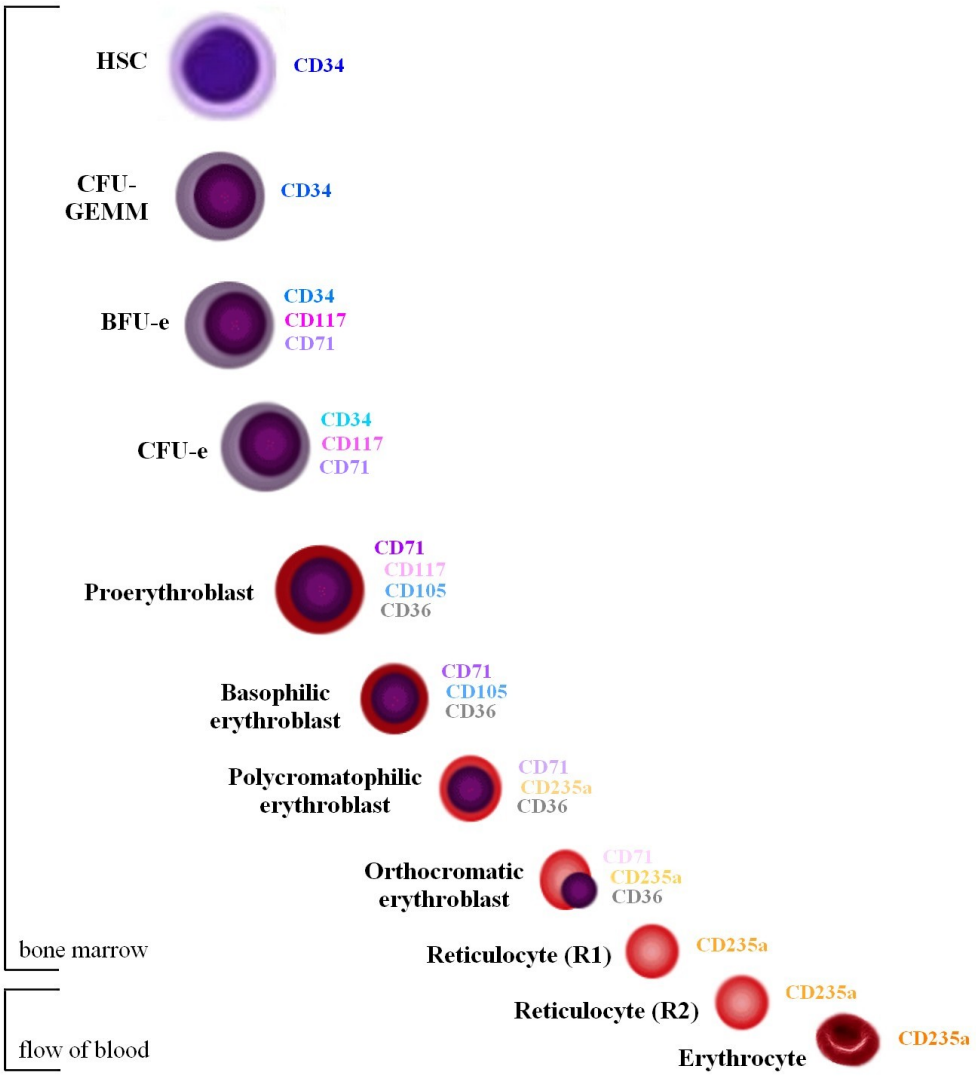

Fig. 5: Maturation during erythropoiesis. The most representative markers expressed during erythroid maturation steps are indicated. The intensity colour variation corresponds to expression levels.

CD34 is a marker of activated early progenitors (HSC and CFU-GEMM) and committed erythroid progenitors (BFU-e and CFU-e) (Furness SG, 2006). Being a marker expressed only by activated progenitors its principal function is to promote HSC proliferation due to its anti-adhesion property. CD34 expression levels slowly decrease and it is absent in proerythroblasts. BFU-e and CFU-e express also CD117 (proto-oncogene c-Kit) (Andre C, 1997). CD117 expression decreases during development. It is still

expressed, at low levels, by proerythroblasts. Proerythroblasts are, also, characterized by CD105 and CD71. The first one is member of TGFβ receptor complex involved in TGFβ modulation signalling as well as cytoskeletal organization (Sanz-Rodriguez F, 2004). CD105 is expressed also by basophilic erythroblasts, but at low levels. On the other hand CD71 levels increase from proerythroblast to orthocromatic erythroblast when it is expelled by reticulocytes through vesicle formation (Fajtova M, 2011). CD71 is the cluster differentiation name for transferrin receptor protein (TFR), a membrane glycoprotein whose function is to mediate cellular uptake of iron from transferrin. The highest amount of transferrin receptor is found on erythroid cells because they need to acquire iron for haemoglobin synthesis. It is released from reticulocytes during their maturation in erythrocytes by EXO secretion (Ponka P, 1999).

The last marker to be expressed is CD235a (glycophorin A). It appears at the proerythroblast stage and its expression increases through maturation being the highest in erythrocytes (Fajtova M, 2011). Glycophorin A is one of the sialoglycoproteins that are expressed on red blood cell membranes. It is the major contributor to the negative surface charge of red blood cells. This negative charge is important for red cells interaction with the vascular endothelium (Griffiths RE, 2012).

Fajitova *et al* identified antigen CD36 as a marker of late differentiation. It is expressed mostly on basophilic erythroblasts, but also on proerythroblasts, polycromatophilic and orthocromatic erythroblasts. The same authors identified CD38 and CD45 in both preoerythroblasts and basophilic erythroblasts (Fajtova M, 2011) although these are typical markers of immune cells (Jackson DG, 1990), (Brown VK, 1994).

1.6.1 Extracellular vesicles from reticulocytes

During maturation, a remodelling of plasma membrane is observed with reduction of cell volume and surface area (Géminard C d. G., 2002). Autophagy and membrane shedding have been shown to be involved in this

process (Seelig LL., 1972), (Simpson CF, 1968). More recently, Johnstone *et al* demonstrated that vesicle secretion is the principal process (Johnstone RM M. A., 1991), (Pan BT J. R., 1983). Johnstone and Stahl demonstrated that TFR shedding is associated to small vesicle release in reticulocytes maturation (Pan BT J. R., 1983), (Harding C, 1983). It now is apparent that EXO secretion during reticulocyte maturation is an integral part of the red cell development program (Blanc L V. M., 2010). Considering that EXOs have a diameter around of 60 nm, each reticulocyte releases between 800 to 2600 EXOs equivalent to 10^{14} EXOs released every day in circulation (Blanc L D. G.-B., 2005).

TFR is, of course, the most studied protein released in EXOs. During reticulocyte maturation this receptor is internalized into the cells through coated pits. Then it can be recycled to plasma membrane or segregated in multivesicular endosomes (Fig. 6). Multivesicular bodies evolve and release TFR positive EXOs (Géminard C d. G., 2002). Huebers *et al* demonstrated that the concentration of TFR reflects erythropoiesis rate. For this reason patients affected by erythroid hypoplasia induced by marrow-suppressive drugs showed a low amount of TFR as compared with controls (Huebers HA, 1990). Furthermore, EXOs released by reticulocytes are enriched with lipid and proteic markers. Beside lipid rafts (de Gassart A, 2003), other molecules are released with EXOs, including AChE, a glycosylphosphatic-dylinisitol-anchored protein (Johnstone RM A. M., 1987), as well as CD55 and CD59, whose loss has been observed in patients with paroxysmal nocturnal hemoglobinuria (Ware RE, 1995). Other EXO markers, such as hsc70 and Alix, have been observed in EXOs released from reticulocytes. They follow the TFR fate. Hsc70 has been demonstrated to interact with TFR during proteasome degradation (Géminard C D. G., 2004), whereas Alix interacts with TFR cytosolic domain and with ESCRT machinery involved in multivesicular body formation (von Schwedler UK, 2003).

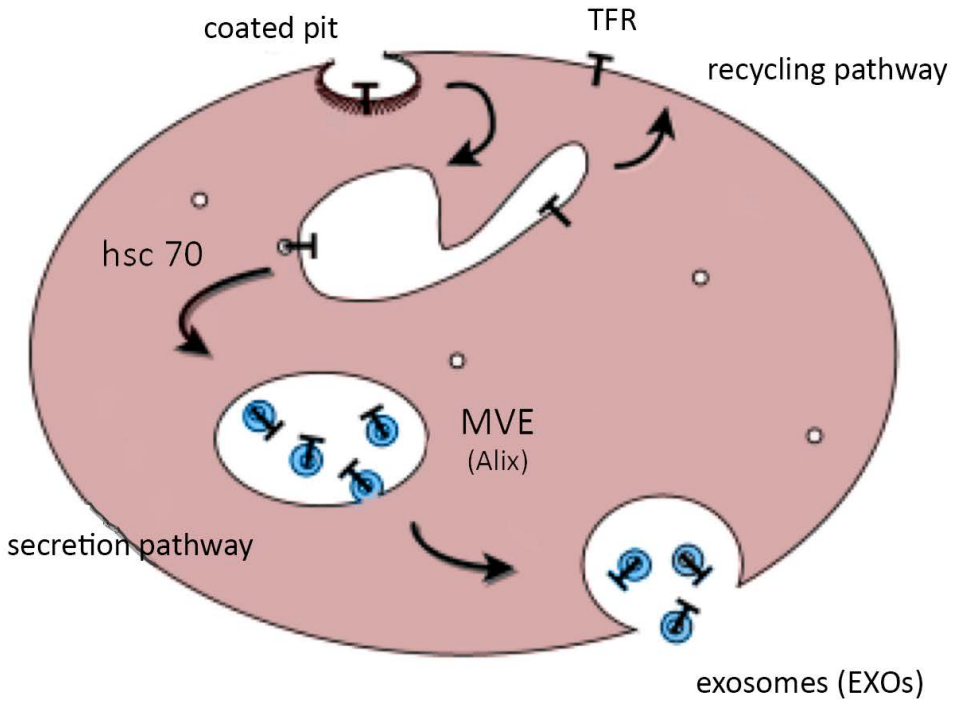

Fig 6: TFR pathway during reticulocyte maturation. Modified from Blanc L *et al*, 2005.

Exosomal secretion is an integral part of erythropoiesis (Blanc L V. M., 2010). Vesicles could be involved in all passages of erythroid progenitor maturation. Further studies are needed to investigate this exciting possibility and to ascertain whether impairment EV secretion could be involved in pathophysiology of red blood cell disorders.

1.7 Extracellular vesicles released during cellular stress – p53 involvement

Cells are subjected to many different endogenous and exogenous stress types. Many responses have been developed to address each stress type, such as cell cycle arrest, apoptosis, senescence, autophagy (Yu X R. T., 2009).

In the last ten years the role of EVs in the development of adaptive mechanisms against stress conditions has been demonstrated (Kucharzewska P, 2013). Much of what we know about the EV function in stress is gathered from studies focused on cancer. As already described, many authors showed that EVs are involved in tumour progression mechanisms, such as angiogenesis and metastasis (Kucharzewska P, 2013). Furthermore, several studies described cell vesiculation in response to different stress types such as hypoxia (Wysoczynski M, 2009), (Zhang HC, 2012), (King HW, 2012), low PH level (Parolini I, 2009), oxidative stress (Eldh M, 2010), (Hedlund M, 2011), (Zhan R, 2009), thermal stress (Zhan R, 2009), (Clayton A T. A., 2005), (Chen T, 2011), radiation (Wysoczynski M, 2009), shear stress (Miyazaki Y, 1996) and drug effects (Lv LH, 2012). It is well documented that stress conditions on parental cells affect the EV content. For example, Choi and co-workers demonstrated that EVs released by primary cells have a very different protein cargo when compared with EVs shed from metastatic cells (Choi DS, 2012). In hypoxic conditions, the EXO amount shed from carcinoma cells (Park JE, 2010) as well as human and murine lung cancer cell lines (Wysoczynski M, 2009) is increased. These EXOs are enriched with proteins potentially able to modulate tumour microenvironment. In breast cancer cell culture increased amount of EXOs depends on HIF-1α. These EXOs are enriched with miR-210, a short RNA well known to be regulated by hypoxia (King HW, 2012). Mesenchymal stem cells release EVs that are similar to those shed by parental cells, but the majority of them are negative for platelet-derived growth factor receptor (Zhang HC, 2012).

Regarding EV response in low PH conditions, Taraboletti *et al* demonstrated that EVs containing VEGF were destroyed under acidic pH conditions (a characteristic of the tumour microenvironment). Consequently, VEGF release led to significantly higher stimulation of cell motility (Taraboletti G, 2006). Moreover, in the same conditions, EVs released from melanoma cells have a less flexible membrane due to a different lipid composition. They are enriched with ganglioside GM3 and

sphyngomyelin. These lipids seem to bestow on EVs a better ability to fuse with plasma membrane of recipient cells (Parolini I, 2009). Eldh *et al* showed that oxidative stress induce a massive change in mRNA content in EXOs from mast cell lines. Furthermore, EXOs are able to confer resistance against oxidative stress and viability improvement in recipient cells (Eldh M, 2010).

Levine and co-workers have investigated the role of p53, a transcriptional factor activated by a wide variety of stress signals. It acts to restore cellular homeostasis and prevents the accumulation of errors on DNA changes (Levine AJ., 1997). In 2006, Yu *et al* observed that, after p53 activation, several proteins encoded by genes that are not p53 transcriptional targets, increased in the cell medium of non small cell lung cancer cell line (H460) and they were released through EXOs. They discovered that the p53 role in EXO production is linked to the expression of a p53 gene target: TSAP6 (Yu X H. S., 2006). TSAP6 is involved in proteins transport (Roperch JP, 1998). Two years later, Telerman and collaborators provided the first genetic evidence that exosome formation is a tightly controlled biological process dependent of TSAP6. TSAP6 deficient mice show microcytic anemia (reticulocytes and erythrocyte were smaller with abnormal shape and osmotic fragility). Reticulocytes from these mice could not expel TFR during their maturation (Lespagnol A, 2008). Absence of TSAP6 resulted in a deficiency of EXO formation delaying the maturation of bone marrow erythroblasts and reticulocytes. Another p53 gene target, CHMP4C, is known to be involved in EXO production. It is part of the ESCRT-III protein complex that is essential for endosome formation (Yu X R. T., 2009). However, a p53 independent mechanism has been shown. An accumulation of ceramide, a lipid molecule involved in EXO formation (Trajkovic K, 2008), has been shown in response to different stress types (Nikolova-Karakashian MN, 2010). It could be interesting to evaluate whether stress-induced ceramide accumulation is paralleled by increase EXO production.

1.8 Ribosomal stress: cell proliferation inhibition through p53-dependent and -independent mechanisms

p53 activation is induced by cells exposed to different stress types as UV radiation, heat shock, hypoxia (Horn HF, 2007). Also an aberrant ribosome biogenesis leads to increased p53 levels. This condition is named "ribosomal stress" (or "nucleolar stress") (Pestov DG, 2001), (Rubbi CP, 2003).

Ribosome biogenesis occurs in the nucleolus and is the result of coordinated steps that include rRNA precursor processing. Briefly, RNA polymerase I is involved in transcription of 47S rRNA precursor. The processing of this precursor generates the mature 18S, 5.8S and 28S rRNA, whereas 5S RNA is transcribed independently. rRNA and ribosomal proteins (RPs) are collected in a specialized cellular compartment: the nucleolus, where rRNA and RPs are assembled to form the large 60S and the small 40S subunits. Finally, the subunits are exported to the cytoplasm (Lempiäinen H, 2009).

Perturbation to this complex process includes inadequate rRNA transcription, disruption of rRNA procession or RP imbalance. These abnormalities trigger ribosomal stress followed by p53 activation (Deisenroth C, 2010). p53 activity is regulated by the MDM2 oncoprotein that binds to p53 and targets it to degradation. Under normal condition p53 levels are low because it is constantly degraded through MDM2 interaction. In many stress conditions, the interaction MDM2-p53 is disrupted and p53 levels increase (Olausson KH, 2012).

Several tumour suppressor proteins, such as ARF, have been demonstrated to bind MDM2 and inhibit MDM2-p53 interaction (Zhang Y X. Y., 2001). Several RPs are able to bind MDM2 inducing increased p53 levels. "Free" RPs are available to bind MDM2 as consequence of altered ribosome biogenesis (Zhang Y L. H., 2009) (Fig. 7).

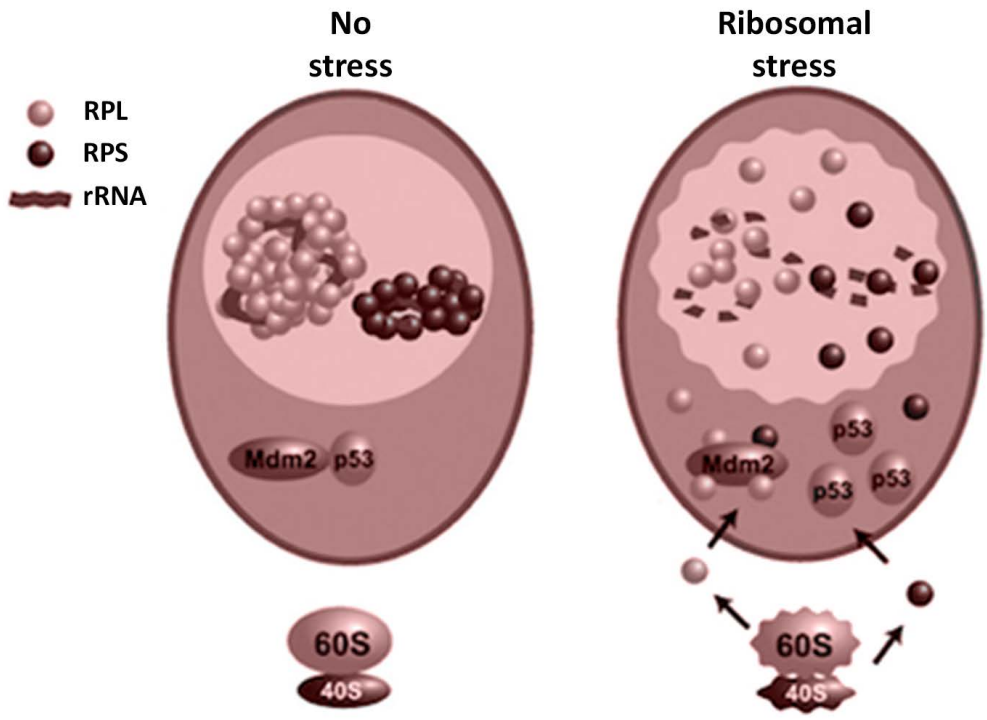

Fig. 7: Schematic p53-dependent mechanism induced by ribosomal stress. Modified from Zhang Y *et al*, 2009.

Several studies demonstrated that several RPs, such as RPL5 (Dai MS L. H., 2004), RPL11 (Zhang Y W. G., 2003), (Lohrum MA, 2003), (Bhat KP, 2004), RPL23 (Dai MS Z. S., 2004), (Jin A, 2004) and RPS7 (Chen D, 2007) could bind MDM2 and inhibit its E3 ubiquitin ligase function.

However, beside p53-dependent pathways, recently a p53-independent mechanism of cell arrest in response to abnormal ribosome biogenesis has been documented (Donati G M. L., 2012). Firstly discovered in Drosophila (Grewal SS, 2007), it has been better documented in recent years. In 2009, Li *at al* investigated the role of pescadillo, a protein involved in processing of pre-rRNA molecules. They demonstrated that knockdown of this protein results in cyclin D1 down-regulation and cyclin-dependent kinase inhibitor p27/Kip1 up-regulation (Li J Y. L., 2009).

Furthermore, a PIM1-dependent pathway has been suggested. Iadevaia *et al* demonstrated that RPs deficiency caused down-regulation of PIM1 expression. Down regulation of RPS19 and other RPs induced PIM1

proteasome degradation. PIM1 is a serine/threonine kinase that reduces the activity of p27/Kip1. PIM1 reduction induces p27/Kip1 stabilization and blocks the cell cycle regardless p53 (Iadevaia V, 2010).
The role of RPL11 in p53-independent mechanisms has been investigated. Inhibiting rRNA transcription, RPL11 protein is "free" and binds MDM2. The result is that E2F-1 protein is not blocked by MDM2 and can induce expression of E2F gene targets that are necessary for the progression through cell cycle (Donati G B. E., 2011). Furthermore, RPL11 together with RPL5 is able to bind c-Myc, a well documented cell proliferation stimulator. The binding of RPL11 to c-Myc induces reduction of c-Myc transcription and c-Myc degradation followed by reduced cell proliferation (Liao JM, 2013).

1.9 Diamond Blackfan Anemia (DBA), a human disease due to ribosomal stress

Mutations in genes encoding for RPs have been identified as the cause of human genetic diseases. Diamond Blackfan Anemia (DBA) is the first human disease shown to be caused by a defect in ribosomal proteins (Draptchinskaia N, 1999). It is a congenital bone marrow failure syndrome due to a specific defect of the erythroid lineage (Hölzel M, 2010). This haematological disorder is member of a class diseases known as "ribosomophaties", characterized by genetic anomalies resulting in defective ribosome biogenesis (Raiser DM, 2013). DBA pathogenesis is due to ribosomal stress triggered by an abnormal ribosome biogenesis.

1.9.1 Clinical features and molecular basis

DBA (MIM 105650) is categorized as a congenital bone marrow failure syndrome, presenting during infancy with an incidence of 4-5 cases/one millions live births (Orfali KA, 2004). It is a hypoplastic anemia

characterized by other haematological characteristic as macrocytosis, reticulocytopenia, high activity of adenosine deaminase (ADA) in red cells (Lipton JM, 2009). Defective erythropoiesis is revealed by a very low number of erythroid precursors and, functionally, by a reduction of BFU−E progenitor cells in the bone marrow. It shows autosomal dominant transmission (Campagnoli MF G. E., 2004). Proliferative and differentiative activity towards the other lineages is normal.

Beside these haematological characteristics, half of patients show physical abnormalies as short stature, thumb abnormalies, heart defect, craniofacial abnormalies and cleaft lip and palate (Lipton JM, 2009).

Standard therapy consists in steroids; about 40% of patients respond to this therapy. The non-responsive patients are treated with red blood cell transfusion, but stem cell transplantation is the only definitive treatment (Vlachos A M. E., 2010)**.** Twenty per cent of patients develop a clinical remission, but the biological reasons are unknown (Quarello P, 2010).

DBA shows an autosomal dominant inheritance and all mutated genes have heterozygous mutations (Ball S., 2011). RPS19 is the first DBA gene identified (Draptchinskaia N, 1999). Mutations in RPS19 have been found in 25% of patients (Campagnoli MF R. U., 2008). Ten genes encoding ribosomal proteins have been found mutated in DBA patients, i.e. RPS19, RPS24, RPS17, RPL5, RPL11, RPS7, RPL35a, RPS26, RPS10, RPL26 (Draptchinskaia N, 1999), (Gazda HT G. A.-L., 2006), (Cmejla R, 2007), (Gazda HT S. M., 2008), (Farrar JE, 2008), (Doherty L, 2010). The most frequently mutated genes, after RPS19, are RPL5 and RPL11 that account for 10% of DBA patients (Gazda HT G. A.-L., 2006). About 60% of patients show mutations in genes encoding ribosomal proteins. Extra-ribosomal factors have been speculated to have a role in those patients that are mutation-negative for *RP* genes. GATA-1, encoding for a hematopoietic transcription factor has been found mutated in four patients with DBA (Sankaran VG, 2012), (Parrella S, 2014).

Several studies in Drosophila, Xenopus, Zebrafish and mouse showed that p53 activation is involved in DBA development (Kongsuwan K, 1985),

(Miller L, 1970), (Danilova N, 2008), (McGowan KA, 2008). As already said, the insufficient RP production could lead to excess of other RPs that can interact with MDM2 inducing cell cycle arrest (Zhang Y L. H., 2009). However, the role of p53 in DBA pathogenesis is still under discussion. Also p53-independent mechanisms have been suggested. Both p53-dependent and -independent mechanisms may cooperate and induce cell cycle arrest with a proapoptotic phenotype in erythroid progenitors.

1.9.2 Global gene expression in p53 null-cell models of DBA suggests activation of p53-independent pathways (Aspesi *et al*, submitted to Gene)

Defects in ribosome synthesis have been shown to activate p53 thereby providing a rationale for the pro-apoptotic phenotype of erythroid progenitor in DBA (Draptchinskaia N, 1999), (Vlachos A B. S., 2008). p53 inhibition has been demonstrated to attenuate the proapoptotic phenotypes in DBA models (Drosophila, Xenopus, zebrafish and mouse) (Kongsuwan K, 1985), (Miller L, 1970), (Danilova N, 2008), (McGowan KA, 2008). However, p53 inhibitors cannot be used in therapy because of their risk of cancer development. We considered that identification of p53-independent pathways could suggest more realistic treatments for DBA. To this aim, we analysed the gene expression changes in three p53-null cell models of DBA as compared with the appropriate controls. Using a microarray approach (Affimetrix GeneChip Human Genome U133A) followed by sophisticated statistical analysis (ranking-PCA), a set of dysregulated genes that are common to the three DBA cell models has been identified. The Gene Onthology classification showed an enrichment of genes involved in amino acid metabolism, negative regulation of cell proliferation, apoptosis and cell redox homeostasis whereas PANTHER Biological annotation identified genes involved in haematopoiesis and amino acid/steroid metabolism. Our results demonstrated that gene expression is altered in DBA cell models in agreement with the proapoptotic phenotype observed in DBA. The

manuscript is attached.

Elsevier Editorial System(tm) for Gene
Manuscript Draft

Manuscript Number:

Title: Dissecting the transcriptional phenotype of ribosomal protein deficiency: implications for Diamond-Blackfan Anemia.

Article Type: Short Communication

Keywords: Ribosomal protein; Diamond Blackfan anemia; ribosomopathy; bone marrow failure

Corresponding Author: Prof. Irma Dianzani,

Corresponding Author's Institution: University of Eastern Piedmont

First Author: Anna Aspesi

Order of Authors: Anna Aspesi; Elisa Pavesi; Elisa Robotti; Rossella Crescitelli; Ilenia Boria; Federica Avondo; Hélène Moniz; Lydie Da Costa; Narla Mohandas; Paola Roncaglia; Ugo Ramenghi; Antonella Ronchi; Stefano Gustincich; Simone Merlin; Emilio Marengo; Steven R Ellis; Antonia Follenzi; Claudio Santoro; Irma Dianzani

Manuscript Region of Origin: ITALY

Abstract: Defects in genes encoding ribosomal proteins cause Diamond Blackfan Anemia (DBA), a red cell aplasia often associated with physical abnormalities. Other bone marrow failure syndromes have been attributed to defects in ribosomal components but the link between erythropoiesis and the ribosome remains to be fully defined. Several lines of evidence suggest that defects in ribosome synthesis lead to "ribosomal stress" with p53 activation and either cell cycle arrest or induction of apoptosis. Pathways independent of p53 have also been proposed to play a role in DBA pathogenesis. We took an unbiased approach to identify p53- independent pathways activated by defects in ribosome synthesis by analyzing global gene expression in various cellular models of DBA. Ranking - Principal Component Analysis (Ranking-PCA) was applied to the identified datasets to determine whether there are common sets of genes whose expression is altered in these different cellular models. We observed consistent changes in the expression of genes involved in cellular amino acid metabolic process, negative regulation of cell proliferation and cell redox homeostasis.
These data indicate that cells respond to defects in ribosome synthesis by changing the level of expression of a limited subset of genes involved in critical cellular processes. Moreover, our data support a role for p53-independent pathways in the pathophysiology of DBA.

Suggested Reviewers: Carlo Dufour
Department of Pediatric Hematology and Oncology, Gaslini Children's Hospital, Genoa, Italy
carlodufour@ospedale-gaslini.ge.it
Pediatrician and hematologist

Johnson M. Liu
Pediatric Hematology & Oncology, The Feinstein Institute for Medical Research, Manhasset, NY, USA
jliu3@nshs.edu
He is a pediatrician specialized in pediatric hematology.

Andrew Bradbury
Los Alamos National Laboratory, USA
amb@lanl.gov
Molecular biologist

Kim De Keersmaecker
Department of Human Genetics, Leuven, Belgium
kim.dekeersmaecker@cme.vib-kuleuven.be
She works on hematologic malignancies

Steven W. Graves
University of New Mexico, USA
graves@unm.edu
Molecular biologist

Clara Camaschella
Università Vita-Salute San Raffaele, Milan, Italy
camaschella.clara@unisr.it
She has a broad research expertise in iron metabolism and inherited disorders of erythropoiesis.

Akiko Shimamura
Fred Hutchinson Cancer Research Center, Seattle, USA
ashimamu@fhcrc.org
She studies ribosomal function in bone marrow failure syndromes and malignant transformation.

Sjaak Philipsen
Erasmus Medical Centre, Rotterdam, Netherlands
j.philipsen@erasmusmc.nl
His laboratory uses gene expression analysis with microarrays to unravel the role of transcription factors in erythropoiesis.

Opposed Reviewers:

Research Highlights

Highlights:

Ribosomopathies such as DBA are caused by ribosome dysfunction that activates p53

p53-independent pathways may suggest possible treatments for DBA

Expression analysis was performed in three p53-null models of DBA

Genes involved in apoptosis and cell redox homeostasis were especially affected

DBA is due to cumulative effects of p53- dependent and independent pathways

Dissecting the transcriptional phenotype of ribosomal protein deficiency: implications for Diamond-Blackfan Anemia.

Anna Aspesi[a], Elisa Pavesi[a], Elisa Robotti[b], Rossella Crescitelli[a], Ilenia Boria[c], Federica Avondo[a], Hélène Moniz[d], Lydie Da Costa[d], Narla Mohandas[e], Paola Roncaglia[f], Ugo Ramenghi[g], Antonella Ronchi[h], Stefano Gustincich[f], Simone Merlin[a], Emilio Marengo[b], Steven R. Ellis[i], Antonia Follenzi[a], Claudio Santoro[a] and Irma Dianzani[a]

[a]Department of Health Sciences, University of Eastern Piedmont, Novara, Italy, [b]Department of Sciences and Technological Innovation, University of Eastern Piedmont, Alessandria, Italy; [c]Department of Chemistry, University of Milan, Italy; [d]U1009, AP-HP, Service d'Hématologie Biologique, Hôpital Robert Debré, Université Paris VII-Denis Diderot, Sorbonne Paris Cité, F-75475 Paris, France; [e]New York Blood Center, New York, USA; [f]International School for Advanced Studies (SISSA/ISAS), Trieste, Italy, [g]Department of Pediatric Sciences, University of Torino, Torino, Italy; [h]Department of Biotechnologies and Biosciences, Milano-Bicocca University; [i]University of Louisville, Kentucky, USA

Correspondence: Irma Dianzani, Department of Health Sciences, University of Eastern Piedmont, via Solaroli17, 28100 Novara, Italy. Phone: +39 0321 660544. E-mail: irma.dianzani@med.unipmn.it

Abstract

Defects in genes encoding ribosomal proteins cause Diamond Blackfan Anemia (DBA), a red cell aplasia often associated with physical abnormalities. Other bone marrow failure syndromes have been attributed to defects in ribosomal components but the link between erythropoiesis and the ribosome remains to be fully defined. Several lines of evidence suggest that defects in ribosome synthesis lead to "ribosomal stress" with p53 activation and either cell cycle arrest or induction of apoptosis. Pathways independent of p53 have also been proposed to play a role in DBA pathogenesis.

We took an unbiased approach to identify p53- independent pathways activated by defects in ribosome synthesis by analyzing global gene expression in various cellular models of DBA. Ranking - Principal Component Analysis (Ranking-PCA) was applied to the identified datasets to determine whether there are common sets of genes whose expression is altered in these different cellular models. We observed consistent changes in the expression of genes involved in cellular amino acid metabolic process, negative regulation of cell proliferation and cell redox homeostasis.

These data indicate that cells respond to defects in ribosome synthesis by changing the level of expression of a limited subset of genes involved in critical cellular processes. Moreover, our data support a role for p53-independent pathways in the pathophysiology of DBA.

Keywords:

Ribosomal protein, Diamond Blackfan anemia, ribosomopathy, bone marrow failure.

Abbreviations:

DBA, Diamond Blackfan anemia; RP, ribosomal protein; RS, ribosomal stress; PCA, principal component analysis; PC, principal component; GO, gene ontology.

1. Introduction

Mutations in genes encoding ribosomal proteins result in Diamond Blackfan Anemia (DBA), a bone marrow failure syndrome characterized by pure erythroid aplasia [1,2]. In addition to bone marrow failure, malformations are observed in approximately one third of the patients. DBA is inherited with an autosomal dominant pattern and results from haploinsufficiency for single ribosomal proteins (RP). To date eleven genes encoding ribosomal proteins have been found mutated in DBA patients, i.e. *RPS19*, *RPS24*, *RPS17*, *RPL5*, *RPL11*, *RPS7*, *RPL35A*, *RPS26*, *RPS10*, *RPL26*, *RPL15* [1,3-6].

In addition to DBA several other ribosomopathies have been described [7]. Many of these are bone marrow failure syndromes but other ribosomopathies where hematopoiesis is unaffected have also been identified [8]. The DBA phenotype has been ascribed to a peculiar sensitivity of the erythron and tissues of the developing embryo to haploinsufficiency for ribosomal proteins. This hypothesis is based on information obtained using both cellular models and model organisms. Deficiencies in factors involved in ribosome synthesis have been studied extensively in Drosophila, Xenopus, zebrafish and mouse [9-12]. These defects cause the induction of a cellular stress response, called ribosomal (or nucleolar) stress (RS) that results in activation of p53-dependent and independent pathways, which block proliferation and/or induce apoptosis [13-15]. Whereas pharmacological or genetic inhibition of p53 is able to attenuate phenotypes in many of these models, treatment based on p53 inhibition appears unrealistic in humans because of attendant cancer risks.

To shed light into pathways that are activated by ribosome stress in human cells expressing reduced levels of ribosomal proteins we have studied the transcriptome of three different cellular models of DBA looking for intersecting patterns of gene expression changes.

2. Design and Methods

2.1. Cell cultures

Human erythroleukemia cell line TF1 (ATCC Number: CRL-2003) was grown in RPMI 1640 medium supplemented with 10% FBS, 2 mM L-glutamine, 100 UI/mL penicillin, 100 µg/mL streptomycin and 5 ng/mL GM-CSF. TF1 cells expressing inducible shRNAs against RPS19 or a scramble shRNA were provided by Dr. Stefan Karlsson [16] (shRNAs SCR, B and C). shRNA expression was induced by 0.5µg/ml doxycycline (DOX) for four days. TF1 cells for transduction were thawed and maintained for minimum two passages before being transduced

with lentivirus prrl-shSCR or prrl-shRPL5A or prrl-shRPL11A [15] with an MOI of 10. Two days after transduction, Green Fluorescent Protein (GFP) positive cells were sorted by flow cytometry, then cultured under the same conditions for four days.
For qRT-PCR validation we also designed and made a third generation lentiviral vector (LV) system expressing scramble or RPS19 shRNA [16] (shRNAs SCR and C). LVs were obtained after transient transfection of 293T cells by the calcium phosphate method [17] with the packaging plasmids (pMDLg/pRRE, pRSV-REV and pMD2-VSVG) and the transfer vectors expressing either the scramble or the RPS19 shRNA. TF1 cells were transduced with 10 MOI of the described LVs [18]. Transduction efficiency was evaluated after three days by detection of GFP. Cells were collected four days after transduction.

2.2. TP53 analysis

Genomic DNA was isolated from TF1 cells using QIAamp DNA Mini kit (Qiagen) according to the manufacturer's protocol. Primers were designed to amplify exons 4-9 and their flanking regions. PCR was performed using AmpliTaq Gold DNA Polymerase (Applied Biosystems) and amplicons were sequenced in both directions using a Big Dye Terminator® v1.1 cycle sequencing kit (Applied Biosystem) and a ABI PRISM® 3100 genetic analyzer. Total RNA was isolated from TF1 cells using RNeasy Plus Mini kit (Qiagen) and reverse transcribed with High Capacity cDNA Reverse Transcription kit (Applied Biosystems). *TP53* was amplified from cDNA and sequenced. Sequencing of *TP53* from primary $CD34^+$ cells was performed in parallel as a wild type control.
For the nuclear localization assay TF1 cells were lysed as previously described [19] and subjected to western blot analysis.

2.3. Western blot

Cells were lysed in Lysis Buffer (50mM Tris-HCl pH 8, 1mM EDTA, 150mM NaCl, 0.5% NP-40) supplemented with protease inhibitors. Cell debris was removed by centrifugation at 13000g for 10 minutes and the supernatant was collected. Proteins were separated on 12% SDS–PAGE, transferred on nitrocellulose membrane and incubated with antibodies specific for RPS19 (Abnova), RPL5 (Abcam), RPL11 (Invitrogen), β-actin (Sigma), p53, nucleolin and GAPDH (Santa Cruz Biotechnology). Detection of immunoblots was carried out with Western Lightning® Plus-ECL (PerkinElmer). Downregulation or overexpression of the proteins of interest were estimated after normalization to the intensity of GAPDH or β-actin.

2.4. RNA isolation and microarray processing

Total RNA for microarray analysis was isolated using either TRIzol® reagent (Invitrogen) or RNeasy Plus Mini kit (Qiagen) according to the protocols supplied by the manufacturers. RNA quantification, quality assessment and labelling were performed as described in Avondo et al. 2009 [20]. Labelled cRNA was hybridized on Affymetrix GeneChip Human Genome U133A 2.0 Arrays. Microarray processing and data analysis was performed as described by Avondo et al. [20].

2.5. Ranking- Principal Component Analysis (Ranking-PCA)

PCA [21,22] is a multivariate pattern recognition method that allows the representation of the original dataset in a new reference system characterised by new variables called principal components (PCs). By the use of a restricted number of significant PCs, experimental noise and random variations can be eliminated. PCA is exploited in Ranking-PCA [23-25] to select the most discriminating variables (i.e. candidate biomarkers) between two groups of samples (e.g. control vs. pathological) and sort them according to their decreasing discrimination ability. Here, Ranking-PCA was applied by calculating PCs in leave-one-out (LOO) cross-validation. The analysis we performed aimed to identify the transcriptome abnormalities found in erythroid human TF1 cells with a defect of RPS19, RPL5 or RPL11.

The data set consisted of measurements from two sets of experiments:

- TF1 cell lines with downregulation of RPS19 (labelled **S19** in Figure 1) and their SCR controls (labelled **CS**);
- TF1 cell lines downregulated for RPL5 and RPL11 (labelled **L5** and **L11** respectively) and their scramble controls (labelled **CL**).

Since the datasets were not directly comparable, they were independently mean centred (i.e. the average value of each variable is substracted from each sample for each dataset separately). Then, Ranking-PCA was applied to the TF1 dataset consisting in 17 samples (7 control and 10 pathological) described by 10194 variables (probes). Only the first PC was selected and provided the correct classification of all the samples, as assessed by calculation of the per cent non-error-rate (NER%), defined as the percentage of correct assignments (NER%=100%).

The performance of Ranking-PCA was compared to other classification tools as Partial Least Squares - Discriminant Analysis (PLS-DA) [26] obtaining similar classification performances

but Ranking-PCA provides an exhaustive set of candidate biomarkers ranked according to their decreasing discriminant ability.

2.6. Quantitative RT-PCR

For qRT-PCR analysis total RNA was isolated using TRIzol® reagent. cDNA was synthesized using the High Capacity cDNA Reverse Transcription Kit (Applied Biosystems). Quantitative PCR was performed with an AbiPrism7000 instrument (Applied Biosystems) using Taqman® Gene Expression Assays (Applied Biosystems). PCR reactions were run in triplicate. Ct values were normalized to GAPDH or β-actin, used as endogenous controls, and expression levels were calculated with the ddCt method [27]. Fold changes in the expression of the target gene were equivalent to 2^{-ddCt}. Fold change data are presented as mean±SD. Data were analyzed with Student's t-test.

3. Results

3.1. Characterization of TF1 cell lines

RPS19-silenced TF1 cells have been widely used to investigate DBA pathophysiology [16,28-30]. In this model, significant suppression of erythroid differentiation, cell growth, and colony formation was observed [16], along with the increase of apoptotic cells [30]. To ascertain the status of p53 in TF1 cell line we sequenced the *TP53* gene. Sequencing of genomic DNA showed two mutations in trans. On one allele, mutation c.693-2A>G in the acceptor splice site of exon 7 is expected to lead to the skipping of this exon and to nonsense mediated mRNA decay (NMD), as confirmed by the absence of this transcript in cDNA sequencing analysis (data not shown).

On the other allele, mutation c.752delT induces frameshift without NMD, since the stop codon of the new reading frame is located in proximity of the last splicing site. This mutation was also detected in p53 mRNA expressed by TF1 cells, as shown by cDNA sequencing (Figure S1A). The aberrant transcript gives rise to a protein with 92 incorrect aminoacids at the C-terminus and with a predicted size of approximately 38 kDa. Accordingly, immunoblotting performed with an antibody against the N-terminal region of p53 revealed a smaller protein in TF1 cells than the full-length p53 expressed by $CD34^+$ cells (Figure S1B). This protein lacks the nuclear localization signal and part of the DNA binding domain, therefore it accumulates in the cytoplasm (Figure S1C) and is presumably inactive.

3.2. Gene expression profiling of cells with RP deficiency

To identify genes associated with a RP defect, we used three cell line models where one of the three most frequently mutated DBA genes was downregulated. This was obtained by the expression of shRNAs against RPS19, RPL5 or RPL11 in the human erythroleukemia cell line TF1. The downregulation of the respective ribosomal proteins was assessed by western blotting (Figure S2). The observed downregulation of RPS19 and RPL5 was to about 50% and that of RPL11 was to about 30%, as compared with scrambled (SCR) controls.

We analysed whole genome expression profiles of the three TF1 cell lines downregulated for RPS19, RPL5 or RPL11 (named hereafter TF1 shRPS19, TF1 shRPL5, TF1 shRPL11) as compared to SCR controls. The expression study was performed using Affymetrix GeneChip Human Genome U133A 2.0 Arrays which allow the screening of 18,400 transcripts. Each dataset showed a decrease in the transcript corresponding to the downregulated RP (fold change RPS19: 0.12; RPL5: 0.26; RPL11: 0.11).

In order to identify the transcriptional signature of RP deficiency in p53-deficient erythroid cells we intersected the three TF1 cell lines downregulated for RPS19, RPL5 and RPL11 using Ranking-PCA. Ranking-PCA is a statistical method that can select and sort the most discriminating variables between groups of pathological and control samples [24]. Figure 1 represents the results of PCA performed on the first 205 variables selected by Ranking-PCA. The first PC accounts for about the 79% of the overall information. The selected variables are reported in Table S1 according to the order in which they were included in the Ranking-PCA model. It is important to note that the results obtained by Ranking-PCA do not necessarily include all the genes that have the highest fold change in RP-deficient cells as compared to their controls. Instead the analysis is carried out to provide the set of dysregulated genes common to the three TF1 cell lines silenced for RPS19, RPL5 or RPL11: a gene is added only if it shows a similar dysregulation in all datasets. Although PC_2 is responsible for only about 4% of the total information, it does reflect effects of the pathology since control and pathological samples from the same cell line (TF1-S and TF1-L cell lines) lie at opposite values along this PC. PC_1 and PC_2 together are able to clearly distinguish the four groups of samples corresponding to two different downregulation models (TF1-S is an inducible model, whereas L is a constitutive downregulation model), both control and pathological, and to RPs pertaining to different ribosome subunits.

3.3. Biological processes altered in cells with RP deficiency

In order to systematically detect impaired biological processes of these cells, we analysed the genes included in the Ranking-PCA list by employing the tool of gene annotation provided by DAVID (Database for Annotation, Visualization and Integrated Discovery) at http://david.abcc.ncifcrf.gov/. The results included classifications according to Gene Ontology (GO) and PANTHER databases. GO categories for Biological Processes showed an enrichment, among others, of genes involved in cellular amino acid metabolic process, negative regulation of cell proliferation, apoptosis and cell redox homeostasis (Table 1). The PANTHER Biological Process annotation identified statistically significant over-representation of genes involved in hematopoiesis and in amino acid and steroid metabolism (Table 2).

Two genes stood out whose expression was increased in this analysis, EPOR and TFRC, whereas another noteworthy gene, SOD2, displayed reduced expression (Table S1).

3.4. Quantitative RT-PCR validation of microarray data

In order to corroborate the microarray gene expression results, we selected eight genes among the top genes of the Ranking-PCA list or among those highlighted by the PANTHER analysis. Real-time RT-PCR was performed on the same RNA samples used for microarray analysis (TF1 shRPL5, TF1 shRPL11) or on different samples with a similar level of RP downregulation (TF1 shRPS19, both DOX-inducible model and transduced cells constitutively expressing shRNAs). The expression level of FTH1 and PLIN2 (up-regulated in RP defective cells) and SLC38A1, TOM1L1, ASNS, CTH, GARS and PHGDH (down-regulated in RP defective cells) was tested. All genes were found concordantly dysregulated in RP depleted cells compared to scramble controls (Figure 2). These data imply that the expression patterns detected by microarray analysis are in good agreement with those detected by qRT-PCR and validate our conclusions.

4. Discussion

Many lines of evidence have underscored the pivotal role of p53 activation in the induction of cell death and proliferation block in cells and organisms subjected to ribosome stress [31,11-13]. The decrease in p53 activity by genetic means or using chemical inhibitors has proven useful to attenuate the proapoptotic phenotype of these models. However, p53 inhibitors cannot be used in the therapy of patients with DBA because they would drastically increase

their cancer risk. The identification of p53-independent pathways that are induced by ribosome stress may suggest new druggable steps that could be modulated to reduce the phenotypic consequences of ribosomal protein haploinsufficiency.

The aim of our work was to identify the p53-independent cellular processes that are altered during ribosome stress due to deficiency of DBA RPs and are erythroid-specific. To this aim we have used human TF1 cell lines that were silenced for the three RPs that are most commonly mutated in DBA patients, i.e. RPS19, RPL5 or RPL11. In fact, TF1 cells carry deleterious mutations on both p53 alleles, which abolish p53 function, as shown by sequencing and functional studies.

To search for impaired processes we have intercepted the transcriptomes of the three TF1 cell lines using Ranking-PCA. We identified genes involved in cell proliferation and apoptosis, in agreement with a previous study that showed abnormal levels of apoptosis related proteins in TF1 cells downregulated for RPS19 [30]. We detected the upregulation of PYCARD, a transcript encoding a proapoptotic protein that triggers the activation of caspases [32]. Overexpression of Pycard in mouse inhibits the proliferation of erythroid cells, promotes their apoptosis, and interferes with their terminal differentiation [33]. Abnormal expression of genes related to apoptosis was also reported in bone marrow $CD34^+$ cells isolated from three DBA patients with mutations in RPS19 and in remission from the disease [34], and in a previous study by our group focused on unraveling the gene expression alterations in fibroblasts isolated from DBA patients with RPS19 mutations [20].

Moreover, a large cluster of significantly underexpressed RPs was described in these two reports [20,34]. On the contrary, both the present study and a previous one which examined RPS19-deficient TF1 cells showed normal levels of RP mRNAs, with the exception of RPL3 [29, Table S1]. This lack of congruence might be explained by the presence or absence of wt p53 in primary cells and TF1 model, respectively. In fact, it is know that p53 can inhibit mTORC1 [35], which mediates the transcription of RP genes [36].

The expression of genes involved in erythroid maturation is increased, in particular, erythropoietin receptor (EPOR), transferrin receptor (TFRC), CDKN2A, that encodes for p16, whose transcriptional upregulation in progenitor cells promotes differentiation [37], and HOXB2, a target of the erythroid transcription factor GATA1 [38].

Interestingly, enrichment of genes involved in hematopoiesis and cell redox homeostasis was observed. Our study shows a downregulation of certain genes that participate in the protection against oxidative stress, in particular superoxide dismutase 2 (SOD2) and thioredoxin reductase 1 (TXNRD1) in cells depleted of RPs. A reduced expression of SOD2 was observed

also in RPL11-deficient zebrafish [39]. These results indicate that cells depleted of RPs may have an enhanced sensitivity to oxidative stress. The same phenomenon has been suggested for two other bone marrow failure syndromes, i.e. Fanconi Anemia (FA) and Shwachman-Diamond Syndrome (SDS). This sensitivity may lead to increased apoptosis and decreased cell growth [40-42].

Finally, we found dysregulation of clusters of genes involved in amino acid metabolism and lipid metabolism. Downregulation of genes involved in biosynthetic processes has been reported also in zebrafish with a RPL11 deficiency [39].

All these data show that when a RP is defective there is a set of biological functions/ molecular processes that are affected in different types of human cells, either primary cells from DBA patients or experimental models. The increased destruction of erythroid progenitors observed in patients with DBA may be due to the cumulative effects of p53-dependent and -independent pathways. Cells that undergo ribosome stress alter the expression profile of a set of genes, which are consistent with the pro-apoptotic and hypo-proliferative phenotype. Further studies are needed to ascertain whether antioxidant treatment may relieve the DBA phenotype in vitro.

Conflict of interest statement

The authors declare no conflicts of interest.

Acknowledgements

This work was funded from grants from Istituto Piemontese per la ricerca sulla Anemia di Diamond-Blackfan and PRIN (to ID and UR), Diamond Blackfan Anemia Foundation, Telethon onlus and ENERCA (to ID), Cariplo 2011-0554 (to ID and AR), Regione Piemonte Ricerca Sanitaria Finalizzata (to UR).We thank the Daniella Maria Arturi Foundation for supporting communication among DBA researchers.

References

[1] Draptchinskaia N, Gustavsson P, Andersson B, Pettersson M, Willig TN, et al. (1999) The gene encoding ribosomal protein S19 is mutated in Diamond-Blackfan anaemia. Nat Genet 21: 169-175.

[2] Vlachos A, Ball S, Dahl N, Alter BP, Sheth S, et al. (2008) Diagnosing and treating Diamond Blackfan anaemia: results of an international clinical consensus conference. Br J Haematol 142: 859-76. doi: 10.1111/j.1365-2141.2008.07269.x

[3] Quarello P, Garelli E, Carando A, Brusco A, Calabrese R, et al. (2010) Diamond-Blackfan anemia: genotype-phenotype correlation in Italian patients with RPL5 and RPL11 mutations. Haematologica 95: 206-13. doi: 10.3324/haematol.2009.011783.

[4] Boria I, Garelli E, Gazda HT, Aspesi A, Quarello P, et al. (2010) The ribosomal basis of Diamond-Blackfan Anemia: mutation and database update. Hum Mutat 31: 1269-79. doi: 10.1002/humu.21383.

[5] Gazda HT, Preti M, Sheen MR, O'Donohue MF, Vlachos A, et al. (2012) Frameshift mutation in p53 regulator RPL26 is associated with multiple physical abnormalities and a specific pre-ribosomal RNA processing defect in diamond-blackfan anemia. Hum Mutat 33: 1037-44. doi: 10.1002/humu.22081.

[6] Landowski M, O'Donohue MF, Buros C, Ghazvinian R, Montel-Lehry N, et al. (2013) Novel deletion of RPL15 identified by array-comparative genomic hybridization in Diamond-Blackfan anemia. Hum Genet 132 : 1265-74. doi: 10.1007/s00439-013-1326-z.

[7] Narla A, Ebert BL. (2010) Ribosomopathies: human disorders of ribosome dysfunction. Blood 115: 3196-205.doi: 10.1182/blood-2009-10-178129.

[8] Freed EF, Bleichert F, Dutca LM, Baserga SJ. (2010) When ribosomes go bad: diseases of ribosome biogenesis. Mol Biosyst 6: 481-93.doi: 10.1039/b919670f.

[9] Kongsuwan K, Yu Q, Vincent A, Frisardi MC, Rosbash M, et al. (1985) A Drosophila Minute gene encodes a ribosomal protein. Nature 317: 555-8.

[10] Miller L, Gurdon JB. (1970) Mutations affecting the size of the nucleolus in Xenopus leavis. Nature 227: 1108-10.

[11] Danilova N, Sakamoto KM, Lin S. (2008) Ribosomal protein S19 deficiency in zebrafish leads to developmental abnormalities and defective erythropoiesis through activation of p53 protein family. Blood 112: 5228-37. doi: 10.1182/blood-2008-01-132290.

[12] McGowan KA, Li JZ, Park CY, Beaudry V, Tabor HK, et al. (2008) Ribosomal mutations cause p53-mediated dark skin and pleiotropic effects. Nat Genet 40: 963-70. doi: 10.1038/ng.188.

[13] Dutt S, Narla A, Lin K, Mullally A, Abayasekara N, et al. (2011) Haploinsufficiency for ribosomal protein genes causes selective activation of p53 in human erythroid progenitor cells. Blood 117: 2567-76.doi: 10.1182/blood-2010-07-295238.

[14] Torihara H, Uechi T, Chakraborty A, Shinya M, Sakai N, et al. (2011) Erythropoiesis failure due to RPS19 deficiency is independent of an activated Tp53 response in a zebrafish model of Diamond-Blackfan anaemia. Br J Haematol 152: 648-54. doi: 10.1111/j.1365-2141.2010.08535.x.

[15] Moniz H, Gastou M, Leblanc T, Hurtaud C, Crétien A, et al. (2012) Primary hematopoietic cells from DBA patients with mutations in RPL11 and RPS19 genes exhibit distinct erythroid phenotype in vitro. Cell Death Dis 3: e356. doi: 10.1038/cddis.2012.88.

[16] Miyake K, Flygare J, Kiefer T, Utsugisawa T, Richter J, et al. (2005) Development of cellular models for ribosomal protein S19 (RPS19)-deficient diamond-blackfan anemia using inducible expression of siRNA against RPS19. Mol Ther 11: 627-37.

[17] Taulli R, Accornero P, Follenzi A, Mangano T, Morotti A, et al. (2005) RNAi technology and lentiviral delivery as a powerful tool to suppress Tpr-Met-mediated tumorigenesis. Cancer Gene Ther 12: 456-63.

[18] Follenzi A, Ailles LE, Bakovic S, Geuna M, Naldini L. (2000) Gene transfer by lentiviral vectors is limited by nuclear translocation and rescued by HIV-1 pol sequences. Nat Genet 25: 217-22.

[19] Andrews NC, Faller DV. (1991) A rapid micropreparation technique for extraction of DNA-binding proteins from limiting numbers of mammalian cells. Nucleic Acids Res 19: 2499.

[20] Avondo F, Roncaglia P, Crescenzio N, Krmac H, Garelli E, et al. (2009) Fibroblasts from patients with Diamond-Blackfan anaemia show abnormal expression of genes involved in protein synthesis, amino acid metabolism and cancer. BMC Genomics 10: 442. doi: 10.1186/1471-2164-10-442.

[21] Massart DL, Vanderginste BGM, Buydens LMC, De Jong S, Lewi PJ, Smeyers-Verbeke J. (1998) Handbook of chemometrics and qualimetrics: part A. Elsevier, Amsterdam.

[22] Massart DL, Vanderginste BGM, Deming SM, Michotte Y, Kaufman L. (1988) Chemometrics: a textbook. Elsevier, Amsterdam.

[23] Marengo E, Robotti E, Bobba M, Gosetti F. (2010) The principle of exhaustiveness versus the principle of parsimony: a new approach for the identification of biomarkers from proteomic spot volume datasets based on Principal Component Analysis. Anal Bioanal Chem 397: 25-41. doi: 10.1007/s00216-009-3390-8.

[24] Robotti E, Demartini M, Gosetti F, Calabrese G, Marengo E. (2011) Development of a classification and ranking method for the identification of possible biomarkers in proteomics based on Principal Component Analysis and variable selection procedures. Molecular Biosyst 7: 677-686. doi: 10.1039/c0mb00124d.

[25] Polati R, Menini M, Robotti E, Millioni R, Marengo E, et al. (2012) Proteomic changes involved in tenderization of bovine Longissimus dorsi muscle during prolonged ageing. Food Chem 135: 2052-69. doi: 10.1016/j.foodchem.2012.06.093.

[26] Marengo E, Robotti E, Bobba M, Milli A, Campostrini N, et al. (2008) Application of partial least squares discriminant analysis and variable selection procedures: a 2D-PAGE proteomic study. Anal Bioanal Chem 390: 1327-42.doi: 10.1007/s00216-008-1837-y.

[27] Livak KJ, Schmittgen TD. (2001) Analysis of relative gene expression data using real-time quantitative PCR and the 2(-Delta Delta C(T)) Method Methods 25: 402-8.

[28] Flygare J, Aspesi A, Bailey JC, Miyake K, Caffrey JM, et al. (2007) Human RPS19, the gene mutated in Diamond-Blackfan anemia, encodes a ribosomal protein required for the maturation of 40S ribosomal subunits. Blood 109: 980-6.

[29] Badhai J, Fröjmark AS, Razzaghian HR, Davey E, Schuster J, Dahl N. (2009) Posttranscriptional down-regulation of small ribosomal subunit proteins correlates with reduction of 18S rRNA in RPS19 deficiency. FEBS Lett 583: 2049-53. doi: 10.1016/j.febslet.2009.05.023.

[30] Miyake K, Utsugisawa T, Flygare J, Kiefer T, Hamaguchi I, et al. (2008) Ribosomal protein S19 deficiency leads to reduced proliferation and increased apoptosis but does not affect terminal erythroid differentiation in a cell line model of Diamond-Blackfan anemia. Stem Cells 26: 323-9.

[31] Ellis SR, Gleizes PE. (2011) Diamond Blackfan anemia: ribosomal proteins going rogue. Semin Hematol 48: 89-96. doi: 10.1053/j.seminhematol.2011.

[32] Ohtsuka T, Ryu H, Minamishima YA, Macip S, Sagara J, et al. (2004) ASC is a Bax adaptor and regulates the p53–Bax mitochondrial apoptosis pathway. Nat Cell Biol 6: 121-128.

[33] Hu W, Yuan B, Flygare J, Lodish HF. (2011) Long noncoding RNA-mediated anti-apoptotic activity in murine erythroid terminal differentiation. Genes Dev 25: 2573-8. doi: 10.1101/gad.178780.111.

[34] Gazda HT, Kho AT, Sanoudou D, Zaucha JM, Kohane IS, et al. (2006) Defective ribosomal protein gene expression alters transcription, translation, apoptosis, and oncogenic pathways in Diamond-Blackfan anemia. Stem Cells 24: 2034-44.

[35] Hasty P, Sharp ZD, Curiel TJ, Campisi J. (2013) mTORC1 and p53: clash of the gods? Cell Cycle 12: 20-5.

[36] Xiao L, Grove A. (2009) Coordination of Ribosomal Protein and Ribosomal RNA Gene Expression in Response to TOR Signaling. Curr Genomics 10: 198-205. doi: 10.2174/138920209788185261.

[37] Minami R, Muta K, Umemura T, Motomura S, Abe Y, et al. (2003) p16INK4a induces differentiation and apoptosis in erythroid lineage cells. Exp Hematol 31: 355–362.

[38] Vieille-Grosjean I, Huber P. (1995) Transcription factor GATA-1 regulates human HOXB2 gene expression in erythroid cells. J Biol Chem 270: 4544-50.

[39] Danilova N, Sakamoto KM, Lin S. (2011) Ribosomal protein L11 mutation in zebrafish leads to haematopoietic and metabolic defects. Br J Haematol 152: 217-28. doi: 10.1111/j.1365-2141.2010.08396.x.

[40] Mukhopadhyay SS, Leung KS, Hicks MJ, Hastings PJ, Youssoufian H, Plon SE. (2006) Defective mitochondrial peroxiredoxin-3 results in sensitivity to oxidative stress in Fanconi anemia. J Cell Biol 175: 225-35.

[41] Bogliolo M, Cabre O, Callen E, Castillo V, Creus A, et al. (2002) The Fanconi anaemia genome stability and tumour suppressor network. Mutagenesis 17: 529-538

[42] Ambekar C, Das B, Yeger H, Dror Y. (2010) SBDS-deficiency results in deregulation of reactive oxygen species leading to increased cell death and decreased cell growth. Pediatr Blood Cancer 55: 1138-44. doi: 10.1002/pbc.22700.

Figure Legends

Figure 1. PCA on RP deficient TF1 cells.

Score plot of the first two PCs calculated on the dataset containing TF1 cell lines downregulated for RPS19, RPL5 and RPL11. Samples are separated along PC_1 in controls (positive scores; empty circles) and pathological (negative scores; full circles).

Labels: **S19** = TF1 downregulated for RPS19; **CS** = scramble controls for RPS19; **L5** and **L11** = TF1 downregulated for RPL5 and RPL11; **CL =** scramble controls for RPL5 and RPL11.

Figure 2. Validation of microarray results by qRT-PCR.

Fold change of the expression of eight altered genes in RP depleted TF1 cells compared to scramble controls (set equal to 1). Data were obtained by qRT-PCR measurement and normalized to GAPDH or β-actin levels. * p value< 0.05 ° p< 0.01 ‡ p < 0.001

Table(s)

Table 1. Genes included in the PC1 were annotated using Gene Ontology biological process.

Term	Count	pValue	Genes
GO:0008610~lipid biosynthetic process	19	4.12E-08	FCER1A, EBP, SPTLC2, SCD, HMGCS1, FDXR, LTC4S, SC4MOL, FDFT1, FAR2, PIGK, PIGF, LPCAT1, SH3GLB1, DHCR7, PBX1, LTA4H, SC5DL, NSDHL
GO:0016053~organic acid biosynthetic process	12	1.99E-06	FCER1A, C8ORF62, SCD, ASNS, LTC4S, SC4MOL, CTH, GOT1, SH3GLB1, PHGDH, LTA4H, PSAT1, SC5DL
GO:0016126~sterol biosynthetic process	7	2.84E-06	EBP, DHCR7, HMGCS1, SC5DL, FDFT1, SC4MOL, NSDHL
GO:0006694~steroid biosynthetic process	9	6.53E-06	EBP, DHCR7, HMGCS1, FDXR, PBX1, SC5DL, FDFT1, SC4MOL, NSDHL
GO:0043436~oxoacid metabolic process	21	7.41E-06	FCER1A, C8ORF62, SCD, CS, GARS, EPRS, ASNS, LTC4S, PCK2, SLC7A5, SC4MOL, MTHFD2, CTH, GOT1, SH3GLB1, GFPT1, PHGDH, LTA4H, DDAH2, PSAT1, SC5DL, ALDH9A1
GO:0044106~cellular amine metabolic process	14	5.98E-05	C8ORF62, GARS, EPRS, ASNS, SLC7A5, CTH, GOT1, GFPT1, PHGDH, SMOX, PAFAH1B1, AMD1, PSAT1, DDAH2, ALDH9A1
GO:0044255~cellular lipid metabolic process	16	0.0013	FCER1A, SPTLC2, SCD, HMGCS1, PIP5K1B, LTC4S, SC4MOL, FDFT1, PIGK, PIGF, LPCAT1, SH3GLB1, LTA4H, PAFAH1B1, SC5DL, NR1H3
GO:0006520~cellular amino acid metabolic process	10	0.0014	C8ORF62, CTH, GOT1, GFPT1, GARS, PHGDH, EPRS, ASNS, PSAT1, DDAH2, SLC7A5
GO:0006633~fatty acid biosynthetic process	6	0.0023	FCER1A, SCD, LTA4H, LTC4S, SC5DL, SC4MOL
GO:0009309~amine biosynthetic process	6	0.0026	C8ORF62, CTH, GOT1, PHGDH, ASNS, PSAT1, AMD1
GO:0008202~steroid metabolic process	9	0.0026	EBP, DHCR7, HMGCS1, FDXR, PBX1, SC5DL, FDFT1, SC4MOL, NSDHL
GO:0006575~cellular amino acid derivative metabolic process	8	0.0034	CTH, PHGDH, PAFAH1B1, SMOX, AMD1, ALDH9A1, SOD2, GLRX2
GO:0008203~cholesterol metabolic process	6	0.0044	EBP, DHCR7, HMGCS1, FDXR, FDFT1, NSDHL
GO:0010243~response to organic nitrogen	5	0.0063	ALDOC, HMGCS1, ASNS, PPP3CA, DDIT3
GO:0019725~cellular homeostasis	13	0.0086	CLNS1A, FTH1, DDIT3, SOD2, GLRX2, LOC100130902, TFRC, FTHL3, FTHL16, EPOR, TXNRD1, PPP3CA, SH3BGRL3, SLC39A4, EIF2B4, FTHL20, ADD1
GO:0008285~negative regulation of cell proliferation	11	0.0099	CEBPA, LST1, FTH1, SOD2, MAGED1, CTH, CDKN2A, FTHL3, BTG3, MYO16, FTHL16, ASPH, EMP3, FTHL20
GO:0006915~apoptosis	15	0.0109	DPF2, ALDOC, LGALS1, SOD2, TRADD, GLRX2, MAGED1, CDKN2A, SHARPIN, SH3GLB1, BRE, PYCARD, AVEN, APAF1, TRAF3
GO:0006259~DNA metabolic process	13	0.0156	GLRX2, MCM6, SOD2, TFAM, CDKN2A, CSNK1D, RRM1, MUS81, BRE, APAF1, OGG1, TRIP13, RBMS1
GO:0043450~alkene biosynthetic process	3	0.0204	FCER1A, LTA4H, LTC4S
GO:0006644~phospholipid metabolic process	7	0.0241	PIGK, PIGF, LPCAT1, SH3GLB1, PIP5K1B, PAFAH1B1, FDFT1
GO:0006691~leukotriene metabolic process	3	0.0269	FCER1A, LTA4H, LTC4S
GO:0006732~coenzyme metabolic process	6	0.0338	MTHFD2, CTH, PANK3, CS, SOD2, GLRX2
GO:0021570~rhombomere 4 development	2	0.0347	HOXA1, HOXB2
GO:0006461~protein complex assembly	12	0.0348	TFAM, CTH, TSPAN4, ALDOC, IRF7, RRM1, EPRS, TUBA4A, HSPA4, WIPF1, SURF1, SOD2
GO:0030262~apoptotic nuclear changes	3	0.0367	CDKN2A, SHARPIN, APAF1
GO:0044271~nitrogen compound biosynthetic process	9	0.0371	CEBPA, C8ORF62, CTH, GOT1, RRM1, PHGDH, ASNS, PSAT1, DDAH2, AMD1
GO:0045454~cell redox homeostasis	4	0.0374	LOC100130902, TXNRD1, SH3BGRL3, DDIT3, GLRX2
GO:0046486~glycerolipid metabolic process	6	0.0416	PIGK, PIGF, SH3GLB1, PIP5K1B, PAFAH1B1, NR1H3
GO:0006749~glutathione metabolic process	3	0.0421	CTH, SOD2, GLRX2
GO:0021610~facial nerve morphogenesis	2	0.0460	HOXA1, HOXB2
GO:0021569~rhombomere 3 development	2	0.0460	HOXA1, HOXB2
GO:0021604~cranial nerve structural organization	2	0.0460	HOXA1, HOXB2
GO:0021612~facial nerve structural organization	2	0.0460	HOXA1, HOXB2
GO:0009888~tissue development	14	0.0479	S100A4, TRIM15, LOC100130902, CDKN2A, HOXB2, SHARPIN, GFPT1, SEMA3C, EPOR, TXNRD1, PBX1, APAF1, CA2, PPP3CA, NSDHL
GO:0006650~glycerophospholipid metabolic process	5	0.0496	PIGK, PIGF, SH3GLB1, PIP5K1B, PAFAH1B1

Table(s)

Table 2. Genes included in the PC1 were annotated using Panther.

Term	Count	PValue	Genes
BP00297:Other steroid metabolism	3	0.0048	SC5DL, FDFT1, SC4MOL
BP00026:Cholesterol metabolism	5	0.0054	EBP, HMGCS1, FDFT1, SC4MOL, NSDHL
BP00284:Hematopoiesis	5	0.0063	CEBPA, STAP1, EPOR, PBX1, TRIM15
BP00013:Amino acid metabolism	8	0.0085	C8ORF62, CTH, GOT1, SLC7A1, CS, PHGDH, ASNS, PSAT1, SLC7A5
BP00014:Amino acid biosynthesis	4	0.0122	C8ORF62, CS, PHGDH, ASNS, PSAT1
BP00295:Steroid metabolism	6	0.0314	EBP, HMGCS1, SC5DL, FDFT1, SC4MOL, NSDHL

1

Figure(s)
Click here to download high resolution image

FIGURE 1

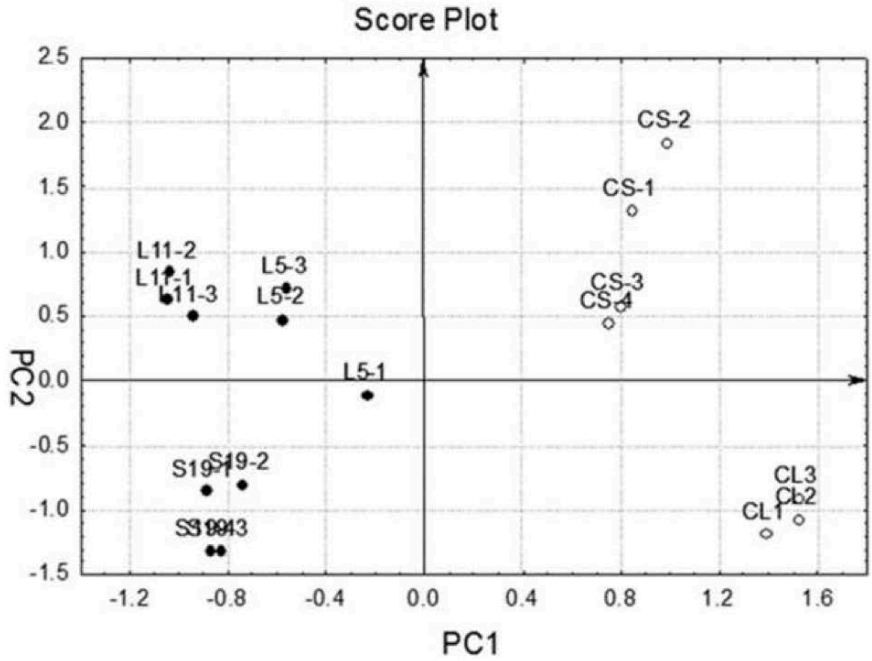

Figure(s)
Click here to download high resolution image

FIGURE 2

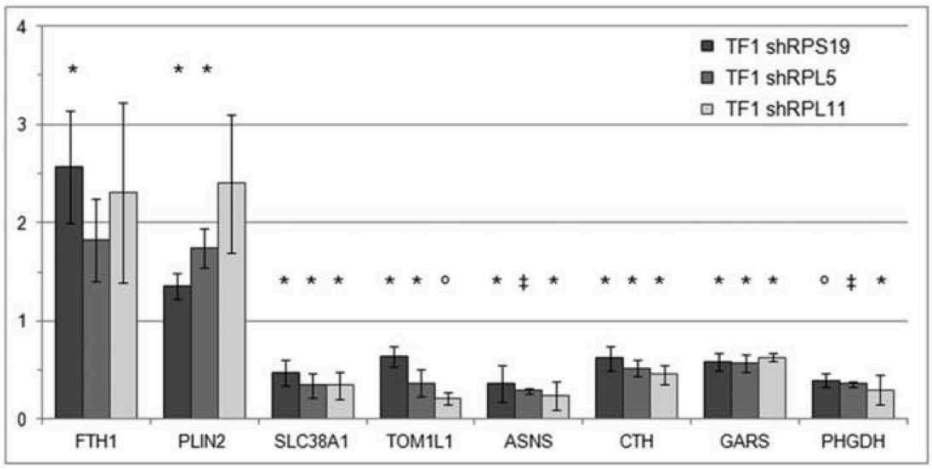

SUPPLEMENTARY MATERIAL

Figure S1. p53 in TF1 cells.

A. Sequencing of the cDNA obtained from TF1 cells reveals a c.752delT frameshift mutation in p53. Wild type p53 from $CD34^+$ primary cells is shown as a control.

B. TF1 cells express a mutated p53 protein. Downregulation of RPS19 increases p53 level. A lysate from U2Os cells is shown as a full-length p53 control.

C. Nuclear and cytoplasmic extracts were obtained from shSCR and shRPS19 TF1 cells. Immunoblot showed that p53 accumulates in the cytoplasm in these cells, especially when RPS19 is downregulated. Nu nuclear extract; Cy cytosolic extract.

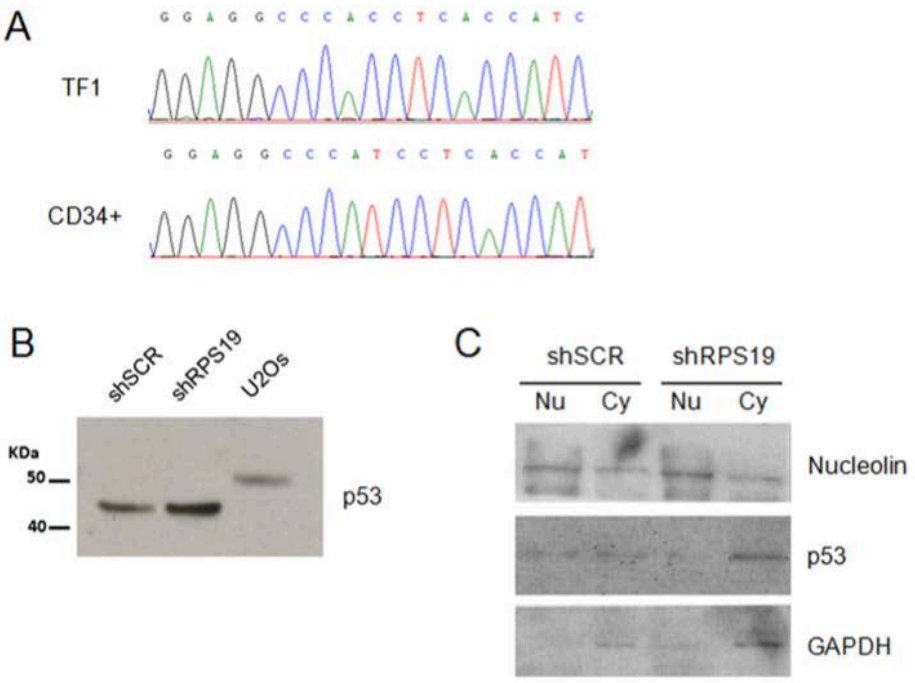

Figure S2. RP silencing in TF1 cells.

Western blot showing the downregulation of RPS19, RPL5 and RPL11 in TF1 cells compared to scramble controls.

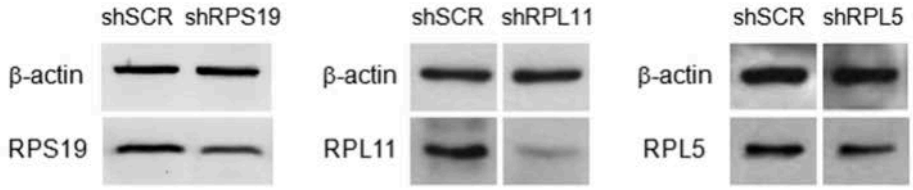

Table S1. Genes describing the first PC calculated on the dataset containing TF1 cell lines downregulated for RPS19, RPL5 or RPL11. FC: fold change values of the genes differentially expressed between silenced cells and scramble controls.

	Probe ID	Gene Name	Gene Symbol	FC S19	FC L5	FC L11
1	217809_at	basic leucine zipper and W2 domains 2	BZW2	0.81	0.84	0.8
2	220059_at	signal transducing adaptor family member 1	STAP1	1.4	1.74	1.76
3	211628_x_at	ferritin, heavy polypeptide pseudogene 1	FTHL5	1.93	1.71	1.93
4	208693_s_at	glycyl-tRNA synthetase	Gars	0.6	0.68	0.69
5	221524_s_at	Ras-related GTP binding D	Rragd	0.66	0.6	0.58
6	200748_s_at	ferritin, heavy polypeptide 1; ferritin, heavy polypeptide-like 16; similar to ferritin, heavy polypeptide 1; ferritin, heavy polypeptide-like 3 pseudogene	FTHL3,FTHL16, FTHL20, FTH1	2.3	1.92	1.66
7	203186_s_at	S100 calcium binding protein A4	S100a4	1.37	1.51	1.62
8	204485_s_at	target of myb1 (chicken)-like 1	TOM1L1	0.56	0.46	0.38
9	201266_at	thioredoxin reductase 1; hypothetical LOC100130902	LOC100130902, TXNRD1	0.71	0.58	0.55
10	201105_at	lectin, galactoside-binding, soluble, 1	LGALS1	1.64	1.28	1.42
11	212877_at	kinesin light chain 1	KLC1	0.6	0.6	0.45
12	218433_at	pantothenate kinase 3	PANK3	0.59	0.58	0.62
13	206480_at	leukotriene C4 synthase	LTC4S	1.8	2.85	2.99
14	203920_at	nuclear receptor subfamily 1, group H, member 3	NR1H3	1.95	1.42	1.3
15	209122_at	adipose differentiation-related protein	PLIN2	1.59	1.79	2.33
16	203882_at	interferon regulatory factor 9	IRF9	1.85	2.94	2.47
17	214909_s_at	dimethylarginine dimethylaminohydrolase 2	ddah2	1.59	1.34	1.54
18	208813_at	glutamic-oxaloacetic transaminase 1, soluble (aspartate aminotransferase 1)	GOT1	0.63	0.5	0.43
19	200809_x_at	ribosomal protein L12 pseudogene 2; ribosomal protein L12 pseudogene 32; ribosomal protein L12 pseudogene 35; ribosomal protein L12 pseudogene 19; ribosomal protein L12 pseudogene 6; ribosomal protein L12; ribosomal protein L12 pseudogene 14	RPL12P6,RPL12P32, RPL12P14, rpl12, RPL12P2, RPL12P35, RPL12P19	0.86	0.85	0.77
20	218237_s_at	solute carrier family 38, member 1	SLC38A1	0.38	0.46	0.41
21	205277_at	PR domain containing 2, with ZNF domain	PRDM2	1.43	1.54	1.95
22	203661_s_at	tropomodulin 1	TMOD1	1.25	1.38	1.32
23	212281_s_at	transmembrane protein 97	TMEM97	0.6	0.73	0.59

24	202721_s_at	glutamine-fructose-6-phosphate transaminase 1	GFPT1	0.77	0.61	0.54
25	211734_s_at	Fc fragment of IgE, high affinity I, receptor for; alpha polypeptide	FCER1A	1.82	1.57	1.97
26	220892_s_at	chromosome 8 open reading frame 62; phosphoserine aminotransferase 1	C8orf62 PSAT1	0.29	0.46	0.28
27	204859_s_at	apoptotic peptidase activating factor 1	Apaf1	0.74	0.63	0.57
28	203127_s_at	serine palmitoyltransferase, long chain base subunit 2	Sptlc2	0.68	0.64	0.49
29	211566_x_at	brain and reproductive organ-expressed (TNFRSF1A modulator)	BRE	1.36	1.9	2.09
30	221666_s_at	PYD and CARD domain containing	pycard	1.65	1.4	1.37
31	205077_s_at	phosphatidylinositol glycan anchor biosynthesis, class F	pigf	1.73	1.48	1.79
32	202616_s_at	methyl CpG binding protein 2 (Rett syndrome)	mecp2	1.59	1.77	2.11
33	207039_at	cyclin-dependent kinase inhibitor 2A (melanoma, p16, inhibits CDK4)	CDKN2A	1.29	1.36	1.51
34	203416_at	CD53 molecule	Cd53	1.43	1.55	1.71
35	220127_s_at	F-box and leucine-rich repeat protein 12	fbxl12	1.27	1.25	1.32
36	219412_at	RAB38, member RAS oncogene family	RAB38	0.74	0.83	0.79
37	201761_at	methylenetetrahydrofolate dehydrogenase (NADP+ dependent) 2, methenyltetrahydrofolate cyclohydrolase	mthfd2	0.61	0.66	0.61
38	203355_s_at	pleckstrin and Sec7 domain containing 3	PSD3	0.57	0.43	0.45
39	209263_x_at	tetraspanin 4	tspan4	1.45	1.61	1.42
40	215127_s_at	RNA binding motif, single stranded interacting protein 1	RBMS1	1.69	1.21	1.35
41	1729_at	TNFRSF1A-associated via death domain	TRADD	1.28	1.31	1.34
42	219247_s_at	zinc finger, DHHC-type containing 14	Zdhhc14	1.75	1.56	1.72
43	209644_x_at	cyclin-dependent kinase inhibitor 2A (melanoma, p16, inhibits CDK4)	CDKN2A	1.14	1.17	1.18
44	205047_s_at	asparagine synthetase	asnS	0.23	0.28	0.18
45	205632_s_at	phosphatidylinositol-4-phosphate 5-kinase, type I, beta	Pip5k1b	1.45	1.33	1.49
46	221750_at	3-hydroxy-3-methylglutaryl-Coenzyme A synthase 1 (soluble)	HMGCS1	0.5	0.45	0.34
47	31845_at	E74-like factor 4 (ets domain transcription factor)	Elf4	1.41	1.4	1.84
48	220560_at	chromosome 11 open reading frame 21	C11orf21	1.41	2.07	1.87
49	218303_x_at	lysine-rich coiled-coil 1	KRCC1	1.61	1.53	1.49
50	219092_s_at	inositol 1,3,4,5,6-pentakisphosphate 2-kinase	IPPK	0.89	0.71	0.73
51	221269_s_at	SH3 domain binding glutamic acid-rich protein like 3	SH3BGRL3	1.55	1.57	2.25
52	202022_at	aldolase C, fructose-bisphosphate	aldoc	0.64	0.48	0.35
53	217127_at	cystathionase (cystathionine gamma-lyase)	CTH	0.33	0.47	0.4
54	212645_x_at	brain and reproductive organ-expressed (TNFRSF1A modulator)	BRE	1.39	1.69	2.07
55	210278_s_at	adaptor-related protein complex 4, sigma 1 subunit	ap4s1	1.55	1.95	1.95
56	209135_at	aspartate beta-hydroxylase	asph	0.66	0.48	0.45
57	203057_s_at	PR domain containing 2, with ZNF domain	PRDM2	0.8	0.63	0.58
58	209301_at	carbonic anhydrase II	CA2	0.31	0.27	0.09
59	218859_s_at	similar to ABT1-associated protein; ESF1, nucleolar pre-rRNA processing protein, homolog (S. cerevisiae)	ESF1	0.62	0.51	0.47
60	205822_s_at	3-hydroxy-3-methylglutaryl-Coenzyme A synthase 1 (soluble)	HMGCS1	0.41	0.28	0.15
61	204033_at	thyroid hormone receptor interactor 13	Trip13	0.65	0.6	0.48
62	219366_at	apoptosis, caspase activation inhibitor	AVEN	1.24	1.44	1.28
63	214271_x_at	ribosomal protein L12 pseudogene 2; ribosomal protein L12 pseudogene 32; ribosomal protein L12 pseudogene 35; ribosomal protein L12 pseudogene 19; ribosomal protein L12 pseudogene 6; ribosomal protein L12; ribosomal protein L12 pseudogene 14	RPL12P6 RPL12P32 RPL12P14 rpl12 RPL12P2 RPL12P35 RPL12P19	0.86	0.86	0.83
64	212886_at	coiled-coil domain containing 69	ccdc69	1.57	1.42	1.87
65	212333_at	family with sequence similarity 98, member A	Fam98a	0.68	0.49	0.47
66	205453_at	homeobox B2	HOXB2	1.24	1.23	1.19
67	212282_at	transmembrane protein 97	TMEM97	0.65	0.72	0.54
68	200842_s_at	glutamyl-prolyl-tRNA synthetase	eprs	0.68	0.48	0.4
69	207917_at	nudix (nucleoside diphosphate linked moiety X)-type motif 13	Nudt13	0.63	0.71	0.59
70	218429_s_at	chromosome 19 open reading frame 66	c19orf66	1.7	1.32	1.66
71	205252_at	zinc finger protein 174	ZNF174	1.34	1.42	1.42
72	202722_s_at	glutamine-fructose-6-phosphate transaminase 1	GFPT1	0.63	0.47	0.41
73	208030_s_at	adducin 1 (alpha)	Add1	1.28	1.42	1.59
74	205760_s_at	8-oxoguanine DNA glycosylase	OGG1	1.56	1.9	2.16
75	212507_at	transmembrane protein 131	TMEM131	1.33	1.35	1.38
76	202847_at	phosphoenolpyruvate carboxykinase 2 (mitochondrial)	pck2	0.65	0.63	0.5
77	218463_s_at	MUS81 endonuclease homolog (S. cerevisiae)	MUS81	1.2	1.24	1.31
78	208660_at	citrate synthase	CS	0.83	0.76	0.77
79	204478_s_at	RAB interacting factor	Rabif	1.31	1.51	1.75
80	208774_at	casein kinase 1, delta	CSNK1D	1.33	1.63	1.87
81	215093_at	NAD(P) dependent steroid dehydrogenase-like	nsdhl	0.78	0.66	0.59
82	218076_s_at	Rho GTPase activating protein 17	arhgap17	0.82	0.7	0.68
83	201306_s_at	similar to Acidic leucine-rich nuclear phosphoprotein 32 family member B (PHAPI2 protein) (Silver-stainable protein SSP29) (Acidic protein rich in leucines); acidic (leucine-rich) nuclear phosphoprotein 32 family, member B	anp32b, LOC646791	0.72	0.89	0.84
84	215501_s_at	dual specificity phosphatase 10	Dusp10	1.41	1.32	1.28

85	209331_s_at	MYC associated factor X	MAX	1.47	1.21	1.29
86	202116_at	D4, zinc and double PHD fingers family 2	dpf2	1.31	1.8	2
87	205550_s_at	brain and reproductive organ-expressed (TNFRSF1A modulator)	BRE	1.4	1.84	2.3
88	202429_s_at	protein phosphatase 3 (formerly 2B), catalytic subunit, alpha isoform	ppp3ca	1.32	1.35	1.45
89	202262_x_at	dimethylarginine dimethylaminohydrolase 2	ddah2	1.65	1.37	1.52
90	208855_s_at	serine/threonine kinase 24 (STE20 homolog, yeast)	stk24	1.22	1.28	1.55
91	210277_at	adaptor-related protein complex 4, sigma 1 subunit	ap4s1	1.6	1.97	2.47
92	216999_at	erythropoietin receptor	EPOR	1.76	1.41	1.91
93	203789_s_at	sema domain, immunoglobulin domain (Ig), short basic domain, secreted, (semaphorin) 3C	SEMA3C	2.5	3.34	5.71
94	206085_s_at	cystathionase (cystathionine gamma-lyase)	CTH	0.3	0.53	0.3
95	208315_x_at	TNF receptor-associated factor 3	TRAF3	0.83	0.68	0.61
96	209486_at	UTP3, small subunit (SSU) processome component, homolog (S. cerevisiae)	UTP3	0.81	0.68	0.73
97	209549_s_at	deoxyguanosine kinase	Dguok	1.27	1.24	1.24
98	204951_at	ras homolog gene family, member H	Rhoh	1.38	2.85	3.43
99	202732_at	protein kinase (cAMP-dependent, catalytic) inhibitor gamma	PKIG	1.27	1.86	1.96
100	206833_s_at	acylphosphatase 2, muscle type	Acyp2	1.3	1.59	1.67
101	218079_s_at	gametogenetin binding protein 2	GGNBP2	1.27	1.26	1.52
102	213386_at	chromosome 9 open reading frame 125	c9orf125	0.67	0.67	0.59
103	219933_at	glutaredoxin 2	GLRX2	1.43	1.34	1.46
104	219215_s_at	solute carrier family 39 (zinc transporter), member 4	SLC39A4	1.23	1.51	1.73
105	205662_at	B9 protein domain 1	B9D1	0.78	0.58	0.53
106	208771_s_at	leukotriene A4 hydrolase	LTA4H	0.47	0.78	0.67
107	213292_s_at	sorting nexin 13	Snx13	0.7	0.62	0.47
108	215963_x_at	ribosomal protein L3 pseudogene 7	RPL3P7	0.68	0.88	0.73
109	214639_s_at	homeobox A1	hoxa1	1.84	1.83	1.85
110	212151_at	pre-B-cell leukemia homeobox 1	PBX1	1.41	1.55	2.01
111	204039_at	CCAAT/enhancer binding protein (C/EBP), alpha	CEBPA	0.64	0.64	0.5
112	203957_at	E2F transcription factor 6	e2f6	0.83	0.73	0.65
113	220153_at	ectonucleoside triphosphate diphosphohydrolase 7	ENTPD7	0.65	0.67	0.47
114	220615_s_at	fatty acyl CoA reductase 2	FAR2	0.71	0.5	0.45
115	205812_s_at	transmembrane emp24 protein transport domain containing 9	tmed9	0.89	0.75	0.72
116	212039_x_at	ribosomal protein L3; similar to 60S ribosomal protein L3 (L4)	RPL3 LOC653881	0.71	0.88	0.71
117	201196_s_at	adenosylmethionine decarboxylase 1	AMD1	0.74	0.61	0.6
118	210044_s_at	lymphoblastic leukemia derived sequence 1	Lyl1	1.26	1.57	1.56
119	221482_s_at	cAMP-regulated phosphoprotein 19 pseudogene; cAMP-regulated phosphoprotein, 19kDa	LOC646227 ARPP19 LOC643896	0.62	0.69	0.58
120	210357_s_at	spermine oxidase	SMOX	1.43	1.38	1.77
121	201930_at	minichromosome maintenance complex component 6	MCM6	0.6	0.77	0.59
122	202187_s_at	protein phosphatase 2, regulatory subunit B', alpha isoform	PPP2R5A	1.43	1.42	1.54
123	201305_x_at	similar to Acidic leucine-rich nuclear phosphoprotein 32 family member B (PHAPI2 protein) (Silver-stainable protein SSP29) (Acidic protein rich in leucines); acidic (leucine-rich) nuclear phosphoprotein 32 family, member B	anp32b, LOC646791	0.71	0.83	0.84
124	204122_at	TYRO protein tyrosine kinase binding protein	TYROBP	2.19	1.76	2.92
125	211423_s_at	sterol-C5-desaturase (ERG3 delta-5-desaturase homolog, S. cerevisiae)-like	SC5DL	0.64	0.48	0.35
126	220486_x_at	hypothetical protein LOC100130886		3	1.57	2.57
127	204634_at	NIMA (never in mitosis gene a)-related kinase 4	NEK4	0.7	0.54	0.47
128	207813_s_at	ferredoxin reductase	fdxr	0.73	0.5	0.37
129	202617_s_at	methyl CpG binding protein 2 (Rett syndrome)	mecp2	1.67	1.75	2.66
130	203729_at	epithelial membrane protein 3	emp3	1.38	1.46	1.94
131	211162_x_at	stearoyl-CoA desaturase (delta-9-desaturase)	scd	0.62	0.41	0.37
132	200816_s_at	platelet-activating factor acetylhydrolase, isoform Ib, subunit 1 (45kDa)	Pafah1b1	1.36	1.37	1.48
133	219347_at	nudix (nucleoside diphosphate linked moiety X)-type motif 15	NUDT15	0.7	0.69	0.63
134	211581_x_at	leukocyte specific transcript 1	Lst1	1.29	1.41	1.64
135	209014_at	melanoma antigen family D, 1	MAGED1	0.66	0.46	0.38
136	208691_at	transferrin receptor (p90, CD71)	TFRC	1.17	1.21	1.26
137	215537_x_at	dimethylarginine dimethylaminohydrolase 2	ddah2	1.61	1.37	1.56
138	208839_s_at	cullin-associated and neddylation-dissociated 1	CAND1	0.83	0.65	0.59
139	200843_s_at	glutamyl-prolyl-tRNA synthetase	eprs	0.72	0.7	0.54
140	209413_at	UDP-Gal:betaGlcNAc beta 1,4- galactosyltransferase, polypeptide 2	b4galt2	0.71	0.86	0.8
141	201791_s_at	7-dehydrocholesterol reductase	DHCR7	0.69	0.39	0.28
142	212740_at	phosphoinositide-3-kinase, regulatory subunit 4	PIK3R4	0.66	0.72	0.83
143	209820_s_at	transducin (beta)-like 3	tbl3	0.85	0.79	0.73
144	201818_at	lysophosphatidylcholine acyltransferase 1	lpcat1	0.67	0.38	0.25
145	205078_at	phosphatidylinositol glycan anchor biosynthesis, class F	pigf	2	1.38	1.42
146	201612_at	aldehyde dehydrogenase 9 family, member A1	ALDH9A1	0.8	0.78	0.85
147	209382_at	polymerase (RNA) III (DNA directed) polypeptide C (62kD)	POLR3C	1.4	1.19	1.3

148	202664_at	WAS/WASL interacting protein family, member 1	WIPF1	1.42	1.4	1.57
149	211016_x_at	heat shock 70kDa protein 4	HSPA4	0.87	0.59	0.57
150	203044_at	chondroitin sulfate synthase 1	CHSY1	1.61	1.37	2.04
151	221529_s_at	plasmalemma vesicle associated protein	Plvap	2.23	1.98	2.81
152	36742_at	tripartite motif-containing 15	TRIM15	0.81	0.65	0.63
153	203846_at	tripartite motif-containing 32	trim32	0.76	0.49	0.44
154	212825_at	PAX interacting (with transcription-activation domain) protein 1	PAXIP1	0.68	0.48	0.47
155	205786_s_at	integrin, alpha M (complement component 3 receptor 3 subunit)	ITGAM	1.82	1.92	1.91
156	209143_s_at	chloride channel, nucleotide-sensitive, 1A	CLNS1A	0.71	0.82	0.68
157	212509_s_at	matrix-remodelling associated 7	mxra7	0.77	0.74	0.63
158	209707_at	phosphatidylinositol glycan anchor biosynthesis, class K	PIGK	2.12	1.74	2.88
159	218168_s_at	chaperone, ABC1 activity of bc1 complex homolog (S. pombe)	cabc1	0.72	0.87	0.82
160	219639_x_at	poly (ADP-ribose) polymerase family, member 6	parp6	1.32	1.29	1.57
161	201876_at	paraoxonase 2	PON2	0.72	0.49	0.53
162	201397_at	phosphoglycerate dehydrogenase	PHGDH	0.29	0.6	0.53
163	336_at	thromboxane A2 receptor	tbxa2r	2	1.26	2.05
164	AFFX-r2-Bs-phe-3_at	Sporulation initiation phosphotransferase B	spo0B	0.81	0.6	0.54
165	218321_x_at	serine/threonine/tyrosine interacting-like 1	STYXL1	1.3	1.26	1.33
166	208117_s_at	LAS1-like (S. cerevisiae)	LAS1L	0.84	0.73	0.64
167	202735_at	emopamil binding protein (sterol isomerase)	EBP	0.79	0.71	0.59
168	209090_s_at	SH3-domain GRB2-like endophilin B1	sh3glb1	1.26	1.73	1.56
169	201195_s_at	solute carrier family 7 (cationic amino acid transporter, y+ system), member 5	SLC7A5	0.54	0.53	0.61
170	218870_at	Rho GTPase activating protein 15	ARHGAP15	1.41	1.37	1.24
171	218106_s_at	mitochondrial ribosomal protein S10	mrps10	1.72	1.7	2.65
172	218375_at	nudix (nucleoside diphosphate linked moiety X)-type motif 9	nudt9	0.79	0.78	0.71
173	205171_at	protein tyrosine phosphatase, non-receptor type 4 (megakaryocyte)	PTPN4	0.77	0.66	0.58
174	210644_s_at	leukocyte-associated immunoglobulin-like receptor 1	Lair1	1.82	1.56	2.05
175	208913_at	golgi associated, gamma adaptin ear containing, ARF binding protein 2	Gga2	0.75	0.7	0.63
176	204295_at	surfeit 1	SURF1	1.22	2.07	2.37
177	212290_at	solute carrier family 7 (cationic amino acid transporter, y+ system), member 1	SLC7A1	0.69	0.72	0.6
178	205743_at	SH3 and cysteine rich domain	Stac	1.39	2.54	3.55
179	204000_at	guanine nucleotide binding protein (G protein), beta 5	GNB5	0.7	0.66	0.67
180	203177_x_at	transcription factor A, mitochondrial	TFAM	0.75	0.67	0.57
181	38149_at	Rho GTPase activating protein 25	Arhgap25	1.27	1.44	1.84
182	209383_at	DNA-damage-inducible transcript 3	DDIT3	1.67	3.63	6.04
183	219013_at	UDP-N-acetyl-alpha-D-galactosamine:polypeptide N-acetylgalactosaminyltransferase 11 (GalNAc-T11)	galnt11	0.77	0.78	0.74
184	209146_at	sterol-C4-methyl oxidase-like	SC4MOL	0.55	0.37	0.31
185	202886_s_at	protein phosphatase 2 (formerly 2A), regulatory subunit A, beta isoform	ppp2r1b	0.78	0.68	0.6
186	205527_s_at	gem (nuclear organelle) associated protein 4	GEMIN4	0.8	0.63	0.5
187	208647_at	farnesyl-diphosphate farnesyltransferase 1	FDFT1	0.71	0.69	0.71
188	212242_at	tubulin, alpha 4a	TUBA4A	0.65	0.54	0.32
189	208436_s_at	interferon regulatory factor 7	IRF7	1.55	2.78	3.48
190	200868_s_at	ring finger protein 114	RNF114	1.18	1.62	1.61
191	201576_s_at	galactosidase, beta 1	Glb1	0.79	0.83	0.68
192	201477_s_at	ribonucleotide reductase M1	Rrm1	0.63	0.83	0.74
193	215482_s_at	eukaryotic translation initiation factor 2B, subunit 4 delta, 67kDa	EIF2B4	1.4	1.48	1.21
194	215119_at	myosin XVI	Myo16	1.69	1.35	1.74
195	214749_s_at	similar to armadillo repeat containing, X-linked 6; armadillo repeat containing, X-linked 6	LOC653354 Armcx6	1.44	1.77	2.05
196	216841_s_at	superoxide dismutase 2, mitochondrial	Sod2	0.77	0.8	0.83
197	208078_s_at	salt-inducible kinase 1	Sik1	0.69	0.58	0.45
198	220973_s_at	SHANK-associated RH domain interactor	Sharpin	1.37	1.58	1.84
199	213134_x_at	BTG family, member 3	BTG3	0.67	0.36	0.24
200	209681_at	solute carrier family 19 (thiamine transporter), member 2	SLC19A2	0.56	0.63	0.46
201	213625_at	zinc finger with KRAB and SCAN domains 4	ZKSCAN4	1.3	1.58	2
202	219770_at	glycosyltransferase-like domain containing 1	GTDC1	1.35	1.17	1.43
203	205169_at	retinoblastoma binding protein 5	RBBP5	0.72	0.62	0.46
204	211582_x_at	leukocyte specific transcript 1	Lst1	1.3	1.34	1.56
205	204882_at	Rho GTPase activating protein 25	Arhgap25	1.4	1.35	1.91

2. Overview of the objectives

In the last years, the field of extracellular vesicles (EVs) has been characterized by an increasing interest due to their possible use as biomarkers for different diseases and their therapeutic potential.

However, a great challenge still needs to be solved, i.e. the standardization of methods used to separate EV subpopulations. It is crucial to distinguish the different EV subpopulations to avoid cross contamination that could lead to data misinterpretation.

Therefore, the first aim of this thesis has been to analyse different isolation methods to obtain the following objectives:

1. To evaluate the potential of centrifugation-based protocols to separate apoptotic bodies, microvesicles and exosomes and characterize them by RNA profile analysis, electron microscopy and flow cytometry.
2. To analyse the effect of a filtration step on exosome pellet purity, looking at the RNA profile of the isolated exosomal fractions.
3. To compare the different EV populations obtained using protocols detailed at points 1 and 2 and looking at their RNA profiles.

A significant numbers of studies focused on the role of EVs in response to biological stress (hypoxic conditions, low pH level, oxidative stress, thermal stress, radiation, shear stress and drugs effect). However, nobody has analysed EV release during ribosomal stress. Diamond Blackfan Anemia (DBA) is a disease due to abnormal ribosome biogenesis that induces apoptosis in erythroid progenitors. DBA research is hampered by the inability to study erythroid progenitors. The characterization and quantitative analysis of EVs from erythroid progenitors could be useful to overcome this limitation. The following objectives were attempted:

4. To investigate the miRNAs pattern in EVs shed by a DBA cell model.
5. To characterize and quantify microparticles from erythroid progenitors released in blood of patients with Diamond Blackfan Anemia.

3. Results and discussion

3.1 Isolation and characterization of EVs: RNA profile analysis distinguishes EV subpopulations

The EV field is rapidly expanding, but isolation methods, classification and quality assessment methods are still under discussion (Simpson RJ., 2012). EV isolation methods are based on sedimentation time, density, size and surface markers that are different in EV subpopulations. Despite distinct features, numerous similarities exist among different EVs so the overlap and pellet "contamination" could be greater than believed.

3.1.1 Centrifugation based protocols to separate ABs, MVs and EXOs (Crescitelli *et al*, 2013)

This project was performed at Krefting Research Centre, Department of Internal Medicine, University of Gothenburg, Sweden under the supervision of Prof. Jan Lötvall.

Our aim was to properly separate subpopulations of extracellular vesicles and analyse their different molecular characteristics.

We compared a differential centrifugation-based protocol used to isolate ABs and MVs (protocol 1) (Turiák L, 2011) and another protocol to isolate EXOs after removal of ABs and MVs (protocol 2) (Valadi H, 2007). In short, for both of protocols, cells were harvested and pelleted by centrifugation at 300 × *g*, vesicles were collected from the supernatant at differential centrifugation steps.

Protocol 1: ABs were collected at 2000 × *g*. Supernatant was filtered through 0.8 μm pores and MVs were pelleted by ultracentrifugation at 12200 × *g*.

Protocol 2: ABs and MVs were collected together at 16500 × *g*. Supernatant was filtered through 0.22 μm pores and EXOs were pelleted by ultracentrifugation at 120000 × *g*.

We utilized these protocols to isolate different vesicles from supernatant of three cell lines (HMC-1, TF-1 and BV-2). First of all, EV RNA profiles were analysed. We demonstrated that distinct vesicle fractions have clearly different RNA profiles. rRNA was primarily detected in ABs from all cell lines, whereas little or no RNA was contained in MVs, except for those from TF-1 cells. In EXO, the RNA profiles from all cell lines lacked rRNA peaks, but showed small RNAs. In the pellet containing both ABs and MVs, RNA profiles similar to those observed for ABs, were observed in vesicles from all cell lines. To verify if the contribution to the rRNA in the ABs+MVs pellet was provided by ABs and not by MVs, a modification of protocol 2 was utilized. In this protocol, the 2000 $\times g$ step was added, aiming to separate ABs and MVs otherwise collected in the same pellet in the original protocol 2. The comparisons of the RNA profiles showed that the rRNA peaks were predominant in ABs from the HMC-1 and TF-1 cell lines. We can thus conclude that ABs are likely to contribute the majority of the rRNA present in the pellet composed by a mixture of ABs and MVs.

Considering that RNA content of EVs can change depending on the state of the cell, we analysed RNA profiles from EVs shed by cells subjected to TRAIL-induced apoptosis. We demonstrated that the RNA profile was maintained during apoptosis, but RNA concentration was increased in ABs, but also in EXOs. It is well known that EXO secretion is increased during apoptosis (Yu X H. S., 2006).

Furthermore, electron microscopy revealed a morphology compatible with ABs, MVs and EXOs. Elements with chromatin condensation and marginalization and a size range of 800-5000 nm was present in the pellet composed by ABs; round and oval shaped, membrane-bound structures with a size between 200-800 nm characterized MVs and finally, EXOs showed cup shape with a diameter of 40-100 nm. As expected, the pellet composed by both ABs and MVs showed elements with 200-5000 nm diameter, with typical characteristics of both ABs and MVs. The pellets morphology characteristics were similar for pellets isolated from all three cell lines considered. This finding shows that separation was correctly achieved.

Finally, in order to better characterize the different subpopulations of EVs, flow cytometry-based evaluation of the tetraspanins CD9, CD63 and CD81 was performed on vesicles from HMC-1 and TF-1 cells. CD9, CD63 and CD81 were considered specific for EXOs (Escola JM, 1998). We observed that all pellets contained vesicles captured by anti-CD63-coated beads. This shows that CD63 marker is not exclusively present on EXOs, as previously suggested (Escola JM, 1998), (Bobrie A C. M., 2012). CD63 positive vesicles were also positive for all other markers investigated except for CD9 that was not expressed by TF-1-derived vesicles since TF-1 cells do not express this tetraspanin. Our results demonstrated that anti-CD63-coated beads and flow cytometry is not a robust method for EXO characterization.
Our results, demonstrated that centrifugation-based protocols are simple and fast systems to distinguish subpopulation of EVs. Different EV types show different RNA profiles and peculiar morphological characteristics, but they are indistinguishable using anti-CD63-coated beads for flow cytometry.

ORIGINAL RESEARCH ARTICLE

COACTION

Distinct RNA profiles in subpopulations of extracellular vesicles: apoptotic bodies, microvesicles and exosomes

Rossella Crescitelli[1,2], Cecilia Lässer[1], Tamas G. Szabó[3], Agnes Kittel[4], Maria Eldh[1], Irma Dianzani[2], Edit I. Buzás[3]* and Jan Lötvall[1]*

[1]Department of Internal Medicine and Clinical Nutrition, Krefting Research Centre, University of Gothenburg, Gothenburg, Sweden; [2]Department of Health Sciences, University of Eastern Piedmont, Novara, Italy; [3]Department of Genetics, Cell and Immunobiology, Semmelweis University, Budapest, Hungary; [4]Institute of Experimental Medicine, Hungarian Academy of Sciences, Budapest, Hungary

Introduction: In recent years, there has been an exponential increase in the number of studies aiming to understand the biology of exosomes, as well as other extracellular vesicles. However, classification of membrane vesicles and the appropriate protocols for their isolation are still under intense discussion and investigation. When isolating vesicles, it is crucial to use systems that are able to separate them, to avoid cross-contamination.

Method: EVs released from three different kinds of cell lines: HMC-1, TF-1 and BV-2 were isolated using two centrifugation-based protocols. In protocol 1, apoptotic bodies were collected at 2,000 × g, followed by filtering the supernatant through 0.8 μm pores and pelleting of microvesicles at 12,200 × g. In protocol 2, apoptotic bodies and microvesicles were collected together at 16,500 × g, followed by filtering of the supernatant through 0.2 μm pores and pelleting of exosomes at 120,000 × g. Extracellular vesicles were analyzed by transmission electron microscopy, flow cytometry and the RNA profiles were investigated using a Bioanalyzer®.

Results: RNA profiles showed that ribosomal RNA was primary detectable in apoptotic bodies and smaller RNAs without prominent ribosomal RNA peaks in exosomes. In contrast, microvesicles contained little or no RNA except for microvesicles collected from TF-1 cell cultures. The different vesicle pellets showed highly different distribution of size, shape and electron density with typical apoptotic body, microvesicle and exosome characteristics when analyzed by transmission electron microscopy. Flow cytometry revealed the presence of CD63 and CD81 in all vesicles investigated, as well as CD9 except in the TF-1-derived vesicles, as these cells do not express CD9.

Conclusions: Our results demonstrate that centrifugation-based protocols are simple and fast systems to distinguish subpopulations of extracellular vesicles. Different vesicles show different RNA profiles and morphological characteristics, but they are indistinguishable using CD63-coated beads for flow cytometry analysis.

Keywords: *apoptotic bodies*; *microvesicles*; *exosomes*; *extracellular vesicles*; *ultracentrifugation*; *characterization*; *RNA*; *electron microscopy*

Received: 20 February 2013; Revised: 31 July 2013; Accepted: 16 August 2013; Published: 12 September 2013

Extracellular vesicles (EVs) are membranous vesicles naturally released by most cells (1–9). EVs can be broadly classified into three main classes, based primarily on their size and presumed biogenetic pathways: (a) apoptotic bodies (ABs), 800–5,000 nm diameter and released by cells undergoing programmed cell death, (b) microvesicles (MVs), also referred to as shedding MVs, are large membranous vesicles (50–1,000 nm diameter) that are produced by budding from the plasma membrane (c) and finally exosomes (EXOs), 40–100 nm diameter vesicles considered to be of endocytic origin (10,11).

Despite some presumed distinct features, numerous similarities exist among the different EVs with respect to

Citation: Journal of Extracellular Vesicles 2013, **2**: 20677 - http://dx.doi.org/10.3402/jev.v2i0.20677
(page number not for citation purpose)

their physical characteristics and biochemical composition (12–15), which make the separation of different subsets challenging (12). Because of their small size, many EVs are below the detection range of conventional detection methods such as light microscopy. Consequently, recovery and contamination among vesicles in the separation process cannot be reliably controlled. Furthermore, isolation protocols and the nomenclature are not fully standardized in the field at this point. In most studies, vesicles are isolated by differential centrifugation steps which are considered to be the "golden standard" to isolate different types of EVs (16). Differential centrifugation involves multiple sequential centrifugations, each time removing the pellet and the supernatant, and includes increasing the centrifugal force to isolate smaller and less dense components in the subsequent steps. In general, centrifugal force at 200–1,500 × g are used to pellet cells and "cellular debris," 10,000–20,000 × g to pellet vesicles with a size between 100 and 800 nm (generally called MVs) and between 100,000 and 200,000 × g to pellet the smallest vesicles with a diameter <100 nm (generally referred to as EXOs) (17).

Besides the size and density of vesicles, the efficiency to isolate vesicles depends on the shape and viscosity of the solution, as well as on temperature, centrifugation time and the type of rotor used for the centrifugation (fixed-angle rotor or swinging buckets). As vesicles are heterogeneous, complete separation of vesicles with a certain diameter and/or density is still unlikely with this approach. Besides differential centrifugations, filtration has also been applied to remove larger vesicles from smaller ones. Although the pore size of filters is often well defined, increasing forces have to be applied with decreasing pore size, which can result in artefacts (12,17).

Although flow cytometry and Western blot has been utilized to identify and characterize nano-sized vesicles (18), the golden standard remains to be transmission electron microscopy (TEM) (19), which is the only method by which both the size and morphology of the isolated vesicles can be determined simultaneously (12). Attempts to separate different vesicles to allow analysis of their diverse functions and description of their different contents also remain crucial for the development of the field.

In this study, we have used differential centrifugation steps to achieve a relative separation of ABs, MVs and EXOs from several different cell lines, with the hypothesis that the RNA profiles are different in different types of vesicles, but similar among vesicles from different types of cells. To do this, three fundamentally different cell lines were cultured *in vitro*, including a human mast cell line (HMC-1), a human erythroleukemia cell line (TF-1) and a mouse microglia cell line (BV-2). Different EVs were isolated to determine their respective RNA profiles. To determine the morphology of the different vesicles, the subpopulations of EVs from the different cells were visualized using TEM of sectioned vesicle pellets.

Materials and methods

Cell cultures

The HMC-1 (J. Butterfield, Mayo Clinic, Rochester, MN, USA) used in our earlier studies (20,21) was cultured in IMDM (Sigma-Aldrich, St. Louis, MO, USA) containing 10% foetal bovine serum (FBS, Sigma-Aldrich), 100 U ml^{-1} penicillin, 100 µg ml^{-1} streptomycin, 2 mM L-glutamine and 1.2 mM α-thioglycerol (Sigma-Aldrich). The cytokine-dependent erythroleukemia cell line TF-1 (ATCC number: CRL-2003) was grown in RPMI 1640 medium supplemented with 10% FBS, 100 U ml^{-1} penicillin, 100 µg ml^{-1} streptomycin, 2 mM L-glutamine (all reagents were from Sigma-Aldrich) and 5 ng ml^{-1} GM-CSF (granulocyte-macrophage colony-stimulating factor, Miltenyi Biotec, Lund, Sweden). The BV-2 murine microglia cells were grown in RPMI supplemented by 10% FBS (Gibco Invitrogen Corporation, Carlsbad, CA, USA) and 4 µg ml^{-1} ciprofloxacin (Fresenius Kabi Deutschland GmbH, Bad Homburg v.d.H, Germany). For all FBS used in the cell cultures, pure foetal bovine serum was depleted from EXOs prior to use, by ultracentrifugation at 120,000 × g for 18 hours, using a Ti45 rotor (Beckman Coulter, Brea, CA, USA). Cell viability was assessed using trypan blue exclusion methods.

Vesicle isolation

Vesicles were prepared from the supernatant of HMC-1, TF-1 and BV-2 cells ($1–2 \times 10^6$ cells ml^{-1}) using two different centrifugation-based protocols. Briefly, for both protocols, cells were isolated and removed by pelleting with centrifugation at 300 × g for 10 minutes. Vesicles were then collected from the supernatant through differential centrifugation steps (Fig. 1).

Protocol 1: ABs and MVs were isolated by differential centrifugations and micro-filtration as previously described (22). The supernatant harvested from the cells was centrifuged at 2,000 × g for 20 minutes to collect ABs. This supernatant was then filtered by gravity through 0.8 µm filters (GE healthcare, Whatman®, UK) to remove particles >800 nm. The supernatant was again collected and further used to isolate MVs. MVs were pelleted by centrifugation at 12,200 × g for 40 minutes (Fig. 1A). All centrifugation steps in both protocols 1 and 2 were performed at 4°C.

Protocol 2: ABs + MVs and EXOs were isolated by differential centrifugations and nano-filtration as previously described (21). ABs + MVs were collected together in this protocol by a centrifugation of the cell supernatant at 16,500 × g for 20 minutes. The supernatant from this step was filtered through 0.2 µm filters (with gentle

Citation: Journal of Extracellular Vesicles 2013, **2**: 20677 - http://dx.doi.org/10.3402/jev.v2i0.20677

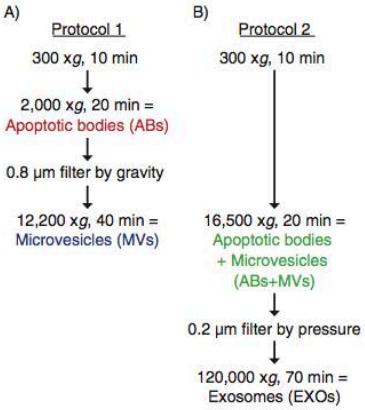

Fig. 1. Flow chart over two different differential centrifugation-based protocols. Apoptotic bodies (ABs) and microvesicles (MVs) were isolated separately using protocol 1 (A). ABs and MVs were isolated together (ABs+MVs) followed by exosome (EXO) isolation, using protocol 2 (B).

pressure) (Sarstedt, Nümbrecht-Rommelsdorf, Germany) to remove particles larger than 200 nm. EXOs were then pelleted by ultracentrifugation at 120,000 × g for 70 minutes (Fig. 1B).

RNA isolation and detection

RNA was isolated from vesicles (n = 4 for HMC-1 and TF-1 cells and n = 3 for BV-2 cells) using miRCURY™ RNA Isolation Kit (Exiqon, Vedbaek, Denmark) according to the manufacturer's protocol. Detection, quality, yield and size of the vesicular RNA were analyzed using capillary electrophoresis (Agilent RNA 6000 Nano Kit on an Agilent 2100 Bioanalyzer®, Agilent Technologies, Santa Clara, CA, USA). One microlitre RNA in solution was analyzed according to the manufacturer's protocol as previously described (23).

Induction and determination of apoptosis

To induce apoptosis, TF1 cells were incubated with 100 ng ml^{-1} of recombinant human TNF-related apoptosis-inducing ligand (TRAIL; PeproTech Inc., Rocky Hill, NJ, USA). Apoptosis was assessed after 2, 4, 8, 24 and 48 hours by using PE Annexin V Apoptosis Detection Kit I (BD-Pharmingen™, San Jose, CA, USA) according to the manufacturer's protocol. Briefly, after two washes in cold PBS, cells were resuspended in 1 × binding buffer (10 ×: 0.1 M Hepes/NaOH (pH 7.4) 1.4 M NaCl, 25 mM $CaCl_2$) at 1×10^6 cells ml^{-1}. One hundred microlitres of cellular suspension was transferred in a FACS tube and 5 µl of Annexin V-PE antibody and 5 µl of the vital dye 7-Amino-Actinomycin (7-AAD) were added. Cells with intact membranes exclude 7-AAD, whereas the membrane of necrotic cells is permeable to 7-AAD. Apoptotic cells are identified by positivity for Annexin-V. After 15 minutes of incubation at room temperature (RT) in the dark, 400 µl of 1 × binding buffer was added and the fluorescence was determined by a FACSAria (BD Biosciences, San Jose, CA, USA). The flow cytometry data were analyzed using the FlowJo Software (Tri Star Inc., Ashland, OR, USA) (n = 2). ABs were collected after 4, 24 and 48 hours of TRAIL treatment, while the other populations of EVs (MVs, AB+MVs and EXOs) were collected after 48 hours only. The RNA profiles were analyzed in all samples as described above (n = 2).

Transmission electron microscopy

The vesicular pellets obtained by the two differential centrifugation-based protocols were submitted to TEM. Briefly, after isolation (see "vesicle isolation" section) pellets were fixed at 4°C overnight. The fixative contained 4% paraformaldehyde in 0.01 M phosphate buffer with pH 7.4 (filtered through 0.22 µm filters). After washing with PBS, the preparations were post-fixed in 1% OsO_4 (Taab Laboratories Equipment Ltd., Aldermaston, England, UK) for 30 minutes. After rinsing with distilled water, the pellets were dehydrated in graded ethanol, including block staining with 1% uranyl-acetate in 50% ethanol for 30 minutes, and embedded in Taab 812 (Taab). After overnight polymerization at 60°C and sectioning for TEM, the ultrathin sections were analyzed with a Hitachi 7100 electron microscope equipped by Megaview II (lower resolution, Soft Imaging System) digital camera.

Flow cytometry of vesicles

The protein concentration of the vesicle preparations was measured using the BCA™ Protein Assay Kit (Pierce, Thermo Scientific, Rockford, IL, USA). Antibody-coated beads were prepared as previously described (20,24). Briefly, for the immune-isolation, 4-µm-diameter aldehyde/sulfate latex beads (Interfacial Dynamics, Life Technologies, Carlsbad, CA, USA) were incubated with 12.5 µg purified anti-CD63 antibody (clone H5C6, BD Biosciences), with the same volume of MES buffer under gentle agitation at RT overnight.

Vesicles (20 µg) were resuspended in PBS and loaded onto the anti-CD63-coated beads (6×10^4) and were incubated overnight at 4°C under agitation. Vesicle-coated beads were incubated for 30 minutes with 100 mM glycine to block remaining binding sites. The bead–vesicle complexes were washed twice in PBS with 3% FBS (prior ultracentrifuged at 120,000 × g for 18 hours). The bead–vesicle complexes were resuspended in IgG (Sigma-Aldrich) and incubated for 15 minutes at RT, before being washed twice more. The tetraspanins CD9, CD63 and CD81, known to be enriched in EXOs, were investigated for its presence on the vesicles. The bead–vesicle complexes were incubated with PE-labelled anti-CD9 (clone M-L13), anti-CD63 (clone H5C6, the same antibody as

used to coat the beads), anti-CD81 (clone JS-81) or the corresponding isotype control (all antibodies were from BD Biosciences) for 40 minutes at RT under agitation, washed twice and then acquired by a FACSAria (BD Biosciences) (n = 3). The flow cytometry data were analyzed using the FlowJo Software (Tri Star Inc., Ashland, OR, USA).

Results

Subpopulations of EVs harbour different RNA profiles

RNA profiles in the different vesicular fractions from the three cell lines, HMC-1, TF-1 and BV-2 were analyzed using a Bioanalyzer®. Using the vesicle isolation protocols described in Fig. 1, different RNA profiles were observed in the vesicular fractions considered to harbour ABs, MVs and EXOs (Fig. 2A–D). Thus, the technique reveals two dominant peaks, corresponding to the ribosomal RNA (rRNA) subunits 18S and 28S, in ABs from HMC-1, TF-1 and BV-2 cells (Fig. 2A). The rRNA peaks were lacking or were very low in MVs from HMC-1 and BV-2 cells, but could be observed in MVs from TF-1 cells (Fig. 2B). In the 16,500 × g pellet, which contained both ABs and MVs, similar RNA profiles as seen for ABs were observed in vesicles from all cell lines (Fig. 2C). In EXOs, the RNA profile from all three cell lines lacked the rRNA peaks, but showed the presence of small RNAs (Fig. 2D). Bioanalyzer® RNA profiles from the two different protocols are also illustrated in the same figure from each cell line (Fig. 2E–G). These data argue that the rRNA peaks are mainly contributed by the ABs and not by MVs.

To better understand whether the ABs collected at 2,000 × g (protocol 1, Fig. 1) were indeed representative of cells undergoing programmed cell death, recombinant human TRAIL was used to induce apoptosis in the TF-1 cells, as TRAIL has previously been shown to induce apoptosis (25–27). Apoptosis and primary/secondary necrosis were assessed after 2, 4, 8, 24 and 48 hours by flow cytometry using Annexin V-PE and 7-AAD staining, respectively. Upon induction of apoptosis by TRAIL, a three-fold increase in the proportion of apoptotic cells was detected at both 2 and 4 hours without

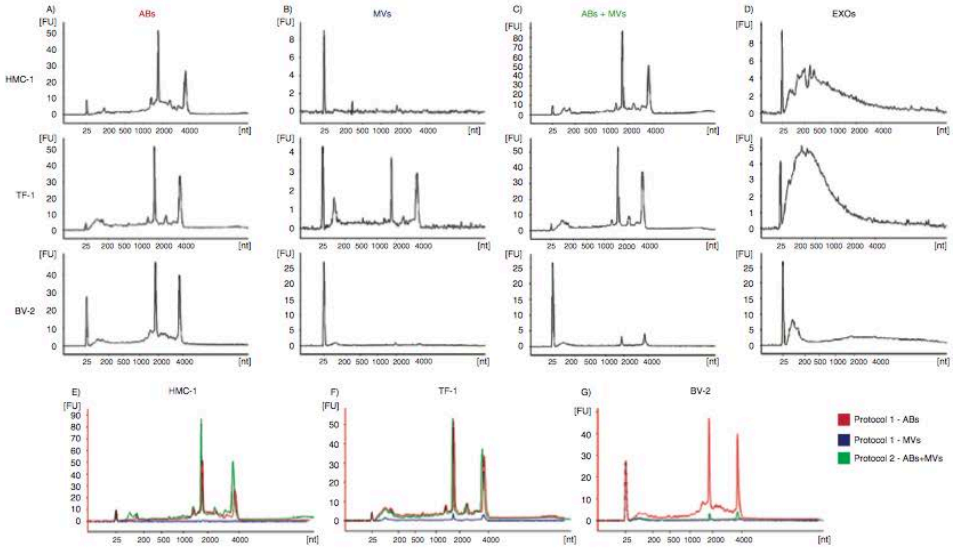

Fig. 2. RNA profiles from different subpopulations of extracellular vesicles (EVs). RNA was extracted from vesicles released by three different cell lines; HMC-1 (human mast cell line), TF-1 (human erythroleukemia cells) and BV-2 (mouse microglia cells). The electropherograms show the size distribution in nucleotides (nt) and fluorescence intensity (FU) of total RNA in apoptotic bodies (ABs), microvesicles (MVs), ABs and MVs together (ABs + MVs) and exosomes (EXOs). The short peak at 25 nt is an internal standard. (A) In ABs the most dominant peaks are the 18S and 28S ribosomal RNA. (B) The 18S and 28S rRNA are not evident in MVs from HMC-1 and BV-2, but only obvious in MVs from TF-1, however at low concentrations. (C) 18S and 28S peaks are evident in the pellet composed by ABs and MVs together (ABs + MVs). (D) In EXOs small RNA is dominating, with no or very small rRNA peaks detected. (E–G) The overlapping profiles from ABs (in red) and MVs (in blue) and both collected together (ABs + MVs – in green), suggesting that the contribution of 18S and 28S rRNA is by ABs. The electropherograms are representative of n = 4.

Citation: Journal of Extracellular Vesicles 2013, **2**: 20677 - http://dx.doi.org/10.3402/jev.v2i0.20677

any increase in the ratio of necrotic cells (data not shown). The percentage of apoptotic cells reached 60.2% by 48 hours. However, from 8 hours there was also an increase in the ratio of necrotic cells (reaching 9.7 and 22.6% by 24 and 48 hours, respectively). ABs were collected at 4 hours (when apoptosis was induced without any necrosis), at 24 hours (when cells showed apoptosis with moderate ($<10\%$) necrosis) and at 48 hours (when cells showed increased necrosis and apoptosis but with three times as much apoptosis). The effect of apoptosis on the RNA content in MVs and EXOs were also determined, but due to low-yield MVs and EXOs were only collected and analyzed at 48 hours. Figure 3 shows RNA profiles in vesicles collected with/without TRAIL treatment. As expected, after induction of apoptosis by TRAIL, the amount of rRNA in vesicular fractions increased, suggesting increased amounts of ABs (Fig. 3A–C). In MVs, prominent rRNA peaks were present after TRAIL treatment. The increased quantities of rRNA could also be explained by an increased presence of ABs in this vesicular fraction (Fig. 3D).

Larger amount of rRNA was observed in the pellet composed by ABs and MVs after TRAIL treatment compared to the pellet obtained without TRAIL treatment (Fig. 3E). In the EXO fraction, the RNA profiles were similar under either condition, but a greater quantity of RNAs was evident in the EXO pellet collected after TRAIL treatment (Fig. 3F).

To verify if the contribution to the rRNA (18S and 28S subunits) in the ABs + MVs pellet was provided by ABs and not by MVs, a modification of protocol 2 from Fig. 1 was utilized (here termed protocol 2b, see Fig. 4A). In this protocol, the 2,000 × g step was added, aiming to separate ABs and MVs otherwise collected in the same pellet in the original protocol 2 (here termed protocol 2a, see Fig. 4A). The comparison of the RNA profiles showed that the rRNA peaks were most dominant in ABs and not in MVs from the HMC-1 and TF-1 cell lines. We can thus conclude that ABs are likely to contribute to a majority of the rRNA present in the pellet composed by a mixture of ABs and MVs (Fig. 4B).

Different morphology of ABs, MVs and EXOs as visualized by TEM

EVs containing pellets of HMC-1, TF-1 and BV-2 were visualized by TEM (Fig. 5). Images revealed that the pellet from the first step of centrifugation using protocol 1 (2,000 × g) is composed by elements with chromatin condensation and/or marginalization with the size range of 800–5,000 nm that are characteristic of ABs (Fig. 5A1–A3). A very pure pellet was obtained from the second step (12,200 × g) after 0.8 μm filtration. It contained predominantly round and oval shaped,

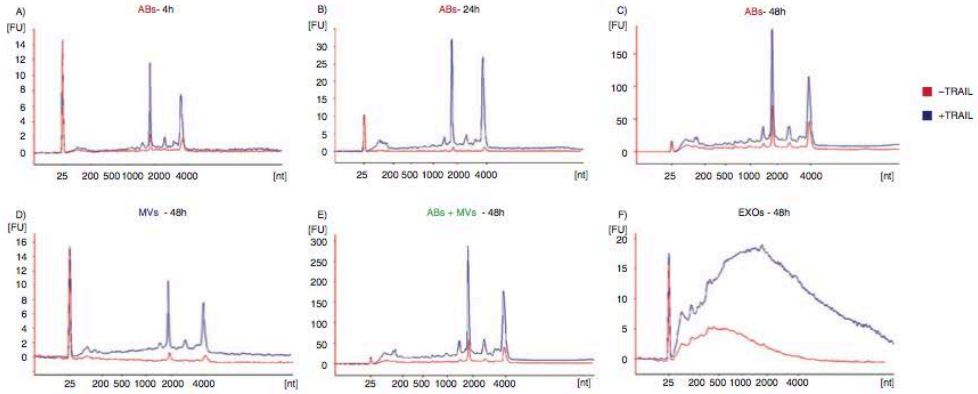

Fig. 3. RNA profiles from different subpopulations of extracellular vesicles (EVs) after TRAIL-induced apoptosis. The electropherograms show the RNA size distribution in nucleotides (nt) and fluorescence intensity (FU) in apoptotic bodies (ABs), microvesicles (MVs), ABs and MVs together (ABs + MVs) and exosomes (EXOs) in TF-1 cells with and without TRAIL treatment. The short peak at 25 nt is an internal standard. (A–C) RNA profiles from ABs released by TF-1 cells after 4, 24, 48 hours of TRAIL treatment (in blue) and without TRAIL (in red). After 4 hours (A), 24 hours (B) and 48 hours (C) of TRAIL treatment, in ABs, the peaks of 18S and 28S rRNAs are more prominent comparing with ABs released in the absence of TRAIL. (D–F) RNA profiles from MVs, ABs + MVs and EXOs released by TF-1 cells after 48 hours of TRAIL treatment (in blue) and without TRAIL (in red). (D) The low 18S and 28S rRNA peaks in MVs without TRAIL (in red) become much more prominent after TRAIL treatment (in blue). (E) The highest rRNA peaks are seen in the pellet composed by ABs and MVs together (ABs + MVs). (F) After 48 hours of TRAIL-induced apoptosis, increased amount of small RNAs is observed in exosomes (EXOs). The electropherograms are representative of n = 2.

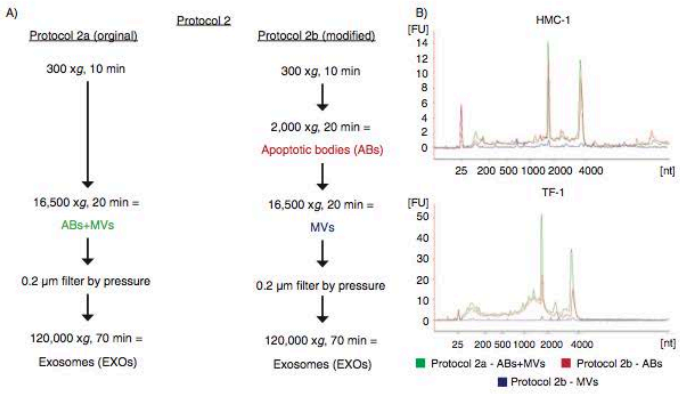

Fig. 4. Flow chart over the original and modified protocol 2. (A) In the modification of protocol 2, a 2,000 × g step was added to isolate apoptotic bodies (ABs) and microvesicles (MVs) separately, prior to EXOs isolation (here called protocol 2b). (B) The RNA profiles from the different subpopulation of extracellular vesicles (EVs) collected using protocol 2a and 2b. RNA was extracted from vesicles releases from two different cell lines; HMC-1 and TF-1. Shown here are the overlapping profiles from ABs (ABs – in red), MVs (MVs – in blue) and both of them collected together (ABs + MVs – in green), indicating that the contribution of 18S and 28S rRNA is primarily by ABs. The electopherograms show the size distribution in nucleotides (nt) and fluorescence intensity (FU) of total RNA. The peak at 25 nt is an internal standard. The electropherograms are representative of n = 3.

membrane-bound structures of variable size and electron density within the diameter range of 200–800 nm (Fig. 5B1–B3). As expected, the first pellet obtained using protocol 2 (16,500 × g) was composed by both ABs and MVs (Fig. 5C1–C3), as it contains elements with both 800–5,000 nm and 200–800 nm diameter, with typical characteristics of ABs and MVs. Finally, pellets from the last step of centrifugation (120,000 × g) were composed of 40–100 nm diameter vesicles, consistent with EXOs (Fig. 5D1–D3).

The electron micrographs thus confirm that the respective pellets contain intact structures primarily within the expected diameter ranges and with typical morphological characteristics of the ABs, MVs and EXOs respectively. The images show similar morphology of the different vesicles from the three different cell lines analyzed, confirming that they produced similar subpopulation of vesicles isolated by the same centrifugation-based protocols.

CD9, CD63 and CD81 are present on ABs, MVs and EXOs

The presence of CD63 and CD81 on the surface of HMC-1 and TF-1 cells was confirmed by flow cytometry, whereas CD9 was only expressed on the HMC-1 cells, and not on the TF-1 cells (Fig. 6A).

In order to better characterize the different subpopulation of EVs, a flow cytometry-based evaluation of the tetraspanins CD9, CD63 and CD81 was performed (24). To do this, we utilized CD63-antibody-coated beads and could capture CD63-containing vesicles from all three types of vesicles (Fig. 6B) and not exclusively EXOs as previously suggested (28,29). As expected based on flow cytometry results from cells, CD63-containing vesicles that were derived from HMC-1 cells, were positive for all markers investigated, whereas TF-1-derived vesicles bound to the CD63-antibody-coated beads expressed also CD81, as well as CD63, but not CD9 (Fig. 6B).

HMC-1 cells exposed less CD63 than CD81 at the cell surface (Fig. 6A), whereas conversely there was a higher level of CD63 than CD81 on the captured vesicles (Fig. 6B). TF-1 cells, instead, exposed both tetraspanins at the same level at their surface, and the released vesicles also expressed these two markers at the same level.

Discussion

In this study, we have applied previously published centrifugation-based protocols considered appropriate for the isolation of ABs and MVs, respectively (22). Furthermore, we used protocols that are considered to remove ABs and MVs, and to more specifically isolate EXOs (21). These protocols were utilized to isolate the different vesicles from the supernatants of cultured HMC-1, TF-1 and BV-2 cells. Here, we provide evidence for the presence of clearly different RNA profiles in the various vesicle fractions, with rRNA being primarily detectable in ABs, and smaller RNAs without prominent rRNA peaks in EXOs. The isolates considered to be MVs contained little or no RNA, except for those from TF-1 cells. Indeed, electron microscopy of sectioned pellets of respective vesicle isolation revealed morphology compatible with predominantly ABs, MVs and EXOs in

Citation: Journal of Extracellular Vesicles 2013, **2**: 20677 - http://dx.doi.org/10.3402/jev.v2i0.20677

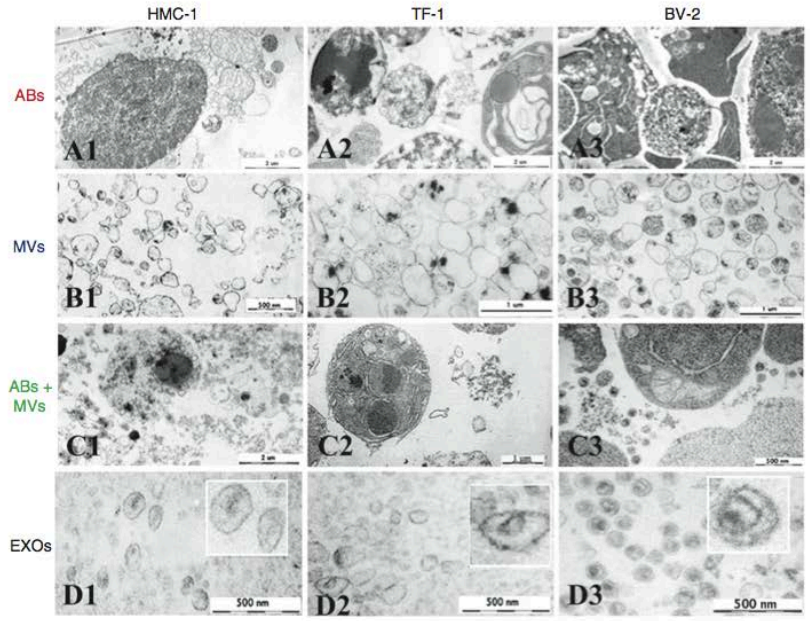

Fig. 5. Analysis of ABs, MVs and EXOs by TEM. Micrographs of vesicles released from three different cell lines; HMC-1 (human mast cell line), TF-1 (human erythroleukemia cells), and BV-2 (mouse microglia cells) are shown. (A1–3) Dense structures show the chromatin substance in the generally round shaped apoptotic bodies (ABs) with a size of 800–5,000 nm. (B1–3) Microvesicles (MVs) are diverse in their shape and density, with a size range between 200 and 800 nm. (C1–3) In the pellet obtained by centrifugation at 16,500 × g presents the mixture of ABs and MVs. (D1–3) The exosome (EXO) fraction from HMC-1 (D1), TF-1 (D2) and BV-2 (D3) cells were found to have a diameter of approximately 40–100 nm.

the different fractions, although some contamination between the fractions cannot be excluded. ABs and MVs were more diverse in their morphology than the EXOs. Flow cytometry revealed the presence of CD63 and CD81 positive vesicles in all fractions from all cell types, as well as CD9 except in the TF-1-derived vesicles.

For the separate isolation of ABs and MVs, we first used a 300 × g centrifugation to remove cells, and a subsequent centrifugation with 2,000 × g to pellet ABs. Subsequently, the supernatant was filtered and centrifuged at 12,200 × g for the pelleting of MVs. Indeed, this approach separated vesicles containing rRNA, which was found primarily in the presumed fraction containing ABs, whereas no or little RNA was found in the MVs fraction, at least from the HMC-1 and BV-2 cells. The TF-1-derived vesicles showed a slightly different RNA profile, as rRNA profiles also could be seen in the MV fraction.

We do not know at this stage whether the rRNA identified in the TF-1-derived MVs fractions is indeed located in MVs, or it is present in other types of vesicles, or even in protein aggregates co-pelleting with MVs. However, electron microscopy of the pellets from the different vesicle isolations shows distinct morphological differences between ABs and MVs from all cells studied, which suggests that the rRNA in MVs from TF-1 cells is not necessarily due to a contamination from ABs, but may argue that MVs from some cells indeed does contain RNA.

With an approach previously utilized in our laboratory (21), a first centrifugation with 16,500 × g was utilized after cell removal to collect ABs and MVs together prior to EXOs isolation. After that, EXOs were isolated by first passing the supernatant through a 200 nm filter, followed by 120,000 × g ultracentrifugation. Thus, the first pellet contains both ABs as well as MVs, and the second pellet only EXOs. Using this approach, the RNA profiles of the mixed AB/MV pellet were similar to that seen in ABs using the first protocol, whereas the EXOs contain primarily small RNA without any prominent rRNA peaks (21). When a first centrifugation with 2,000 × g was utilized prior to this protocol (to isolate ABs), again the rRNA profiles were in the HMC-1 cells seen in the AB fraction, whereas rRNA was found in both the AB and MV fractions from the TF-1 cell line. It cannot,

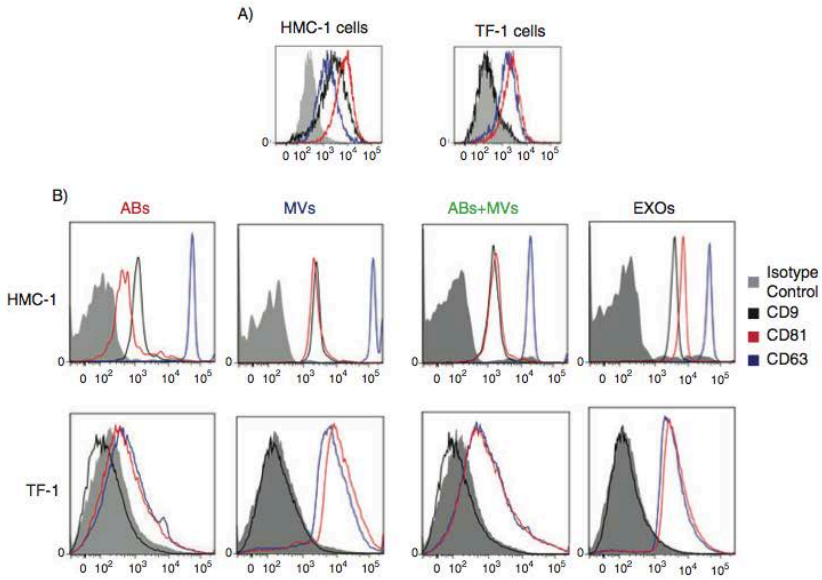

Fig. 6. Detection and characterization of extracellular vesicles (EVs) by flow cytometry. The CD9, CD63 and CD81 expression on HMC-1 and TF-1 cells (A) and their expression on different vesicles, using anti-CD63-coated beads, are shown. (B) Cells and vesicles were immunostained against the tetraspanin (open curve) CD9 (in black), CD63 (in blue) and CD81 (in red) and compared with their appropriate isotype control (filled curve). The graphs are representative of n = 3.

however, be excluded that MVs from different cells have different capacity to carry RNA. Furthermore, it must also be considered that the RNA content of EVs may significantly change depending on the state of the cell (30). After 4 and 24 hours of TRAIL-induced apoptosis, increased concentration of rRNA was observed in the isolated ABs, compared to ABs from untreated cells. After 48 hours of TRAIL-induced apoptosis, a greater concentration of small RNAs was observed also in EXOs. This is in concordance with previously published data, showing that p53-induced apoptosis is associated with increased EXO secretion (31–33).

In many studies, flow cytometry with beads binding different types of micro- and nano-sized vesicles has been utilized (24,28,34), for example to determine the presence of the tetraspanins CD9, CD63 and CD81 on EXOs. Here, we have utilized beads with anti-CD63 antibodies, and could find positive signals in all vesicle fractions, except for CD9 in the TF-1-derived vesicles, which is not surprising, since TF-1 cells do not express this tetraspanin.

Comparing two kinds of cell lines analyzed, and the vesicles from them, HMC-1 cells express less CD63 than CD81 at the cell surface, whereas conversely there is lower level of CD81 than CD63 on the captured vesicles. This result could suggest that part of the CD63-vesicles may be CD81-negative and comes from intracellular compartments, whereas TF-1 cells expose both tetraspanins at the same level at its surface and the released vesicles also express these two markers at a similar level. These data indicate that the levels of CD63 and CD81 must be analyzed both at the surface of vesicle-secreting cells and in the resulting secreted vesicles. Results obtained using flow cytometry indicate that this method is not sufficient to establish that a nano-vesicle fraction studied is EXOs, and only EXOs. This may suggest that these surface molecules are not specific for EXOs, but are also present on ABs ad MVs from both HMC-1 and TF-1 cells. Alternatively, it may suggest that all three EVs population contain detectable amounts of CD63-positive EXOs. Importantly, in all flow cytometry analyses, events were also observed outside of the gates for the beads (data not shown), suggesting that a portion of vesicles do not bind to the CD63 beads, regardless of isolation protocol and vesicle fraction studied, again supporting the notion that non-CD63-expressing vesicles are present in all vesicular fractions.

The TEM analysis of the different vesicular fractions argues strongly that we primarily have ABs, MVs and EXOs in the different fractions from all the cells studied.

Citation: Journal of Extracellular Vesicles 2013, **2**: 20677 - http://dx.doi.org/10.3402/jev.v2i0.20677

Indeed, the morphology of all of these vesicles was characteristically similar to what previously had been described (22). Importantly, the contamination of, for example, EXOs in ABs and MVs is possible, but is not prominent according to the morphological characteristics.

This study shows that ABs, MVs and EXOs contain fundamentally different RNA profiles, and argues that MVs isolated from cell cultures often do not contain considerable amounts of RNA. The rRNA was primarily found in ABs, which should be considered when the functionality of RNA in different vesicles is studied.

Acknowledgements

The authors thank Gunnar Nilsson (Karolinska Institute, Stockholm, Sweden) for the kind gift of the HMC-1 cells. BV-2 cells were kindly provided by Professor Rosario Donato (Perugia, Italy).

Conflict of interest and funding

This work was funded by grants from the Swedish Research Council (K2011-56X-20676-04-6) and Krefting Foundation against Asthma Allergy. R. C. was funded by Istituto Piemontese per la ricerca sulla Anemia di Diamond-Blackfan, Cariplo and EI.B. by OTKA 84043 and FP7-PEOPLE-2011-ITN – PITN-GA-2011-289033 "DYNANO."

References

1. Théry C, Ostrowski M, Segura E. Membrane vesicles as conveyors of immune responses. Nat Rev Immunol. 2009;9: 581–93.
2. Keller S, Sanderson MP, Stoeck A, Altevogt P. Exosomes: from biogenesis and secretion to biological function. Immunol Lett. 2006;107:102–8.
3. Mathivanan S, Ji H, Simpson RJ. Exosomes: extracellular organelles important in intercellular communication. J Proteomics. 2010;73:1907–20.
4. Ratajczak J, Wysoczynski M, Hayek F, Janowska-Wieczorek A, Ratajczak MZ. Membrane-derived microvesicles: important and underappreciated mediators of cell-to-cell communication. Leukemia. 2006;20:1487–95.
5. Cocucci E, Racchetti G, Meldolesi J. Shedding microvesicles: artefacts no more. Trends Cell Biol. 2009;19:43–51.
6. Stoorvogel W, Kleijmeer MJ, Geuze HJ, Raposo G. The biogenesis and functions of exosomes. Traffic. 2002;3:321–30.
7. van Niel G, Porto-Carreiro I, Simoes S, Raposo G. Exosomes: a common pathway for a specialized function. J Biochem. 2006;140:13–21.
8. Johnstone RM. Exosomes biological significance: a concise review. Blood Cells Mol Dis. 2006;36:315–21.
9. Rajendran L, Honsho M, Zahn TR, Keller P, Geiger KD, Verkade P, et al. Alzheimer's disease beta-amyloid peptides are released in association with exosomes. Proc Natl Acad Sci USA. 2006;103:11172–7.
10. Kalra H, Simpson RJ, Ji H, Aikawa E, Altevogt P, Askenase P, et al. Vesiclepedia: a compendium for extracellular vesicles with continuous community annotation. PLoS Biol. 2012;10: e1001450.
11. Simpson RJ, Mathivanan S. Extracellular microvesicles: the need for internationally recognised nomenclature and stringent purification criteria. J Proteomics Bioinform. 2012;5:ii–ii. doi: 10.4172/jpb.10000e10.
12. György B, Szabó TG, Pásztói M, Pál Z, Misják P, Aradi B, et al. Membrane vesicles, current state-of-the-art: emerging role of extracellular vesicles. Cell Mol Life Sci. 2011;68: 2667–88.
13. Choi DS, Yang JS, Choi EJ, Jang SC, Park S, Kim OY, et al. The protein interaction network of extracellular vesicles derived from human colorectal cancer cells. J Proteome Res. 2012;11:1144–51.
14. de Jong OG, Verhaar MC, Chen Y, Vader P, Gremmels H, Posthuma G, et al. Cellular stress conditions are reflected in the protein and RNA content of endothelial cell-derived exosomes. J Extracell Vesicles. 2012;1:18396.
15. Simpson RJ, Kalra H, Mathivanan S. ExoCarta as a resource for exosomal research. J Extracell Vesicles. 2012;1:18374.
16. Gould SJ, Raposo G. As we wait: coping with an imperfect nomenclature for extracellular vesicles. J Extracell Vesicles. 2013;2:20389.
17. van der Pol E, Böing AN, Harrison P, Sturk A, Nieuwland R. Classification, functions, and clinical relevance of extracellular vesicles. Pharmacol Rev. 2012;64:676–705.
18. Chaput N, Théry C. Exosomes: immune properties and potential clinical implementations. Semin Immunopathol. 2011;33:419–40.
19. van der Pol E, Hoekstra AG, Sturk A, Otto C, van Leeuwen TG, Nieuwland R. Optical and non-optical methods for detection and characterization of microparticles and exosomes. J Thromb Haemost. 2010;8:2596–607.
20. Ekström K, Valadi H, Sjöstrand M, Malmhäll C, Bossios A, Eldh M, et al. Characterization of mRNA and microRNA in human mast cell-derived exosomes and their transfer to other mast cells and blood CD34 progenitor cells. J Extracell Vesicles. 2012;1:18389.
21. Valadi H, Ekström K, Bossios A, Sjöstrand M, Lee JJ, Lötvall JO. Exosome-mediated transfer of mRNAs and microRNAs is a novel mechanism of genetic exchange between cells. Nat Cell Biol. 2007;9:654–9.
22. Turiák L, Misják P, Szabó TG, Aradi B, Pálóczi K, Ozohanics O, et al. Proteomic characterization of thymocyte-derived microvesicles and apoptotic bodies in BALB/c mice. J Proteomics. 2011;74:2025–33.
23. Lässer C. Identification and analysis of circulating exosomal microRNA in human body fluids. Methods Mol Biol. 2013; 1024:109–28.
24. Lässer C, Eldh M, Lötvall J. Isolation and characterization of RNA-containing exosomes. J Vis Exp. 2012;(59):e3037. doi: 10.3791/3037.
25. Droin N, Guéry L, Benikhlef N, Solary E. Targeting apoptosis proteins in hematological malignancies. Cancer Lett. 2013;332: 325–34.
26. Suliman A, Lam A, Srivastava RK. Intracellular mechanisms of TRAIL: apoptosis through mitochondrial-dependent and -independent pathways. Oncogene. 2001;20:2122–33.
27. Berent-Maoz B, Piliponsky AM, Daigle I, Simon HU, Levi-Schaffer F. Human mast cells undergo TRAIL-induced apoptosis. J Immunol. 2013;176:2272–8.
28. Escola JM, Kleijmeer MJ, Stoorvogel W, Griffith JM, Yoshie O, Geuze HJ. Selective enrichment of tetraspan proteins on the internal vesicles of multivesicular endosomes and on exosomes secreted by human B-lymphocytes. J Biol Chem. 1998;273: 20121–7.
29. Bobrie A, Marina Colombo M, Krumeich S, Raposo G, Théry C. Diverse subpopulations of vesicles secreted by different intracellular mechanisms are present in exosome preparations

obtained by differential ultracentrifugation. J Extracell Vesicles. 2012;1:18397.
30. Tatischeff I, Larquet E, Falcón-Pérez JM, Turpin P-Y, Kruglik SG. Fast characterisation of cell-derived extracellular vesicles by nanoparticles tracking analysis, cryo-electron microscopy, and Raman tweezers microspectroscopy. J Extracell Vesicles. 2012;1:19179.
31. Yu X, Harris SL, Levine AJ. The regulation of exosomes secretion: a novel function of the p53 protein. Cancer Res. 2006;66:4795–801.
32. Lespagnol A, Duflaut D, Beekman C, Blanc L, Fiucci G, Marine JC, et al. Exosome secretion, including the DNA damage-induced p53-dependent secretory pathway, is severely compromised in TSAP6/Steap3-null mice. Cell Death Differ. 2008;15:1723–33.
33. Lehmann BD, Paine MS, Brooks AM, McCubrey JA, Renegar RH, Wang R, et al. Senescence-associated exosome release from human prostate cancer cells. Cancer Res. 2008;68:7864–71.
34. Freyssinet JM, Toti F. Membrane microparticle determinatio at least seeing what's being sized! J Thromb Haemost. 201 8:311–4.

***Edit I. Buzás**
Department of Genetics, Cell and Immunobiology
Semmelweis University
Budapest, Nagyvarad ter 4,
1089 Hungary
Email: edit.buzas@gmail.com

***Jan Lötvall**
Krefting Research Centre
University of Gothenburg
BOX 424, SE405 30 Göteborg
Sweden
Email: jan.lotvall@gu.se

Citation: Journal of Extracellular Vesicles 2013, **2**: 20677 - http://dx.doi.org/10.3402/jev.v2i0.20677

3.1.2 Effect of filtration on the purity of exosome fraction: identification of two types of exosome-like vesicles

This project was performed at Krefting Research Centre, Department of Internal Medicine, University of Gothenburg, Sweden under the supervision of Prof. Jan Lötvall.

- **Aim of the project**

The experiments in this section are part of a wide project whose aim was to evaluate the effect of filtration on the purity of the exosome fraction. We were interested to determine how the different centrifugation-based protocols affected the isolation of EV populations and their RNA profile. Differently from the first project whose aim was to evaluate the centrifugation effects of time and speed centrifugation steps, here we focused on the filtration step. Therefore we used the same EXO isolation protocol (Valadi H, 2007) with or without 0.22 μm filter.

- **Experimental plan and methods**

The effect of filtration was investigated in two different types of cells: erythroleukemia cell line TF-1 (ATCC: CRL-2003) and primary cells PBMC (Peripheral blood mononuclear cell). TF-1 were cultured in RPMI-1640 supplemented with 10% foetal bovine serum (FBS), 100 units/ml penicillin, 100 μg/ml streptomycin 2 mM L-glutamine and 5 ng/ml granulocyte macrophage colony-stimulating factor (GM-CSF) (all reagent were from Sigma-Aldrich). PBMC were isolated from human buffy coat using Leucosep® Tubes (Greier Bio-One GmbH) according to the manufacturer's protocol. After two washes in 2 mM EDTA in PBS, PBMC were cultured in RPMI-1640 supplemented with 10% FBS, 100 units/ml penicillin, 100 μg/ml streptomycin and 2 mM L-glutamine. The FBS was ultracentrifuged for 18 hours at 120000 × *g* to eliminate exosomes. Cell viability was determinated using the trypan blue dye method. Cells (TF-1 and PBMC) were cultured for three days. At day three the conditional media was used for exosome isolation. Exosomes were isolated by a differential

ultracentrifugation protocol that was previously described (Valadi H, 2007) (Fig. 8A) and the fixed angle rotor, Ti45, was used. Half of the samples were filtered through a 0.22 µm filter, while the other half was unfiltered. In the filtered samples, two separate pellets were identified. One pellet was attached to the tube and corresponds to the standard exosome pellet and we called "exosomes without filter" (or "EXOs w/o filter"). The second pellet was non-fixed but was collected at the bottom of the tube. We will call "additional pellet" (Fig. 8B). The exosome enriched pellet was also found in the filtered samples and is here called "exosomes with filter" ("EXOs w filter"). The "additional pellet" was not detected in the sample were the 0.22 µm filter was used. However, a sample was collected from the bottom of the tube, as a control (here named "Control region") (Fig. 8B). To characterize the pellets isolated with and without filter, as well as the "Control region", the total RNA was isolated using the miRCURY^{TM} RNA isolation kit – Cell and Plant (Exiqon) according the manufacturer's protocol and analysed on a RNA 6000 Pico Chip using an Agilent 2100 Bioanalyzer (Agilent Technologies) following the manufacture's procedures.

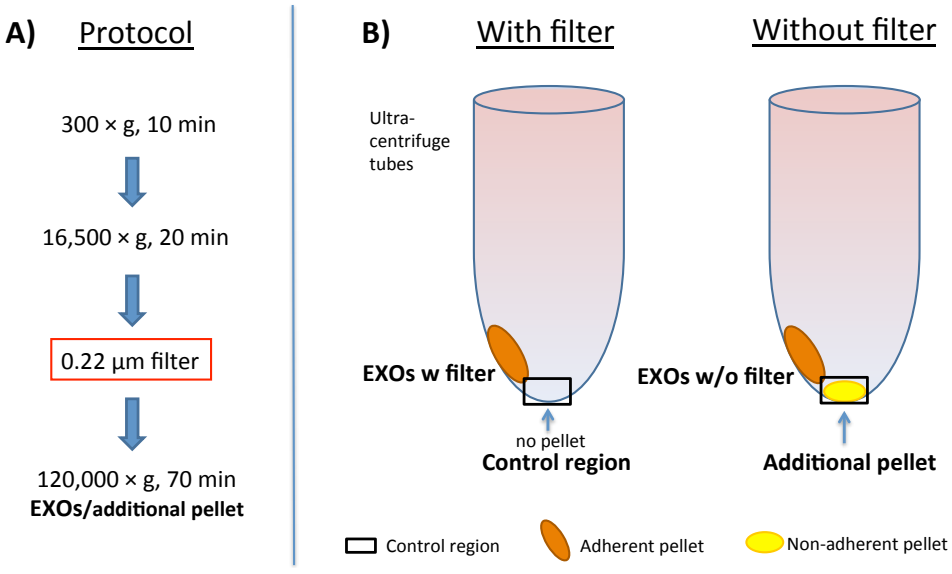

Fig. 8: A) Flow chart describes the differential centrifugation based protocol. Half of the supernatant is filtered through a 0.22 µm filter, while the other half is left unfiltered. B) A schematic representation of the different pellets identified using the protocol shown in figure A with or without the use of filter.

To further characterize and purify the different vesicle types isolated, the "EXOs w filter" and "additional pellet" from TF-1 cells were floated into a sucrose gradient. Sample was dissolved in 2.5 M sucrose and put in ultracentrifugation tubes. Then 15 consecutive 2.2 ml layers of decreasing sucrose concentrations in PBS (2-0.4 M) were layered on top of the sample. Gradients were ultracentrifuged for 16 hours; with no breaks at 4ºC in a SW rotor at 175000 × *g*. Ten fractions were collected and ultracentrifuged in PBS at 120000 × *g* for 70 min in Ti70 rotor. The ten pellets isolated from the sucrose gradient were resuspended in RNA lysis buffer and their RNA profile was analysed using the Bioanalyzer instrument as previously described.

- **Results and discussion**

The pellets were isolated as described and the RNA profiles were analysed. As showed in figure 9A, the exosome pellet from the sample that has been filtrated ("EXOs w filter") contained mostly short RNAs and just small rRNA peaks whereas the sample that was not filtered ("EXOs w/o filter") showed more evident rRNA peaks (18S and 28S). Interestingly, the "additional pellet" contained large rRNA peaks. The "control region" contained no rRNA peaks similarly to the adherent exosome pellet ("EXOs w filter") but with lower RNA concentration. These results were confirmed in primary cells (PBMC) where RNA profile was very similar with that of TF-1 cells (Fig. 9B).

It is clear that, when using 0.22 μm filtration step, vesicles containing rRNA are lost whereas the "additional pellet" obtained without filtration contain rRNA. Small rRNA peaks could be observed in the pellet attached to the wall ("EXOs w/o filter"), indicating a probable contamination from "additional pellet".

These data are consistent with other reports showing that EXO RNA profile is characterized by no or little rRNA, but enriched with small RNAs (Valadi H, 2007), (Miranda KC, 2010).

It could be interesting to investigate the effect of filtration using filters with different sizes. However, there is no consensus about the rRNA EXO content. Some studies demonstrated rRNA peaks in EXOs (Miranda KC, 2010), others did not (Valadi H, 2007), (Lässer C A. V., 2011). Similarly, there is no consensus about using or not a filtration step and pore size. Our results demonstrated that the differences shown in exosome studies could be due not only to a different EXO origin, but also to the different filter used. Other explanations about differences in EXO RNA profiles could be due to the centrifugation rotor used: it is impossible to separate adherent and non adherent pellet using a swinging bucket rotor. Furthermore, particles size analysis could be useful to understand why "additional pellet" was stopped in the filter. It is possible that this behaviour was due to the higher size of the particles composing the "additional pellet", but surface charge and protein composition need to be investigated.

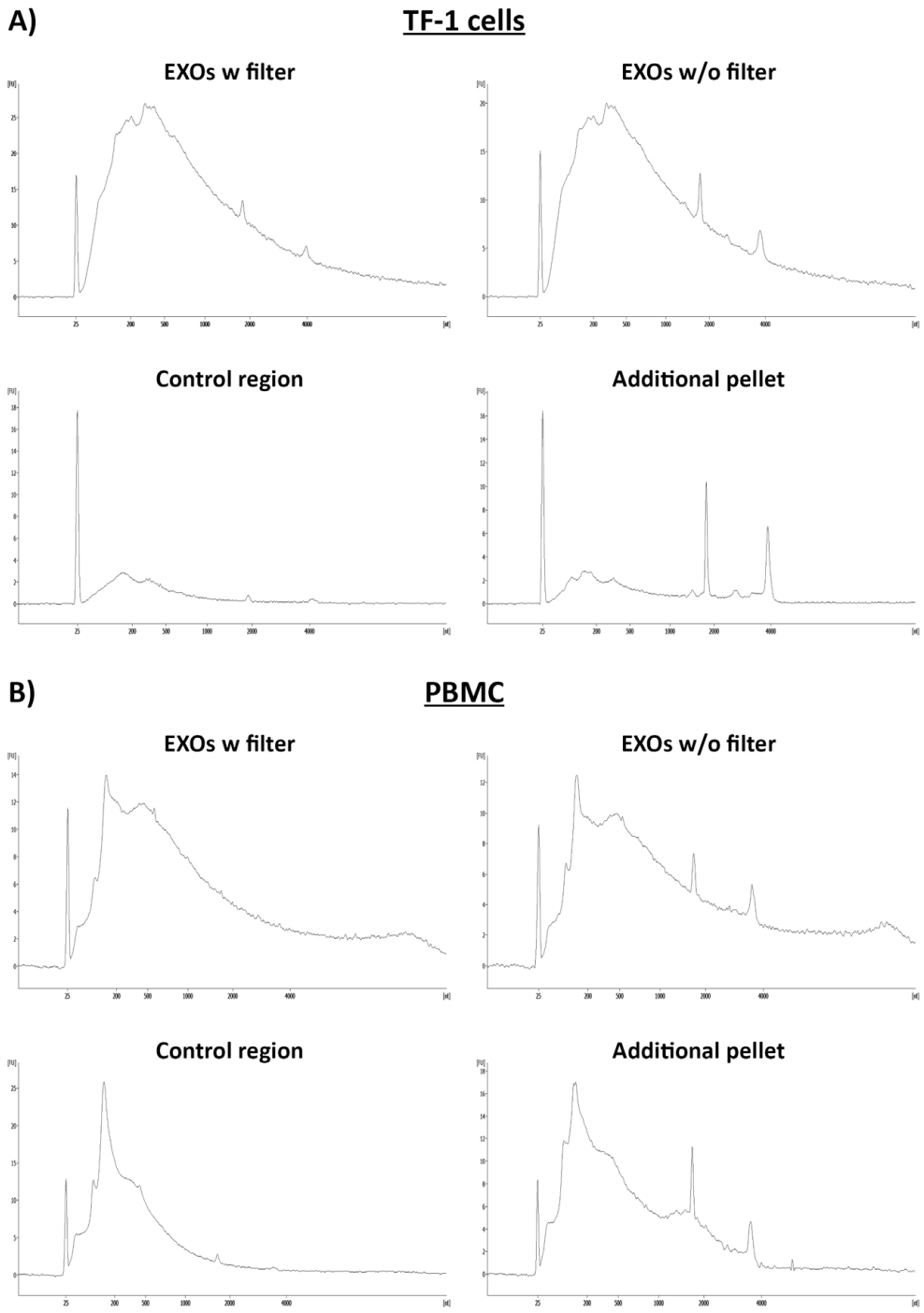

Fig. 9: RNA profiles of "EXOs w filter", "EXOs w/o filter", "Control region" and "Additional pellet". A) RNA profiles were analysed in the four pellets isolated from TF-1 cells B) and primary cells (PBMC: peripheral blood mononuclear cells). RNA profiles are representative of three experiments.

To further purify and characterize these pellets, the adherent pellet obtained with filtration ("EXO w filter") and the pellet collected at the bottom of tube not using filter ("additional pellet") were loaded on sucrose gradient and RNA profile was analysed. The results are shown in figure 10. In "EXO w filter", small RNA was found in fractions 8-10 (1.24-1.31 g/cm^3). The density range was calculated as the average of three different experiments (collaboration with Cecilia Lässer – Kreafting Research Centre, Gothenburg). Interestingly, the RNA from the additional pellet showed both rRNA-positive and -negative fractions. In particular, the rRNA peaks were mainly found in fractions 3-6, (1.12-1.21 g/cm^3) whereas the small RNA peaks, similar to what observed in "EXO w filter", were mainly detected in fractions 8-10. These results indicate that rRNA-negative vesicles have lower density, while the rRNA-positive vesicles have higher density. In conclusion, our data show that the inclusion of a sucrose gradient step after centrifugation allows a further vesicle separation.

Although EXO density was considered to be between 1.13-1.19 g/cm^3, several studies demonstrated that they have a higher density (Caby MP, 2005), (Vella LJ, 2008). Our results show that EXO density could be different from what indicated so far.

A lipidic and protein composition analysis needs to be done to better characterize these two exosome-like vesicles.

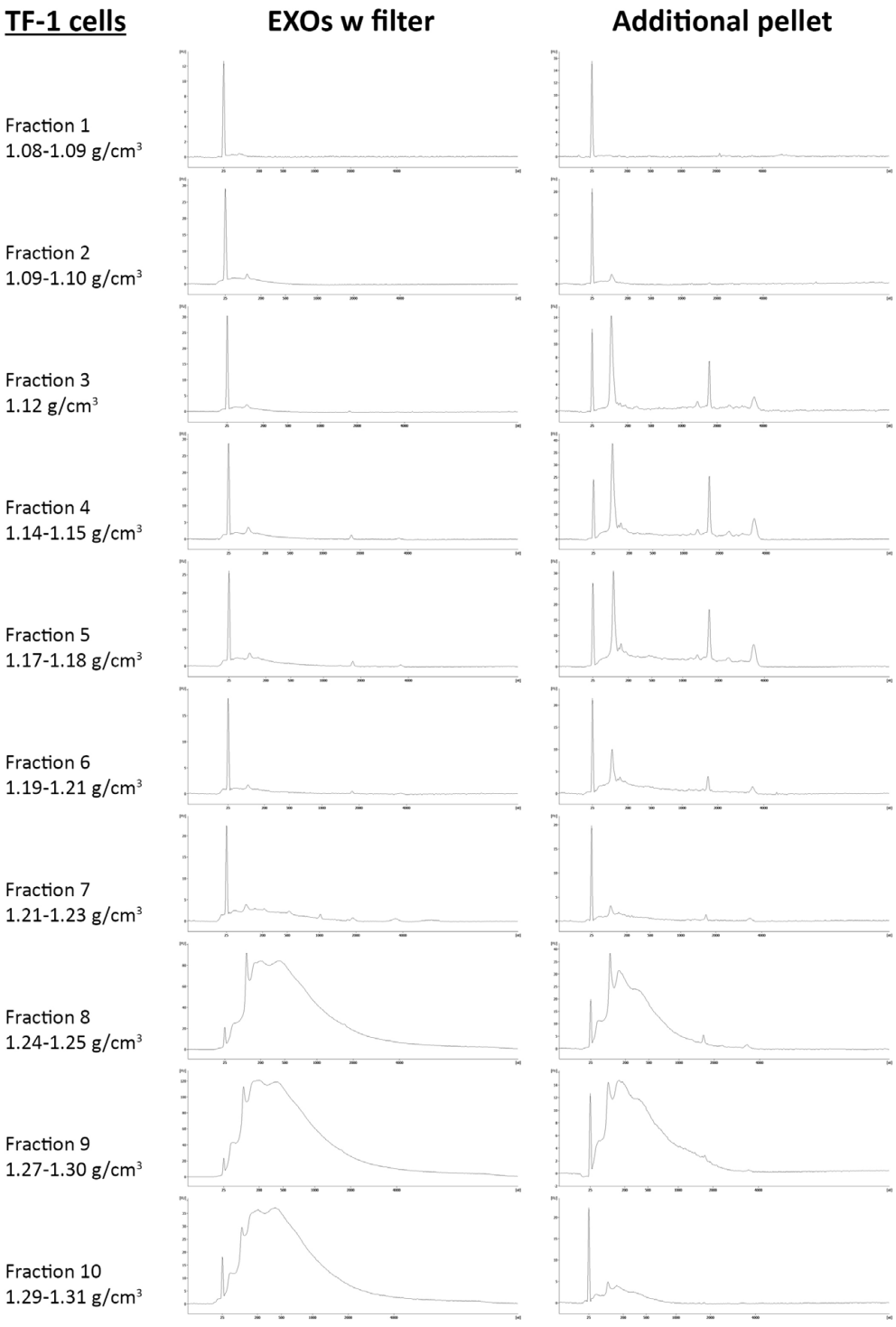

Fig. 10: RNA profiles from ten fractions obtained loading "EXOs w filter" and "Additional pellet" on a sucrose gradient. "EXO w filter" and "Additional pellet" were isolated from TF-1 cells supernatant. RNA profiles are representative of two experiments.

3.1.3 RNA characterization in EV subpopulations: RNA profile comparison between exosomes-like vesicles and ABs, MVs and EXOs

This project was performed at Krefting Research Centre, Department of Internal Medicine, University of Gothenburg, Sweden under the supervision of Prof. Jan Lötvall.

- **Aim of the project**

The data presented in the previously fraction of this thesis show that EV subpopulations need to be further characterized and distinguished. The general perception is that authors often investigated the same type of vesicles, but called them in different ways. Furthermore, specific EV characteristics are still not well documented and we cannot exclude that similar features could be showed by different vesicle types. To investigate this hypothesis, we loaded the following subpopulations on sucrose gradient: ABs, MVs, EXOs (isolated using a centrifugation protocol) as well as "EXO w filter" and "additional pellet" obtained using and not using filter. We compared RNA profiles from ten fractions obtained from each samples.

- **Experimental plan and methods**

ABs, MVs and EXOs as well as "EXOs w filter" and "additional pellet", were isolated from supernatant of TF-1 cells. TF-1 (ATCC: CRL-2003) were cultured in RPMI-1640 supplemented with 10% foetal bovine serum (FBS) 100 units/ml penicillin, 100 µg/ml streptomycin 2 mM L-glutamine and 5 ng/ml GM-CSF (all reagent were from Sigma-Aldrich). The FBS was ultracentrifuged for 18 hours at 120000 × *g* to eliminate exosomes. Cells were cultured for three days. At day three the conditional media was used for EV isolation. ABs, MVs and EXOs were isolated by a differential ultracentrifugation protocol. A modified protocol from Valadi *et al* (Valadi H, 2007) was used (protocol A). Briefly, the 2000 × *g* step was added to the original protocol, aiming to separate ABs and MVs otherwise collected in the same pellet in the original protocol (Fig. 11A). Protocol B was used to

obtain "EXO w filter" and "additional pellet" with or without a 0.22 µm filter as described in the previous section (Fig. 11B). Protocols A and B were described in Crescitelli *et al* 2013 and in the previously section of this thesis.

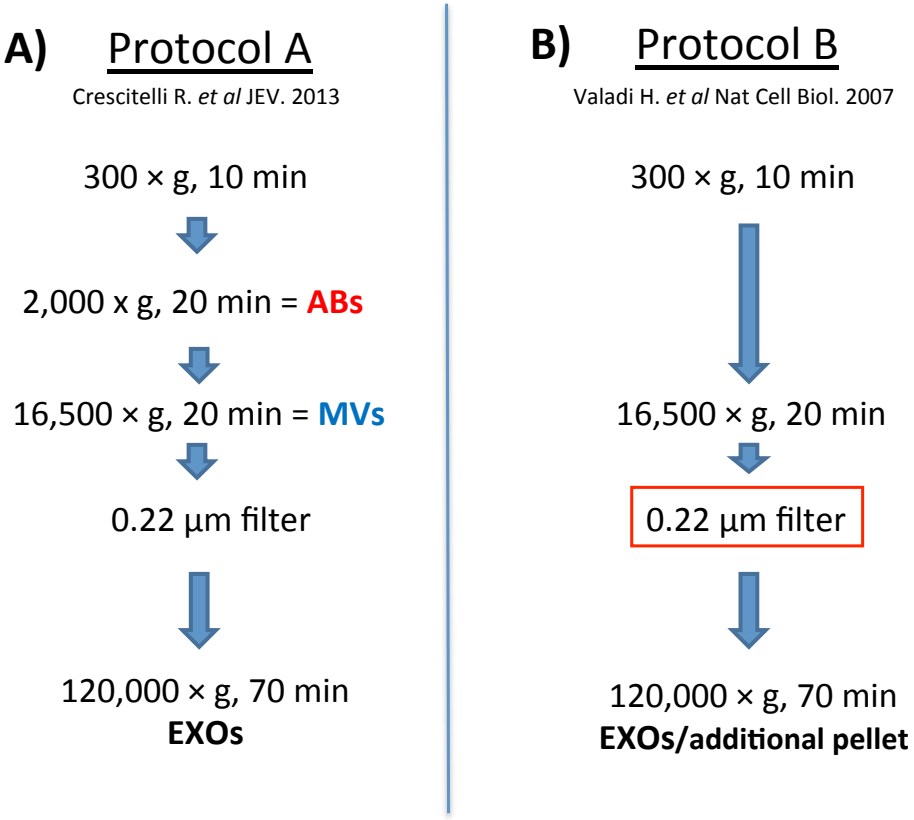

Fig. 11: Flow chart reporting two differential centrifugation-based protocols. A) ABs, MVs and EXOs are isolated at different centrifugation steps using protocol A. B) Protocol B is used to isolate EXO pellet including 0.22 µm filtration step. The same protocol is applied without a filtration step to isolate EXOs ("EXOs w/o filter") and "Additional pellet".

EVs collected were floated into a sucrose gradient. Pellets were resuspended in 2.5 M sucrose in PBS and transferred to ultracentifugation tubes. Fifteen consecutive 2.2 ml layers of decreasing sucrose concentrations in PBS (from 2-0.4 M) were layered on top of the samples. Gradients were ultracentrifuged for 16 hours, with no breaks at 4ºC in a SW rotor at 175000 × *g*. Ten fractions were collected and ultracentrifuged in PBS at 120000 × *g*

for 70 min in Ti70 rotor. The total RNA was isolated from ten pellets using the miRCURY^{TM} RNA isolation kit – Cell and Plant (Exiqon) according the manufacturer's protocol and analysed on a RNA 6000 Pico Chip using an Agilent 2100 Bioanalyzer (Agilent Technologies) following the manufacturer's procedures.

- **Results and discussion**

The RNA profile analysis of the ten AB fractions showed that all of them contain RNA but with the different profiles (Fig.12). This heterogeneity parallels the morphological heterogeneity shown at electron microscopy (Crescitelli R. 2013, Fig. 5 A1-A3). The rRNA is only contained in fraction 4-6 with very small peaks. This is very far from what expected. ABs pellet are known to contain very prominent rRNA peaks (Crescitelli R, 2013), but these experiments show that the rRNA peaks are not so evident. rRNA could be outside of vesicles. If this is the case, rRNA not protected by lipid membrane, could be degraded during the sucrose layers preparation and the very long centrifugation. Regarding density, our results are consistent with Thery *et al* that described AB density between 1.16-1.28 g/cm^3 (Théry C B. M.-C., 2001).

MV density is not known. Sucrose gradient was performed and RNA profiles from ten fractions analysed. The comparison with fractions separated from "additional pellet" is shown in figure 13. MV pellet seems to include two different kinds of vesicles. When loaded on sucrose gradient, rRNA-positive vesicles were identified mainly in fractions 2-7 (1.12-1.23 g/cm^3) similar to what observed in "additional pellet", whereas RNA-negative vesicles were found in lower fractions 8-10 (1.24-1.31g/cm^3), as showed for "additional pellet". MV and "additional pellet" fractions seem to be very similar in vesicle composition (rRNA-positive and rRNA-negative vesicles), but MV pellet seems to be more heterogeneous. In the "additional pellet", two vesicle populations appear well separated (fractions 2-6 (1.09-1.23 g/cm^3) rRNA-positive vesicles, fractions 8-10 (1.24-1.31 g/cm^3) rRNA-negative vesicles).

In these experiments, pellets have been extracted from TF-1 cells supernatant. In agreement with results showed in Crescitelli *et al,* 2013, MVs from TF-1 cells show rRNA peaks. Since MVs from HMC1 cells did not contain rRNA peaks (Crescitelli R, 2013), it should be interesting to compare RNA profiles in MV and "additional pellet" fractions shed from HMC1 cells where the absence of rRNA is expected (Crescitelli R, 2013).

Fractions obtained from EXO pellet are composed only by rRNA-negative vesicles and they were found in fractions 8-10, the same rRNA-negative fractions were detected in "EXO w filter" loaded on sucrose gradient (Fig. 14). This result was expected because the protocols used were exactly the same at this centrifugation step (120000 × *g* after filtration step).

The results confirmed that there is a density overlap between different vesicles. This underlines the nomenclature problem. In fact, what we indicated as MVs using protocol A seems to be the same pellet extract using protocol B ("additional pellet") without filtration step (Fig. 8 and Fig. 11).

In conclusion, the isolation and characterization of EV subpopulations is a still open challenge. Other investigations such as transcriptomic and proteomic analyses may be used to distinguish different vesicle types.

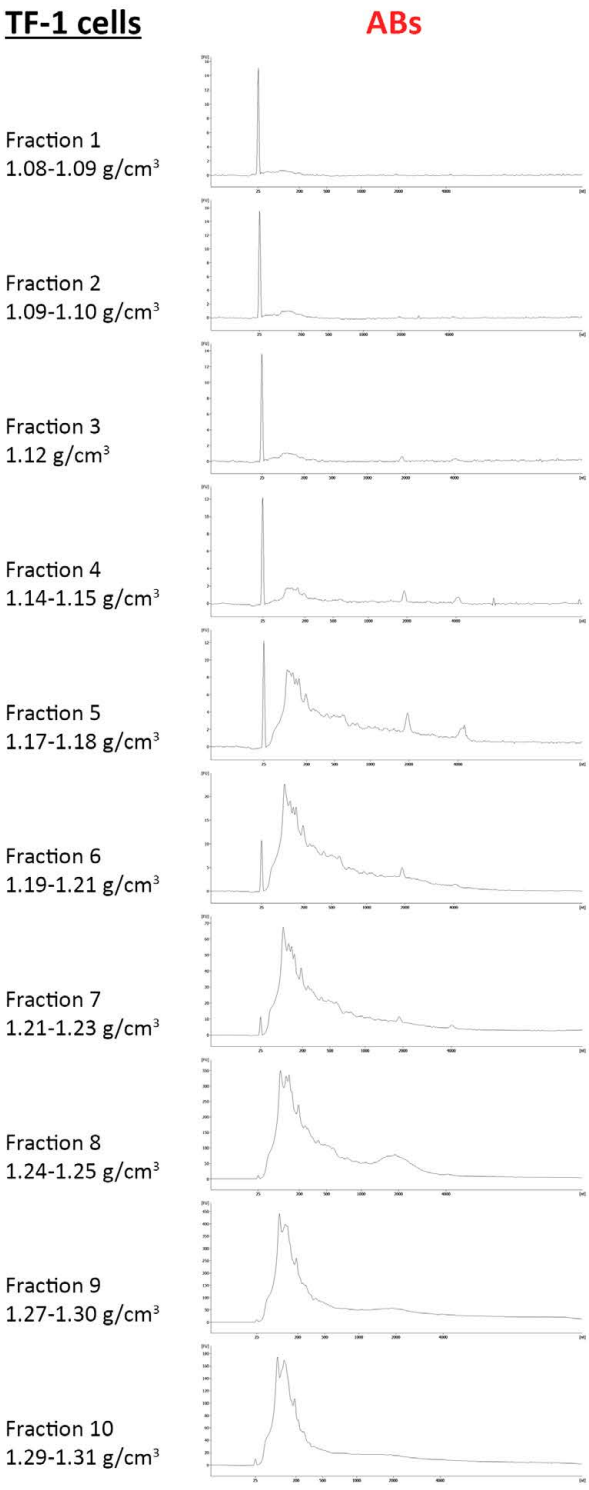

Fig. 12: RNA profiles from ten fractions obtained after loading AB pellet on sucrose gradient. ABs were extracted from TF-1 cells supernatant. RNA profiles are representative of two experiments.

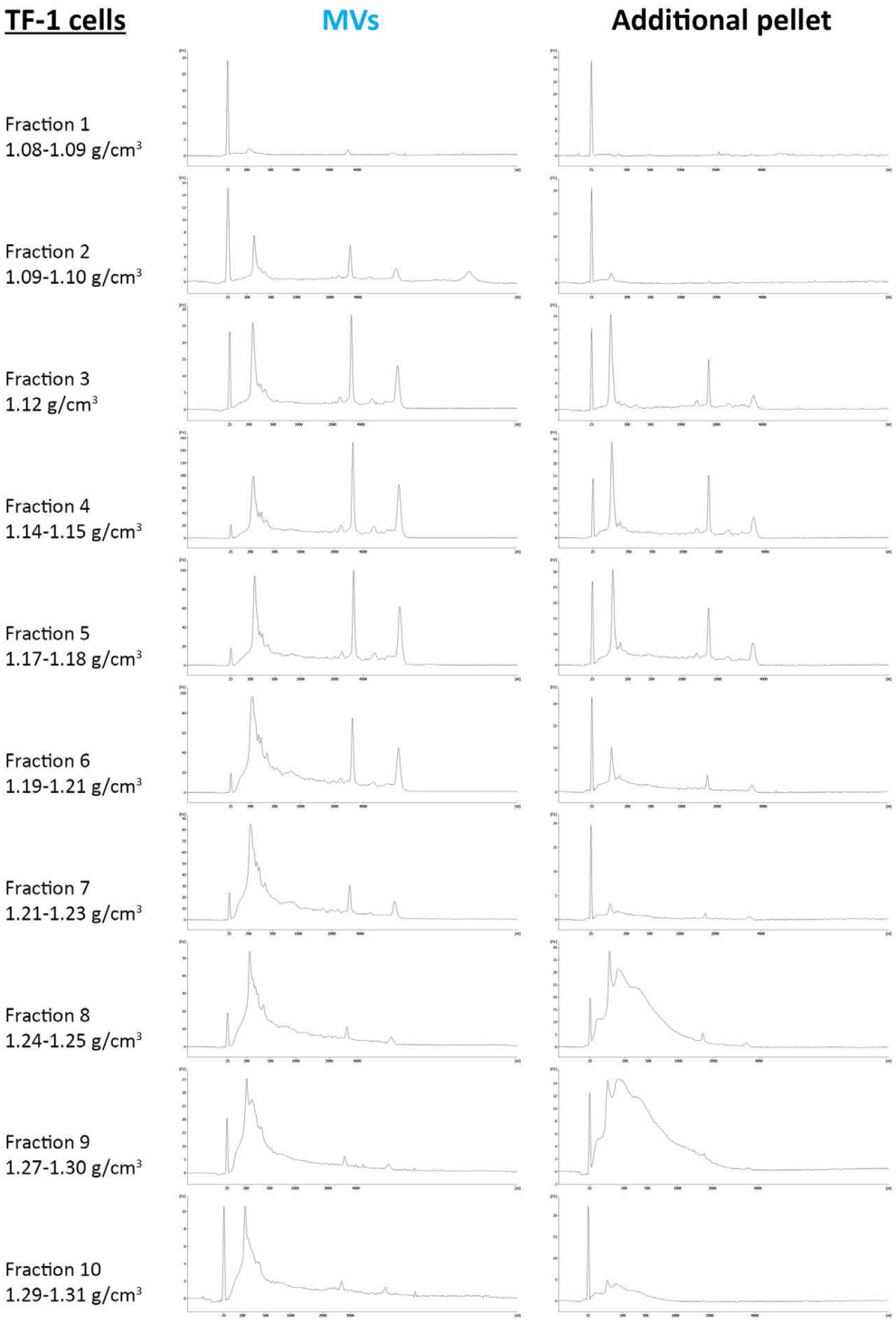

Fig. 13: RNA profiles from ten fractions obtained after loading MV pellet on sucrose gradient. The comparison with the fraction obtained from "Additional pellet" is shown. MVs and "Additional pellet" were extracted from TF-1 cells supernatant. RNA profiles are representative of two experiments.

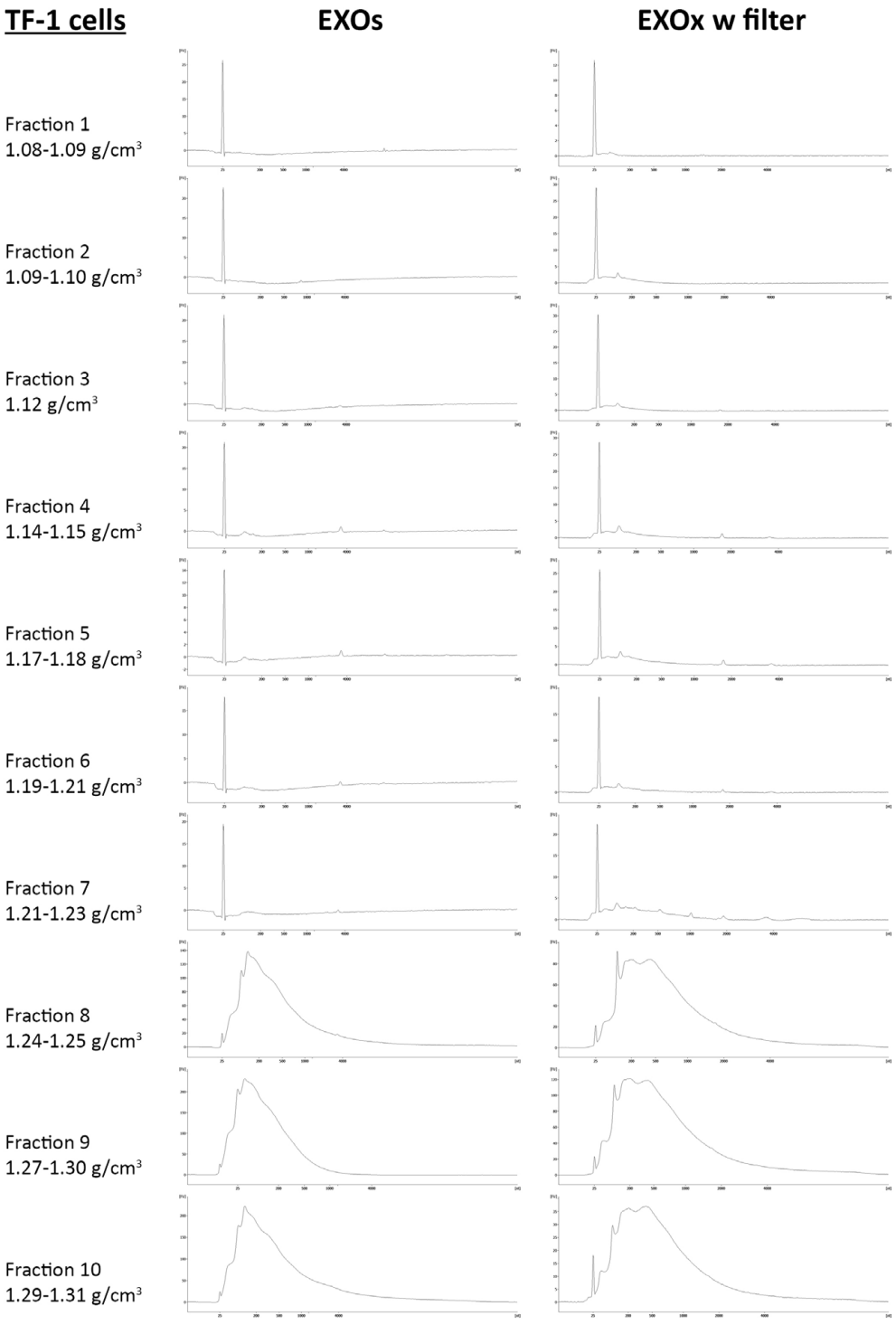

Fig. 14: RNA profiles from ten fractions obtained after loading EXO pellet on sucrose gradient. The comparison with fractions obtained from "EXO w filter" is shown. EXOs and "EXOs w filter" were extracted from TF-1 cells supernatant. RNA profiles are representative of two experiments.

3.2 Study of extracellular vesicles in ribosomal stress

Vesicle production is induced by p53 activation in response to different stress types (hypoxia, low PH level, oxidative, thermal stress, radiation, shear stress and drugs effect) (Wysoczynski M, 2009), (Zhang HC, 2012), (King HW, 2012), (Parolini I, 2009), (Eldh M, 2010), (Hedlund M, 2011), (Zhan R, 2009), (Clayton A T. A., 2005), (Chen T, 2011), (Miyazaki Y, 1996).

Moreover, p53 activation is also caused by "ribosomal stress", a condition caused by aberrant ribosome biogenesis (Pestov DG, 2001), (Rubbi CP, 2003). Consequently, defects of ribosome biogenesis lead to a number of ribosomal diseases (Raiser DM, 2013). Diamond Blackfan Anemia (DBA) is the first human disorder discovered in this group.

To date, there are no studies about vesicle production in ribosomal stress. To analyse EV production during ribosomal stress, we carried out the following objectives:

1. We investigated EV miRNAs composition in $CD34^+$ cells after induction of ribosomal stress due to silencing of RPS19 (DBA cell model) because miRNAs are the EV principal component (Valadi H, 2007), (Lässer C, 2013) and the alteration in miRNA profile reflects the cell host condition (Théry C Z. L., 2002), (Mathivanan S J. H., 2010)
2. We evaluated EVs in blood from patients with DBA to better understand the pathogenesis of DBA and to develop a diagnostic test.

3.2.1 MicroRNA signature in MVs/EXOs shed from CD34+ cells down-regulated for RPS19 (DBA cell model)

This project was performed in collaboration with Prof. Yong Song Gho and co-workers who performed statistic analysis (Department of Life Science,

Pohang University of Science and Technology, Pohang, Kyungbuk, Republic of Korea) and with Prof. Antonia Follenzi who improved the viral construct (Department of Health Science, University of Eastern Piedmont "Amedeo Avogadro", Novara, Italy).

- **Aim of the project**

EV content is representative of host cell and any perturbations in the homeostasis result in alterations of EV content (Skog J, 2008). From 2007 when Valadi and colleagues demonstrated that EXOs released from human and murine mast cell lines contain miRNA molecules (Valadi H, 2007), many researchers focused on the investigation of miRNA release in vesicles (Bellingham SA, 2012), (Hunter MP, 2008), (Lässer C A. V., 2011). miRNA expression changes have been demonstrated in many diseases (Zang W, 2013), (Sayed AS, 2013). miRNAs are released by cells not only within EXOs (Mathivanan S L. J., 2010), but also within MVs (Ratajczak J., 2006) and ABs (Zernecke A, 2009).

In this project, we investigated miRNA signature in MVs and EXOs released in ribosomal stress. For this purpose, we used $CD34^+$ cells silenced for RPS19. After miRNA extraction from MVs and EXOs the intra-vesicles miRNome was identified.

- **Experimental plan and methods**

$CD34^+$ cells were purified from cord blood collected from healthy donors. Mononuclear cells were isolated by Ficoll-Paque™ Premium (GE Healthcare), and then $CD34^+$ cells were separated by immunomagnetic procedure (Miltenyi Biotech) and cultured in StemSpan® Serum-Free Expansion Medium (SFEM) (STEMCELL Technologies) in the presence of SCF (50ng/ml), Flt3-L (50ng/ml), TPO (20ng/ml), IL-3 (10ng/ml) and IL-6 (10ng/ml) (all cytokines were from ImmunoTools).

To transiently silence RPS19, $CD34^+$ cells were transduced with 70 MOI (Multiplicity Of Infection) of a third generation pCCL lentivirus vector (Follenzi A, 2000), expressing scramble or RPS19 shRNA (Miyake K, 2005). $CD34^+$ cells transduced by RPS19 shRNA are indicated as $CD34^+C$,

whereas, $CD34^+$ cells transduced with the virus expressing scramble shRNA are called $CD34^+S$ and were used as negative control. Transduction efficiency was evaluated after three days by detection of GFP with a FACSCalibur flow cytometer (BD Biosciences). Cells were cultured four days after transduction and then RNA was extracted from MVs and EXOs shed from cells. To analyze vesicular miRNAs, a method based on filter isolation of vesicles has been used. This method is based on size only, thus vesicle characterization is less accurate than that obtained using the procedures reported in section 3.1 of this thesis. We used ExoMir™ PLUS Kit (Bioo Scientific) according to the manufacturer's protocol. Briefly, using this kit, cell supernatant is passed over three syringes filters connected in series; the top filter (filter 1) has pore size of ~700 nm, the middle filter (filter 2) has a pore size of ~200 nm, and the bottom one (filter 3) has the smallest pore size of ~20 nm. RNAs from captured particles were extracted flushing filters with a RNA lysis buffer included in the kit. Only RNA samples extracted from filter 2 and filter 3 were used for miRNA array analysis. In this work, particles captured by filter 2 are within the size of microvesicles (MVs, with a size of 700-200 nm) whereas those ones from filter 3 are in the range size of exosomes (EXOs, with a size of 200-20 nm) (Crescitelli R, 2013).

To evaluate RNA quality and concentration, RNA samples were analysed with Agilent 2100 Bioanalyzer (Agilent Technologies) following the manufacturer's procedures. Then, 100 ng of RNA from MVs and EXOs were analysed using The Nanostring® nCounter system (Nanostring® Technologies). RNA was incubated in presence of miRNA specific capture and reporter probes. Non-hybridized probes were removed and the purified hybridized complexes were immobilized and aligned for data collection as previously reported (Geiss GK, 2008). The Nanostring® nCounter miRNA Expression Assay Kit allows miRNA profiling with superior specificity and sensitivity and with lower cost than microarrays. The nCounter Analysis System delivers direct, multiplexed measurement of miRNA expression, providing digital readouts of the relative abundance of 800 miRNAs

simultaneously. The system is based on target-specific probe pairs that are hybridized to the sample in solution.

RNA expression was normalized by quantile normalization with MATLAB (version 2010a). Significant miRNA changes were selected using the following criteria:

- Statistical significance – miRNA expression changes were identified using a *p*-value threshold of 0.05;
- Fold change expression – a minimum of 1.5-fold difference in either direction was required.

Fold changes (log_2-ratio) were calculated also by MATLAB (version 2010a). Quality control was performed not only by depicting the *scatter plots* of relative RNA expression, but also by performing principal component analysis (PCA), which is provided by MATLAB (version 2010a). The PCA has been performed on three independent experiments. PCA analysis showed that miRNA expressions in MVs shed from $CD34^+S$ in experiment three were outliers (probably because of RNA degradation). This experiment was disregarded before further analysis.

- **Results and discussion**

We used an innovative method to obtain a miRNA signature from MVs and EXOs released in ribosomal stress. miRNAs that were included in MVs/EXOs released during ribosomal stress ($CD34^+C$) were compared with those identified in their scramble control ($CD34^+S$). As shown in figure 15, similar overall patterns were observed both in MVs and EXOs. Both comparisons showed and high correlation: ρ =0,9065 in MVs C *vs* MVs S and ρ =0,8984 in EXOs C *vs* EXOs S.

Setting up the statistic significance (*P*-value=0.05) and the fold change (<-0.5 or >0.5), *volcano dot plot* was obtained illustrating the overall pattern of miRNAs (Fig. 16). Specifically, in MVs C versus MVs S, three miRNA were up-regulated (miR-412, miR-1281, miR-1273f) and eight were down-regulated (miR-153, miR-1248, miR-526b-5p, miR452-5p, miR-105-5p, miR-374a-5p, miR-148a-3p and miR-588).

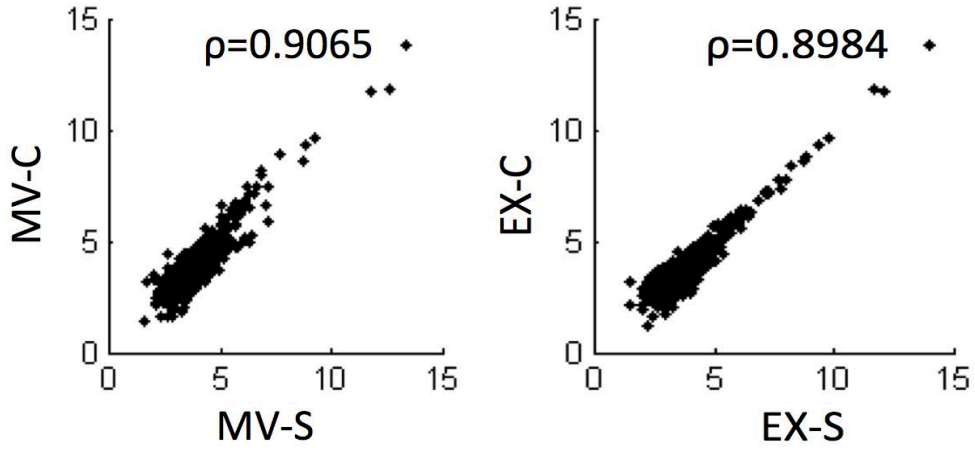

Fig 15: Correlation between miRNA expression in MVs and EXOs shed from RPS19 silenced cells (C) *vs* scramble control (S). Each dot represents one miRNA with its respective mean log2 intensity in different samples. Spearman correlation coefficient (ρ) is indicated.

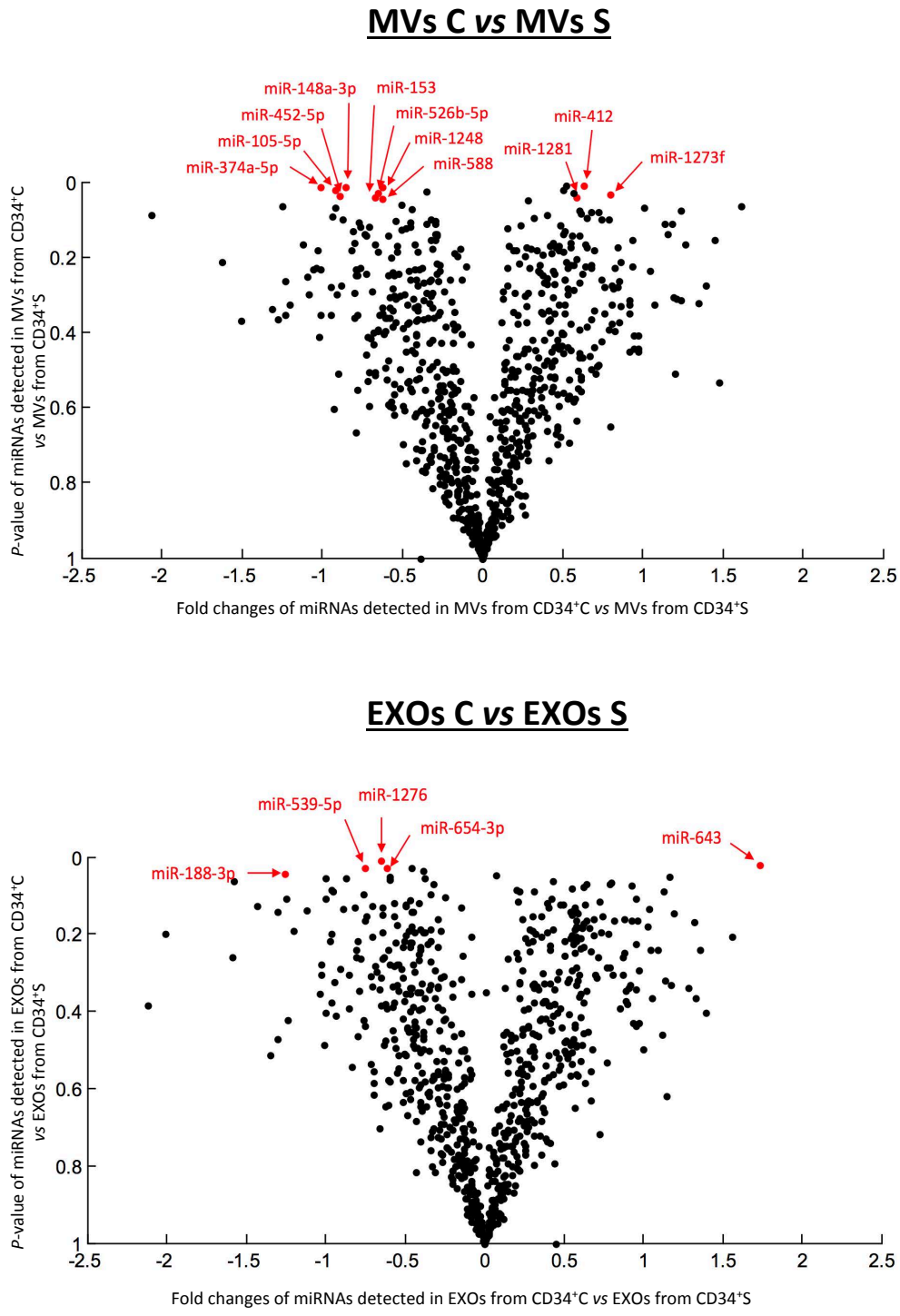

Fig. 16: miRNAs signature in MVs and EXOs shed from CD34$^+$ cells silenced for RPS19 (MVs/EXOs C) compared with negative control (MVs/EXOs S). Probe sets corresponding to miRNAs from different vesicles (MVs and EXOs) and different conditions (C and S) are displayed on *volcano plot*. The miRNAs with high fold change (*x*-axis, fold-change >1,5 or fold change <-1,5) and low *p*-value (*y*-axis, $p<0.05$) are annotated and indicated in red.

Comparing miRNAs changed in EXOs C versus EXOs S, just one miRNA showed to be up-regulated (miR-643), whereas four miRNAs were down-regulated (miR-654-3p, miR-1276, miR-539-5p and miR-188-3p).
Abnormally expressed miRNAs are listed in table 1 (*P*-value and fold change for each miRNA are indicated). Fold change variations are shown in figure 17A-B. The different pattern for MVs and EXOs reflects the different biological processes in EV production and in cargo loading.

Table 1: Up- and down-regulated miRNAs in MVs and EXOs shed from cells silenced for RPS19 (MVs C *vs* MVs S and EXOs C *vs* EXOs S)

miRNAs	*P*-values	Fold changes C *vs* S
MVs up-regulated		
hsa-miR-412	0,0087	0,6
hsa-miR-1281	0,0392	0,6
hsa-miR-1273f	0,0349	0,8
MVs down-regulated		
hsa-miR-153	0,0423	-0,7
hsa-miR-1248	0,0453	-0,6
hsa-miR-526b-5p	0,0298	-0,7
hsa-miR-452-5p	0,0353	-0,9
hsa-miR-105-5p	0,0231	-0,9
hsa-miR-374a-5p	0,0119	-1,0
hsa-miR-148a-3p	0,0144	-0,9
hsa-miR-588	0,0153	-0,6
EXOs up-regulated		
hsa-miR-643	0,0200	1,7
EXOs down-regulated		
hsa-miR-654-3p	0,0281	-0,6
hsa-miR-1276	0,0098	-0,6
hsa-miR-539-5p	0,0290	-0,8
hsa-miR-188-3p	0,0419	-1,3

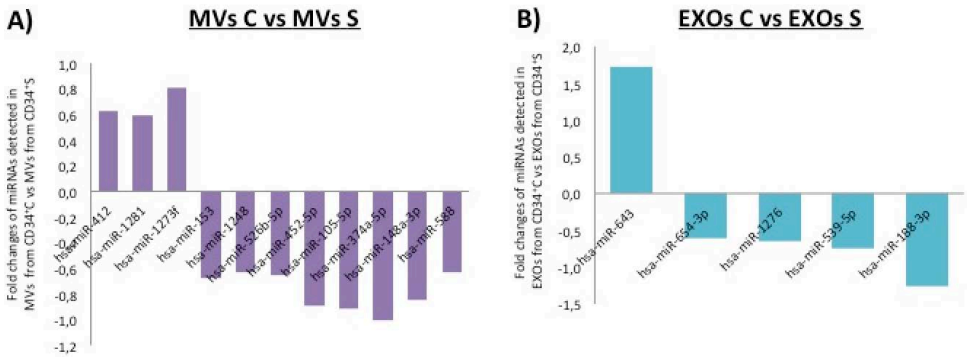

Fig. 17: Fold-change variations between miRNAs in vesicles shed from CD34+ silenced for RPS19 (C) versus negative control (S). A) miRNAs that vary in MVs and B) in EXOs. Only significant variations (P<0.05) are presented.

Most of the altered miRNAs (miR-412, miR-1281, miR-153, miR-526b-5p, miR-452-5p, miR-105-5p, miR-374a-5p, miR-148a-3p, miR-643, miR-654-3p, mir-1276, mir-539-5p and mir-188-3p) are listed in EVpedia (http://www.evpedia.info), the most accurate database of molecules enriched in EVs.

To understand more thoroughly how these miRNAs may contribute to pathways activated in ribosomal stress, we examined miRNA targets as predicted using TargetScan 6.2. Unfortunately, not all 16 miRNAs are listed in this database or some of them are annotated in other species. We identified 752, 148 and 697 genes that were predicted to be targeted by miR-153, mir-588 and miR-539-5p respectively. Setting up the total context score+ <-0.31, no overlap among target genes from these three different miRNAs have been found. However, one gene was targeted both by miR-539-5p and miR-153 i.e. BTBD7, a regulatory gene involved in embryonic development of mammalian salivary glands and lungs (Onodera T, 2010) and in hepatocellular carcinoma progression (Tao YM, 2013).

Several altered miRNAs are related to haematopoiesis and blood cells such as miR-155 (Georgantas RW 3rd, 2007), miR-15b, miR-16, miR-221, miR-185 and many others (Choong ML, 2007). A study focused on miRNA expression in blood cell lineages and stages of hematopoietic stem cell

differentiation demonstrated that miR-148a have a role in DNA methylation of CD34+ cells (Merkerova M, 2010).

Many miRNAs found in our analysis are included in human cancer signatures. For example, miR-412 and miR-1281 are found to be involved in lung cancer (Gao W, 2011) and muscle-invasive bladder cancer (Pignot G, 2013) signature respectively. miR-452 is involved in hepatocarcinoma (Chiu LY, 2013) and breast cancer (van Schooneveld E, 2012), whereas miR-374a is up-regulated in osteosarcoma cell lines (Namløs HM, 2012) and in follicular lymphoma (Wang W, 2012). Furthermore, a potential diagnostic use was proposed for miR-1248, miR-526b-5p and miR-452 in asthma (Panganiban RP, 2012), pregnancy (Kotlabova K, 2011) and uveal melanomas (Ragusa M, 2013) respectively.

Interestingly, two of these miRNAs are involved in cell death i.e. miR-412 (Melamed Z, 2013) and miR-153 (Wu Z, 2013). Melamed *et al* demonstrated that tissue-specific alternative splicing regulates maturation of miR-412, whose targets encode a protein network involved in neuronal cell death processes (Melamed Z, 2013).

miR-153 is the only one whose gene targets are predicted in three databases (TargetScan, MicroCosm and PicTar). miR-153 has an anti-apoptotic function. In breast cancers cells a decrease of miR-153 expression increased apoptosis and inhibited proliferation (Anaya-Ruiz M, 2013). Differently, other authors demonstrated that miR-153 is over-expressed in prostate cancer, where it induces cell cycle transition and cell proliferation. miR-153 up-regulation promotes cell proliferation through down regulation of its target PTEN. Consequently to PTEN decrease, cyclin D1 is overexpressed and p21(Cip1) down-regulated (Wu Z, 2013). miR-153 is down-regulated in MVs shed from CD34+ cells after RPS19 silencing, but we do not know if it has the same behaviour within these cells. Thus, miR-153 levels need to be evaluated in these cells. If miR-153 levels are decreased also in cells, this miRNA may have a role in DBA by inducing apoptosis. Interestingly, PTEN may have an important role in ribosomal stress because of its ability to repress RNA polymerase I transcription and indirectly regulate rRNA

transcription (Zhang C, 2005). Furthermore, PTEN regulates expression of genes involved in apoptosis via Bcl2 and Mcl1 in glioblastoma cell line (Xu J, 2011). It controls FOXO1 expression in endometrial cancer cell lines (Myatt SS, 2010). miR-153 involvement in stretch stress (Song L, 2012) could support its role in other stress types such as ribosomal stress.

In conclusion, a miRNA signature in MVs and EXOs released in ribosomal stress has been identified. These results need to be validated using other methods such as qRT-PCR. Functional analyses are also mandatory. Assays such as MTT, colony formation and BrdUrd incorporation may be performed to investigate miRNAs involved in cell proliferation. Investigation of miRNAs from EVs could be useful to shed light on molecular process involved in ribosomal stress and to understand pathophysiology of DBA.

3.2.2 Diagnostic potential of extracellular vesicles – characterization and quantification of microparticles in patients with Diamond Blackfan Anemia (DBA)

This project was performed in collaboration with Prof. Giorgio Bellomo and co-workers, (Chemical Clinical Analysis laboratory, SCDU, Azienda Ospedaliera Universitaria Maggiore della Carità, Novara, Italy) and with Prof. Ugo Ramenghi and co-workers, (Department of Pediatric and Public Health, University of Turin, Torino, Italy).

- **Aim of the project**

The finding of abnormalities in vesicles shed from cells representing a model for DBA prompted us to explore the diagnostic potential of erythroid vesicles in patients with DBA.

DBA is a genetic disorder induced by a defect in ribosome biogenesis. It is characterized by a deficiency of red cell progenitors, that show a pro-apoptotic phenotype and die in the bone marrow. One of the major factors

limiting DBA research has been the inability to study the patients' erythroid progenitors in the bone marrow.

Our hypothesis was that peripheral blood from DBA patients contained EVs derived from erythroid progenitors. A quantification and a detailed characterization of these EVs could be useful not only to investigate the pathophysiology of the disease, but also as a useful tool for diagnosis.

It is important to note that the isolation of microvesicles derived from erythroid precursors has never been attempted so far.

To test our hypothesis, EVs were collected from blood of patients with DBA and appropriate controls. Vesicle markers were then studied by flow cytometry.

- **Experimental plan and methods**

In this section I will refer to EVs as microparticles (MPs) because EVs from blood are commonly named in this way in literature. MPs corresponding to vesicles have a size less than 1000 nm (Simak J, 2006) (Freyssinet JM, 2010), (Hargett LA, 2013), (Rubin O, 2012).

Peripheral blood samples were drawn from healthy controls (*n*=19), patients with non-DBA haematological disease (*n*=10) and patients with DBA (*n*=8). All patients or their parents signed and informed consent form (Department of Pediatric and Public Health, University of Turin, Italy). Venipuncture was performed using Safety-Lok^{TM} Blood Collection Set (Becton Dickinson Vacutainer®) and blood samples collected in sodium citrate (3.2%) tubes (2.7ml). MPs were isolated using differential-centrifugation steps. Blood was centrifuged at 2400 × *g* for 10 min at RT, plasma without platelets (about 2ml) was centrifuged at 1800 × *g* for 30 min at 4 degrees. Supernatant was transferred to ultracentrifugation tubes and MPs collected at 100000 × *g* for 1 hour at 4°C. Pellet was resuspended in 1 ml of 0.22 μm pore size membrane-filtered PBS 1% and kept at 4°C over night. At the last centrifugation steps (100000 × *g*) all vesicle types should be collected. However, MP pellet was further centrifuged after labeling with antibodies as described below. At that centrifugation step (1800 × *g* for 30 min) only

ABs should be collected (Crescitelli R, 2013). However, we showed that MPs are variably positive to phosphatydilserine (Fig. 26). This may indicate that the MP pellets were composed by both ABs and MVs.

MP signals were acquired by flow cytometry using the FACSCanto II (Beckton Dickinson) instrument and analysed using FacsDiva software (Beckton Dickinson).

Standard size micro beads (1-2 µm) were used to set the MP gate (Flow Cytometry Size Calibration Kit, Invitrogen) (Fig. 18).

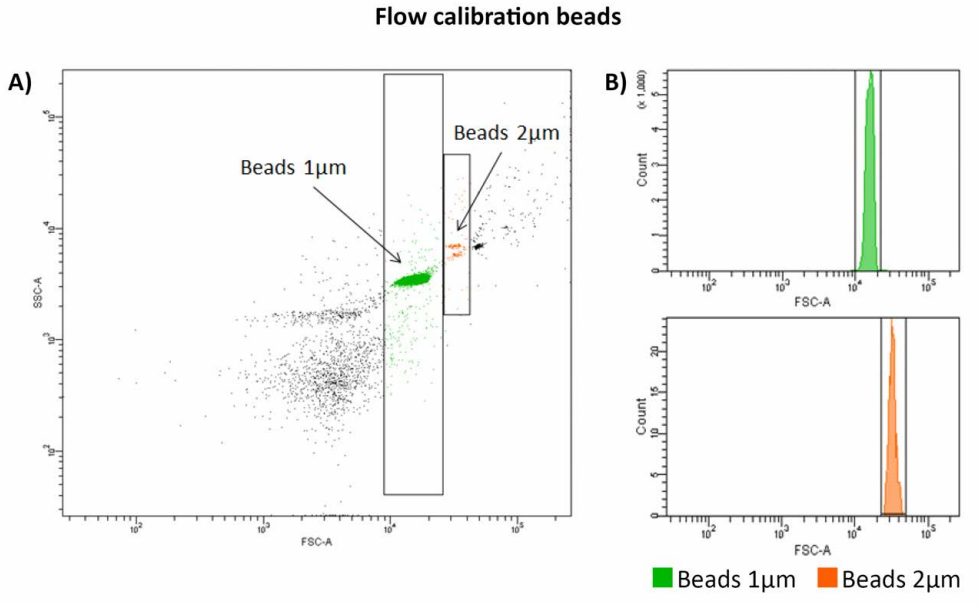

Fig: 18: Flow calibration test. Beads with two diameters (1 and 2 µm) were used to set the upper and lower size limit. Beads were analysed in FSC *vs* SSC plot (A) and in FSC *vs* number of events histogram (B).

The lower limit (500 nm) was set taking into account the instrument limit (Freyssinet JM, 2010), (Lacroix R, 2010), the upper one (1000 nm) has been used to avoid analysing cell debris, platelets, MP aggregates or apoptotic bodies. 1 µm, in fact, is considered as the upper size limit when defining MPs (Gelderman MP, 2008).

To characterize MPs from erythroid progenitors we tested MP positivity to the following markers: CD34, CD71 (markers of erythroid progenitors) (Furness SG, 2006), (Fajtova M, 2011), CD235a (glycophorin A, typical

marker of MPs shed by reticulocytes) (Fajtova M, 2011). Furthermore we tested MP populations for their positivity to phosphatidylserine (PS), a MP marker still under discussion (Connor DE, 2010). It has been demonstrated that only a limited portion of MPs in blood is PS+ (Gelderman MP, 2008), (Nielsen MH, 2014). To set a positive versus negative discrimination limit, samples were incubated also with isotype controls IgG2A/IgG1. The three antibodies and Annexin V (all from Beckton Dickinson) were labelled with different fluorochromes and incubated with sample in three different tubes:

Tube 1: IgG2A-FITC[1]/IgG1-PE[2] (20µl)

Tube 2: CD71-FITC[1] (10µl), CD34-PE[2] (10µl), Annexin V-APC[3] (2,5µl)

Tube 3: CD71-FITC[1] (10µl), CD34-PerCP[4] (10µl), CD235a-PE[2] (10µl), Annexin V-APC[3] (2,5µl)

([1]Fluorescein isothiocyanate, [2]Phycoerythrin, [3]Allophycocyanin, [4]Peridinin Chlorophyll Protein Complex)

100 µl of MPs (resuspended in PBS) were incubated with the three different antibodies combinations (tube 1, tube 2, tube 3) for 15 min in dark conditions. Samples were washed adding 1 ml of 0.22 µm pore size membrane-filtered PBS 1X and centrifuged at 1800 × *g* for 30 min at 4 °C. MP labelled pellet was resuspended in 400 µl of Annexin V buffer (Beckton Dickinson) (diluition 1:10) and Annexin V added to tubes 2 and 3.

The MP absolute numbers of different populations investigated were calculated using TruCount™ Tubes. These tubes contain a defined number of beads which allow to analyse MP number by the following formula: MP count/µl= [(MP event count)/(TruCount™ bead event count)] * [(total TruCount™ beads)/100 µl] *1.1 1.1 is the dilution factor

Student *t*-test and Kruskal-Wallis test have been performed to compare means from the different groups investigated. Mean differences were considered statistically significant if p-value < 0.05.

Receiver operating characteristic (ROC) curves were established to evaluate the diagnostic accuracy needed to differentiate healthy controls versus

patients with DBA and all controls versus patients with DBA. The program Stata V11.0. (Stata Corp. College Station, Texas, USA) was used.

- **Results and discussion**

MPs shed from erythroid cells were analysed in plasma from 19 healthy controls (12 females, 7 males; age range: 10-56), 10 patients showing a non-DBA haematological disease and 8 patients with DBA (3 females, 5 males; age range: 5-42). Clinical data from these patients are reported in table 2 and 3. Clinical characteristics and mutated *RP* genes in patients with DBA were shown in table 3A. BFU-e colony number obtained from peripheral blood and bone marrow of patients with DBA and performed for clinical assessment are reported in table 3B (Dianzani I, 1997). The colony number from both peripheral blood and bone marrow was zero or very small in all patients with DBA analysed.

Individuals #7 and #8, indicated with a different colour, are consanguineous. Patient #7 is the father of patient #8. He is in complete haematological remission, whereas his son, that has never required treatment, shows macrocytosis.

Table 2: characteristics of healthy controls and patients without DBA

HEALTHY CONTROLS #	GENDER	AGE
1	F	24
2	F	25
3	M	33
4	F	32
5	F	26
6	M	35
7	F	26
8	F	26
9	M	26
10	F	56
11	F	25
12	M	26
13	F	24
14	M	10
15	F	32
16	F	24
17	M	24
18	M	26
19	F	25

PATIENTS WITHOUT DBA #	CLINICAL CHARACTERISTICS
20	chronic thrombocytopenia
21	iron deficiency anemia with iron treatment and normal value of Hb
22	heterozygosis for HbS, normal Hb value (12,2 g/dl), age: 2
23	iron overload, microcytosis (Hb: 9g/dl)
24	lymphadenitis
25	congenital dyserythropoietic anemia type II (Hb: 9,9 g/dl)
26	thrombocytopenia
27	autoimmune lymphoproliferative syndrome
28	spherocytosis, splenectomy, normal Hb value (Hb: 14,4 g/dl)
29	spherocytosis, splenectomy, normal Hb value (Hb: 17,5 g/dl)

Table 3: characteristics of patients with DBA

A)

DBA patients #	gender	age	mutation	malformations	low stature	ADA (IU/ml Hb)	therapy
1	M	7	unknown	accessory spleen	NO	0,9	transfusions
2	M	24	RPL11 c. 314-315delTT	turbidity of the vitreous body	YES	3,2	transfusions
3	F	42	del. RPL5	micrognathia, neck cartilage growth	YES	3,9	steroids
4	M	5	unknown	NO	NO	1.4	transfusions
5	F	27	partial del. RPL11	YES	YES	increased	partial remission**
6	F	13	unknown	Tetralogy of Fallot		unknown*	transfusions
7	M	36	RPS24 c.64C>T (Q22X)	heart malformation	YES	5,2	remission***
8	M	8	RPS24 c. 64C>T(Q22X)	heart malformation		2,8	not treated ****

* not analysed because patient has been immediately treated with transfusion
** macrocytosis (Hb: 9g/dl)
*** macrocytosis (Hb: 11g/dl)
**** macrocytosis (Hb: 12g/dl)

B)

DBA patients #	bone marrow conditions	erythroid colonies (BFU-e) *in vitro*	BFU-e colonies source	BFU-e colonies # in basal conditions	BFU-e colonies # using SCF
1	erytroid hypoplasia	reduced growth	PB	1	8
			BM	23	26
2	erytroid aplasia	growth with SCF	PB	0	1
			BM	0	46
3			PB	1, very small	7, small and containing small amount of Hb
4	erytroid aplasia	reduced growth	BM	0	0
5	erytroid aplasia	growth with SCF	BM	0	7
6	erytroid aplasia	growth with SCF	BM	5,20,0*	74,46,2*
			PB	0,0**	2,0**
7	erytroid hypoplasia	growth with SCF	BM	7	41

PB= peripheral blood
BM= bone marrow

* assay has been performed on three independent follow-ups several years apart
* *assay has been performed on two independent follow-ups several years apart

The MP flow cytometry analysis has been performed using a *dot plot* graph. A representative *dot plot* is showed in figure 19. The analysis has been focused on MPs in the MP gate (500-1000 nm) (Fig. 19A).

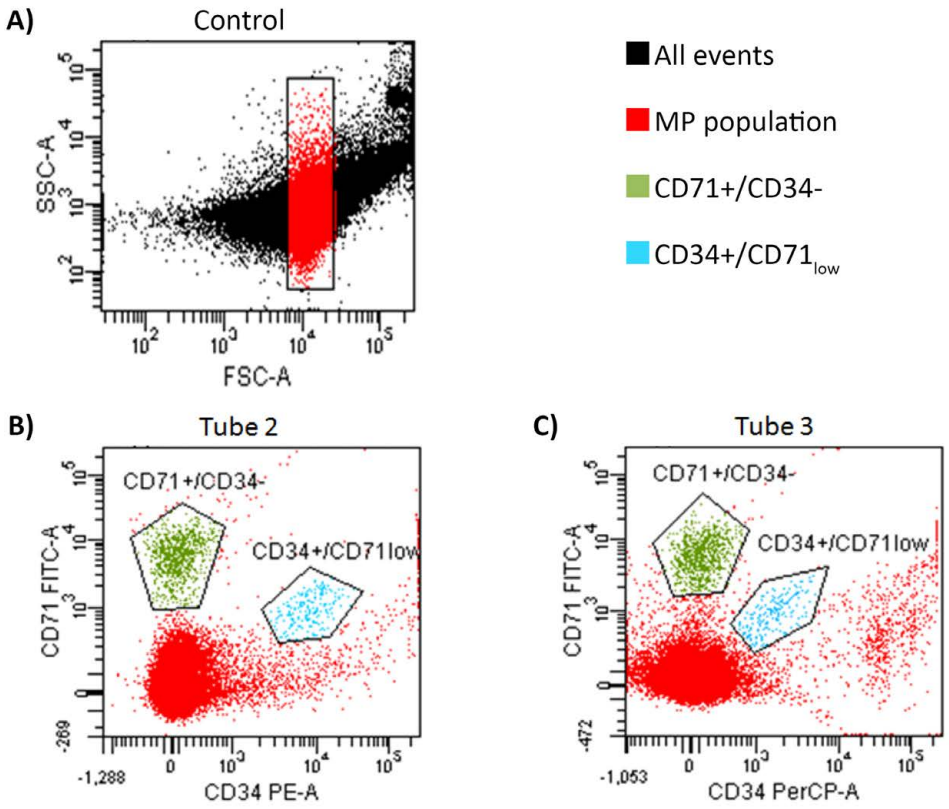

Fig: 19: MP distribution in a *dot plot* graph. (A) The MP gate (500-1000 nm) is indicated and MPs are shown in red. MP population CD71+/CD34- (in green) and MP population CD34+/$CD71_{low}$ (in light blue) are shown as observed in tube 2 (B) and in tube 3 (C).

Looking at markers CD71 and CD34 in both tube 2 (Fig. 19B) and tube 3 (Fig. 19C), two well representative MP clusters are identified: CD71+/CD34- in green and CD34+/$CD71_{low}$ in light blue. The event number has been calculated in the gates observed in tube 2 because of a better technical compensation between the two fluorochromes (FITC and PE) that labelled anti-CD71 and anti-CD34 antibodies.

As shown in figure 20, the MP population CD71+/CD34- varies among different individuals. The graph shows representative experiments for each individual category: a healthy control, a patient with DBA, a patient without DBA, a patient with DBA in remission #7, and patient with a typical DBA mutation but not anemic #8 (Vlachos A B. S., 2008).

On the other hand, the cluster CD34+/CD71$_{low}$ is able to discriminate between patients with DBA and controls. Representative experiments are shown in figure 20 (a healthy control, a patient with DBA, a patient without DBA, a patient with DBA but in remission #7 and patient with a typical DBA mutation but not anemic #8). This cluster is absent in the anemic patient with DBA (black arrow) (Fig. 20).

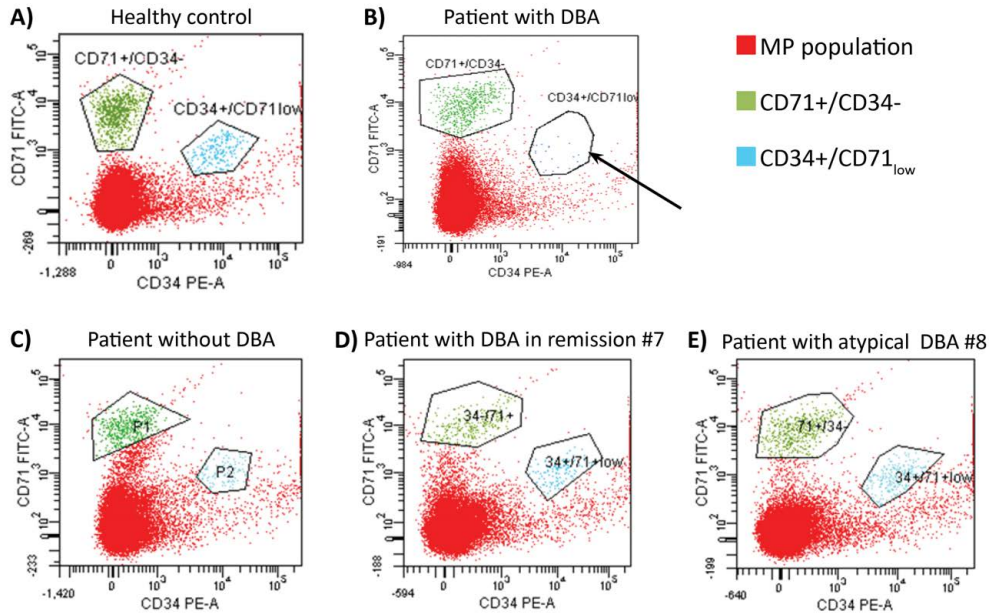

Fig 20: CD71+/CD34- and CD34+/CD71$_{low}$ populations are shown in different individuals: healthy control (A), patient with DBA (B), patient without DBA (C), patient with DBA in remission #7 (D), patient with atypical DBA #8 (E). The black arrow indicates the CD34+/CD71$_{low}$ population that is absent in the anemic patient with DBA, differently from the others.

The MP number in the two populations has been calculated for all samples and the results are reported in table 4.

Control #15 and #16 as well as DBA patient #1 have been analysed from two independent samples (a and b). The second analysis (b) has been performed after six months (clinical conditions were identical). Samples obtained in the two replicates are very similar. This shows that flow cytometry analyses are reproducible.

Table 4: MP absolute number calculated in the gates CD71+/CD34- and CD34+/CD71$_{low}$

HEALTHY CONTROLS #	CD71+/CD34-	CD34+/CD71low
1	6,5	0,8
2	10,0	2,6
3	6,9	17,8
4	4,6	5,9
5	7,1	1,6
6	9,7	2,2
7	0,8	4,9
8	9,6	1,7
9	7,9	5,2
10	4,8	2,2
11	10,2	3,8
12	8,7	1,3
13a*	2,2	6,2
13b*	5,2	1,4
14	3,2	4,2
15a*	134,9	15,9
15b*	188,7	2,9
16	9,5	4,5
17	6,1	6,4
18	6,1	2,4
19	9,3	5,3
PATIENTS WITHOUT DBA #	**CD71+/CD34-**	**CD34+/CD71low**
20	10,3	6,5
21	12,2	4,8
22	6,0	1,2
23**	7,5	0,6
24**	3,7	0,5
25	6,2	3,6
26	9,4	4,1
27	2,8	4,5
28	9,2	1,4
29	7,9	2,1
PATIENTS WITH DBA #	**CD71+/CD34-**	**CD34+/CD71low**
1a*	2,3	0,7
1b*	3,1	0,4
2	3,2	0,7
3	106,3	0,8
4	25,6	0,8
5	9,3	0,4
6	10,0	0,4
7***	3,9	1,6
8***	6,7	3,2

*a, b indicate the analysis performed on the same control or patient in two independent samples.
**patients without DBA #23 and #24, indicated in green, show the MP CD34+/CD71$_{low}$ number similar to that of the anemic DBA patients
***patients with DBA #7 and #8, indicated in violet, carry a DBA mutation (RPS24 c.64C>T) but they do not show anemia. Their MP CD34+/CD71$_{low}$ number is similar to that of controls.

The absolute number of CD71+/CD34- population is shown in table 4 and in figure 21A. Using a Student *t*-test the mean of MP CD71^{+}/CD34^{-} was not statistically significant comparing healthy controls versus patients without

DBA and healthy controls versus patients with DBA. We conclude that this population is not able to distinguish patients from controls.

On the other hand, the MP CD34+/$CD71_{low}$ population was less represented in patients with DBA as compared with healthy controls and patients without DBA (table 4 and Fig. 21B). Specifically, the CD34+/$CD71_{low}$ population was absent in anemic patients with DBA, but was well represented in controls and in patients affected by a non-DBA condition. The difference in MP CD34+/$CD71_{low}$ number between patients with DBA versus healthy controls is statistically significant ($p<0.05$ Kruskal-Wallis test) (Fig. 21B) as well as between patients with DBA versus all controls (healthy controls + patients without DBA) ($p<0.05$ *t*-test). The difference in MP CD34+/$CD71_{low}$ number between patients with DBA versus patients without DBA is not statistically significant, possibly due to the small number of analysed samples. The same result is obtained between patients without DBA and healthy controls. Thus, this population distinguishes DBA patients from controls and this last result supports the specificity of MP CD34+/$CD71_{low}$ analysis for DBA diagnosis.

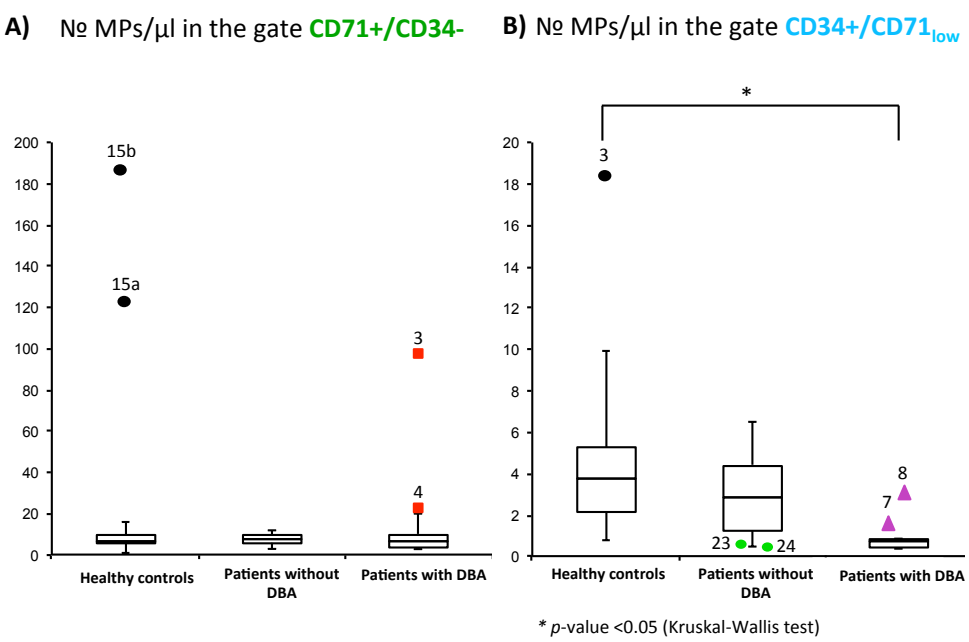

Fig. 21: Absolute MP number in CD71+/CD34- (A) and CD34+/CD71$_{low}$ (B) populations in controls, patients without DBA and patients with DBA. (A) Patient #15 (a and b) in black, and patients #3 and #4, in red, are outliers. In (B) two patients without DBA (#23, #24), in green, show a MP CD34+/CD71$_{low}$ number similar to that of the DBA patients whereas two patients with DBA (#7, #8), in violet, show a MP CD34+/CD71$_{low}$ number similar to that controls. The mean is statistically significant (Kruskal-Wallis, *p*-value <0.05) between patients with DBA and healthy controls. The mean is statistically significant (Student *t*-test, *p*-value <0.05) between patients with DBA and all controls (healthy controls + patients without DBA) (data not shown).

Interestingly, patients with a haematological non-DBA disease showed CD34+/CD71$_{low}$ numbers in the control range. Only patients #23 and #24 do not show the CD34+/CD71$_{low}$ population, as observed in patients with DBA. Patient #23 shows a still undiagnosed anemia, with severe microcytosis and iron overload. Patient #24 shows lymphoadenitis and normal erythroid parameters. We plan to repeat the analyses in this patient. In any case, it should be noted that these patients do not show clinical symptoms of DBA.

On the other hand, two patients with DBA (patients #7 and #8) show a number of MP CD34+/CD71$_{low}$ that is similar to that of controls. They carry

the same *RPS24* mutation, being father and son. Interestingly, they do not show anemia: the father shows a complete haematological remission and the son never displayed anemia. The son's phenotype is named "atypical DBA" (Vlachos A B. S., 2008).

Conversely, DBA patients #3 and #5, who are in partial remission, with a low Hb value, do not show the MP CD34+/$CD71_{low}$ cluster as the other patients with DBA. In conclusion, the low levels of MP CD34+/$CD71_{low}$ parallel Hb values in patients with mutations in DBA genes.

Both CD34 and CD71 are erythroid progenitor markers. DBA is characterized by a deficiency of red cell progenitors (BFU-e/CFU-e), that show a pro-apoptotic phenotype and die in the bone marrow. The CD34+/$CD71_{low}$ cluster absence in blood of patients with DBA parallels the absence of BFU-e colonies grown from peripheral blood or bone marrow of these patients (table 3B). These data support our hypothesis that these vesicles are derived from erythroid progenitors.

The diagnostic value of MP CD34+/$CD71_{low}$ analysis was evaluated using receiver operating characteristic (ROC) curves (Fig. 22). The ROC curve is a fundamental tool for diagnostic test evaluation. In a ROC curve the true positive rate (Sensitivity) is plotted in function of the false positive rate (100-Specificity) for different cut-off points of a parameter. Each point on the ROC curve represents a sensitivity/specificity pair corresponding to a particular decision threshold. The area under the ROC curve (AUC) is a measure of how well a parameter can distinguish between two diagnostic groups (diseased/normal). When the variable under study cannot distinguish between the two groups, i.e. where there is no difference between the two distributions, the area will be equal to 0.5 (the ROC curve will coincide with the diagonal). When there is a perfect separation of the values of the two groups, i.e. there is no overlapping of the distributions; the area under the ROC curve equals 1 (the ROC curve will reach the upper left corner of the plot).

The 95% Confidence Interval is the interval in which the true (population) Area under the ROC curve lies with 95% confidence (Swets JA., 1988).

We analysed patients with DBA *vs* controls (healthy controls + patients without DBA) (AUC 0.88) (Fig. 22A), patients with DBA *vs* healthy controls (AUC 0.92) (Fig. 22B), patients with DBA *vs* patients without DBA (AUC 0.81) (Fig. 22C) and patients without DBA *vs* healthy controls (AUC 0.64) (Fig. 22 D).

In conclusion the results show that MP CD34+/$CD71_{low}$ analysis is a good diagnostic test for DBA.

Further analyses on patients with non-DBA anemia are needed to ascertain the value of this assay in the clinics.

FIG. 22 A **Patients with DBA *vs* healthy controls + patients without DBA**

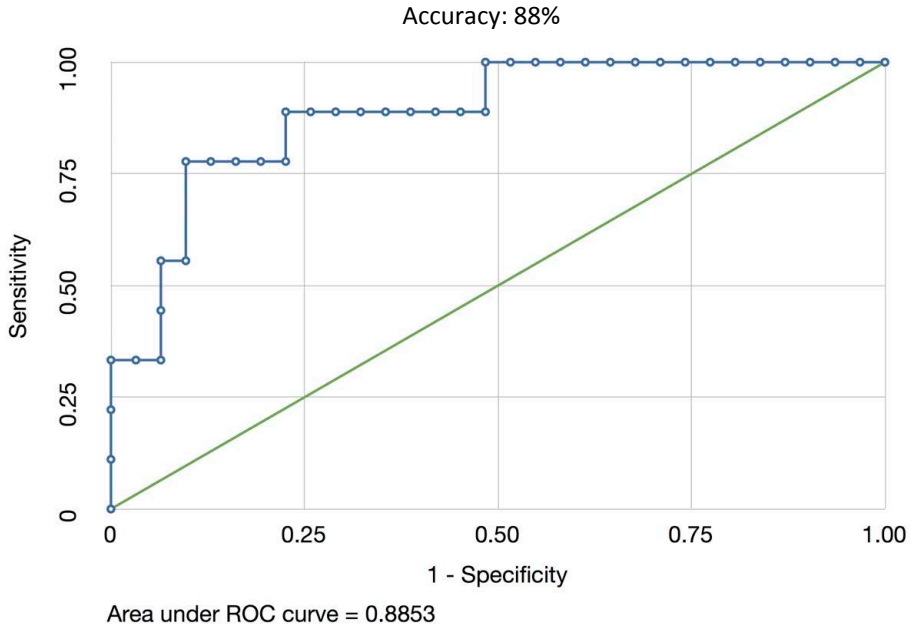

FIG. 22 B **Patients with DBA *vs* healthy controls**

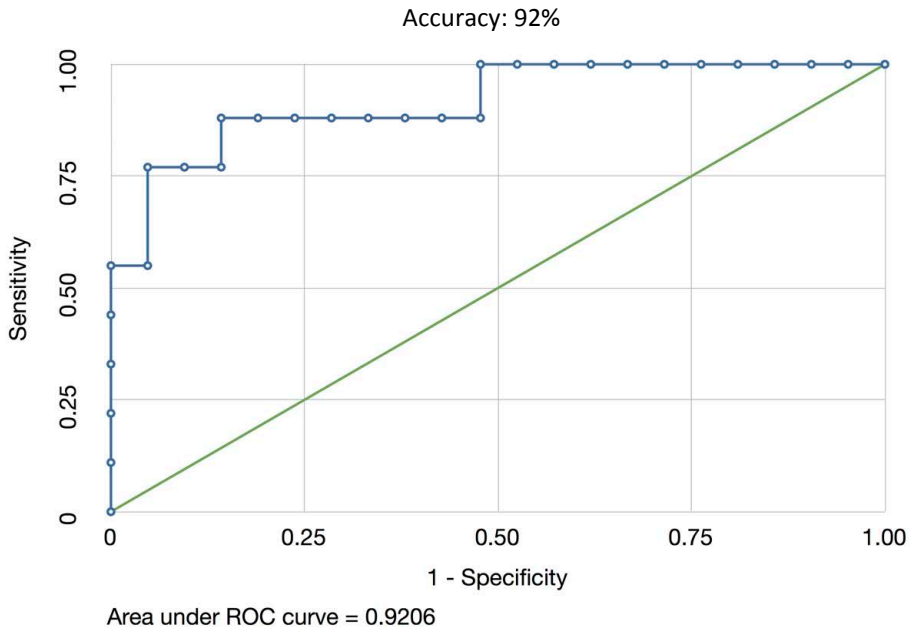

FIG. 22 C Patients with DBA *vs* patients without DBA

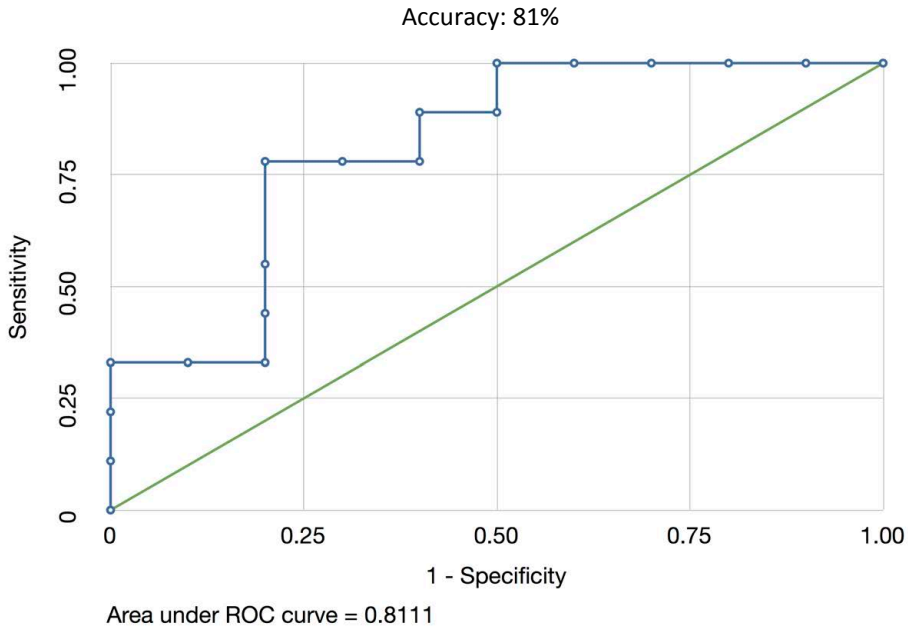

FIG. 22 D Patients without DBA *vs* healthy controls

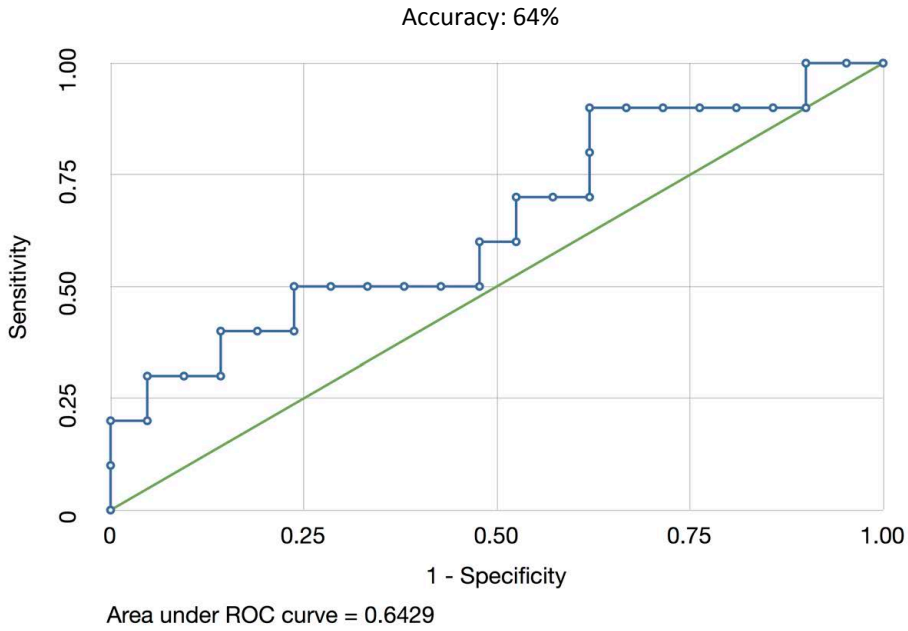

Fig. 22: Receiver operating characteristic (ROC) curve evaluating the accuracy of the MP CD34+/CD71$_{low}$ analysis in A) all controls (healthy controls + patients without DBA) *vs* patients with DBA, in B) healthy controls *vs* patients with DBA, in C) patients with DBA *vs* patients without DBA and in D) patients without DBA *vs* healthy controls.

To obtain a better interpretation about $CD71^{+}/CD34^{-}$ population, we focused on the *dot plot* showing CD71 and CD235a correlation (Fig. 23-24).

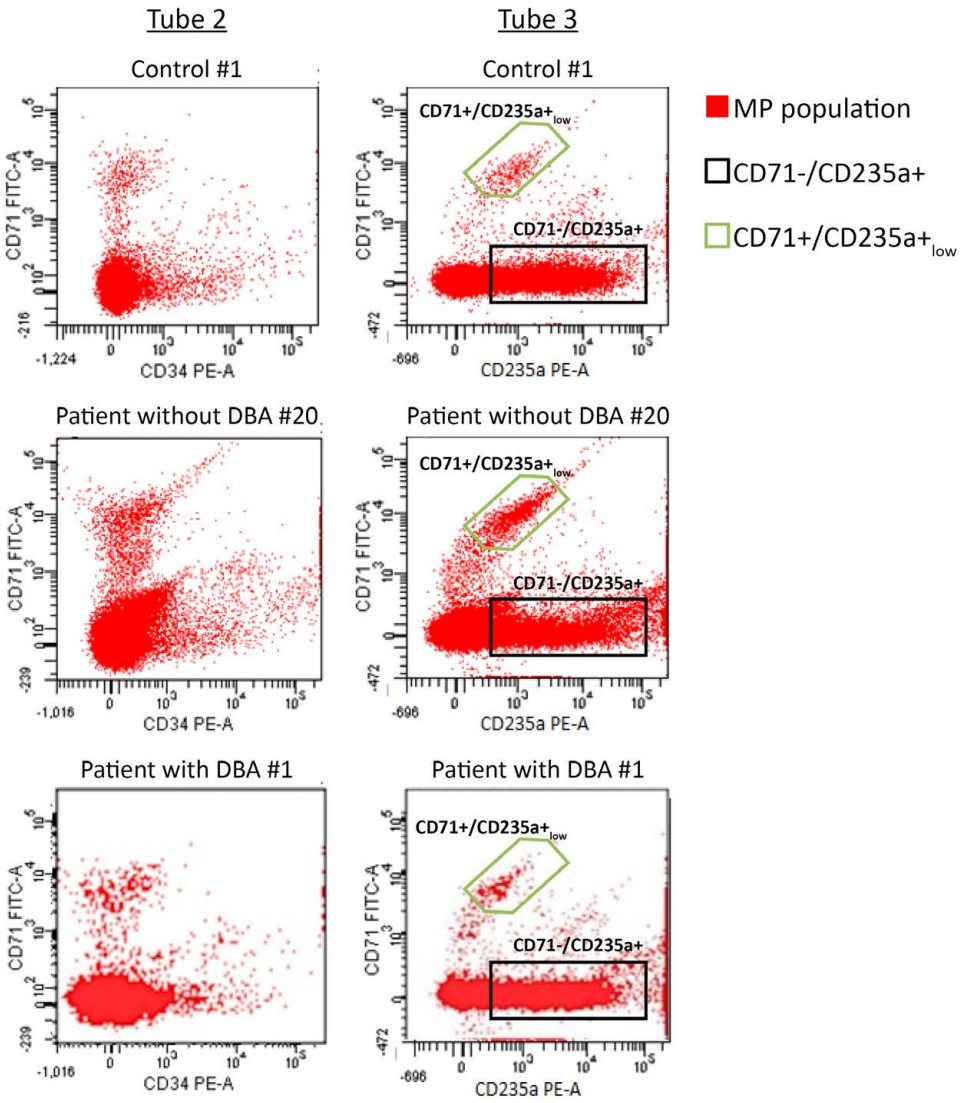

Fig. 23: Qualitative analysis of CD71 and CD235a markers. *Dot plot* CD71-FITC *vs* CD34-PE (tube 2) is showed on the left panel, whereas *dot plot* CD71-FITC *vs* CD235a-PE (tube 3) is on the right. Populations CD71-/CD235a+ and $CD71+/CD235a+_{low}$ are shown in three representative samples.

As shown in figure 23, a well distinct CD235a+ population was observed (CD71-/CD235a+) in many controls, many patients without DBA and one patient with DBA (#1). CD235a (glycophorin a) is expressed on

reticulocytes and erythrocytes (Fajtova M, 2011). Thus, we can conclude that the CD71-/CD235a+ population is shed from reticulocytes and erythrocytes. Moreover, in some samples this population was also positive for CD71 (CD71+/CD235a+ population) (Fig. 24).

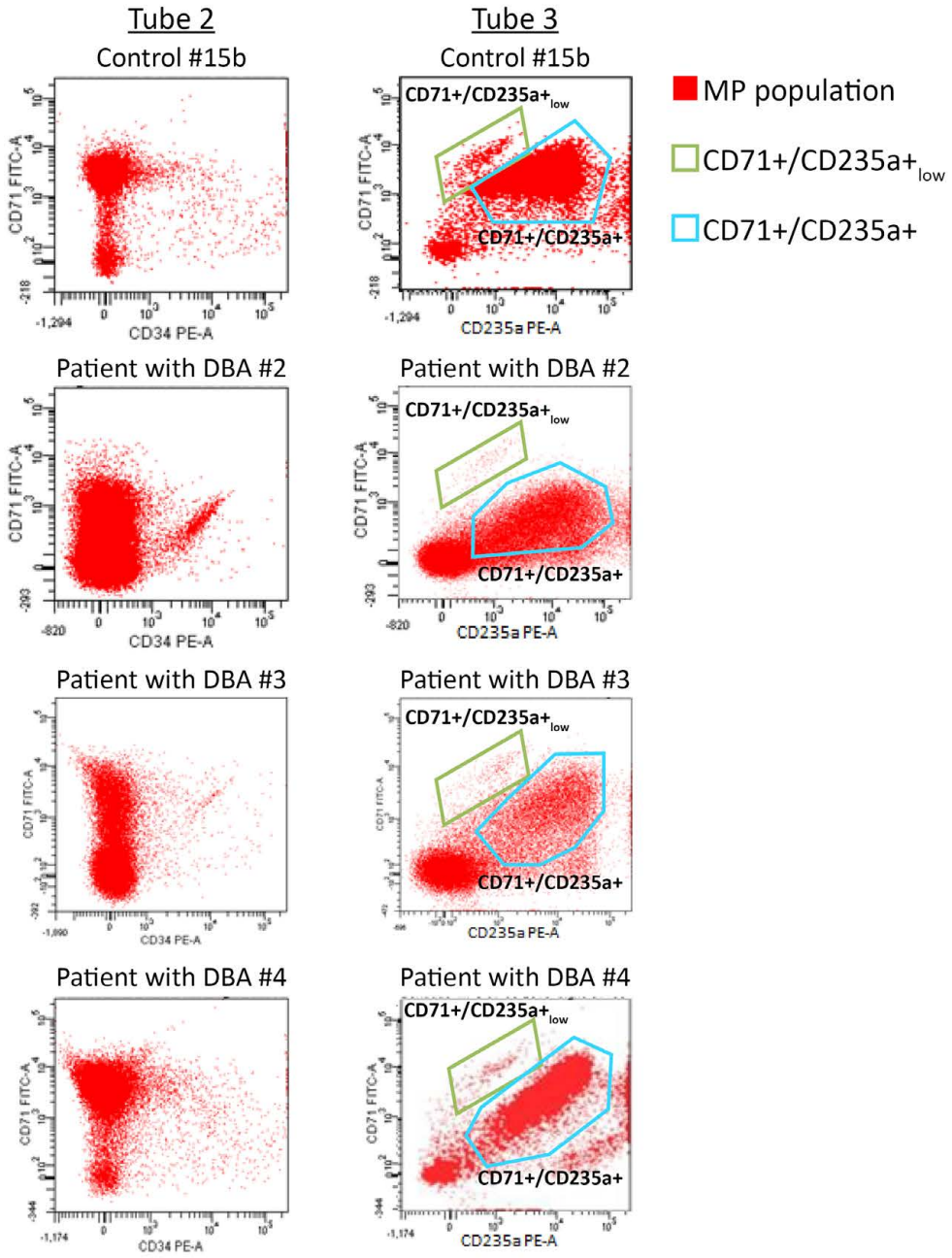

Fig. 24: Qualitative analysis of CD71 and CD235a markers. *Dot plot* CD71-FITC *vs* CD34-PE (tube 2) is showed on the left panel, whereas *dot plot* CD71-FITC *vs* CD235a-PE (tube 3) is on the right. Populations CD71-/CD235a+ and CD71+/CD235a+$_{low}$ are shown in four representative samples.

Normally, CD71 is expressed on erythroid precursors membrane and lost when orthocromatic erythroblast develops in to reticulocyte (Fajtova M, 2011). The CD71+/CD235a+ population could derive from reticulocytes that, for different reasons, retained CD71 on their surface. We can exclude that MP CD71+ are released from cells within bone marrow. In this case we would expect to observe a more heterogeneous MP population, expressing typical markers of cells in all maturation phases and not only CD71.

In all samples (Fig. 23 and 24) a MP CD71+/CD235a+$_{low}$ population has been observed. We assume that it derives from a small amount of erythroid precursors released in blood circulation (Mladenovic J, 1982).

This hypothesis is supported by the CD71+/CD34- cluster analysis in control #15a/b and in patients #3 and #4, where we focused on *dot plots* showing CD34 *vs* CD71 and CD235a *vs* CD71 analysed in tube 3. As shown in figure 25, the cluster CD71+/CD34- is so well represented in these samples because the population CD235a+ was variably positive to CD71 (Fig. 25).

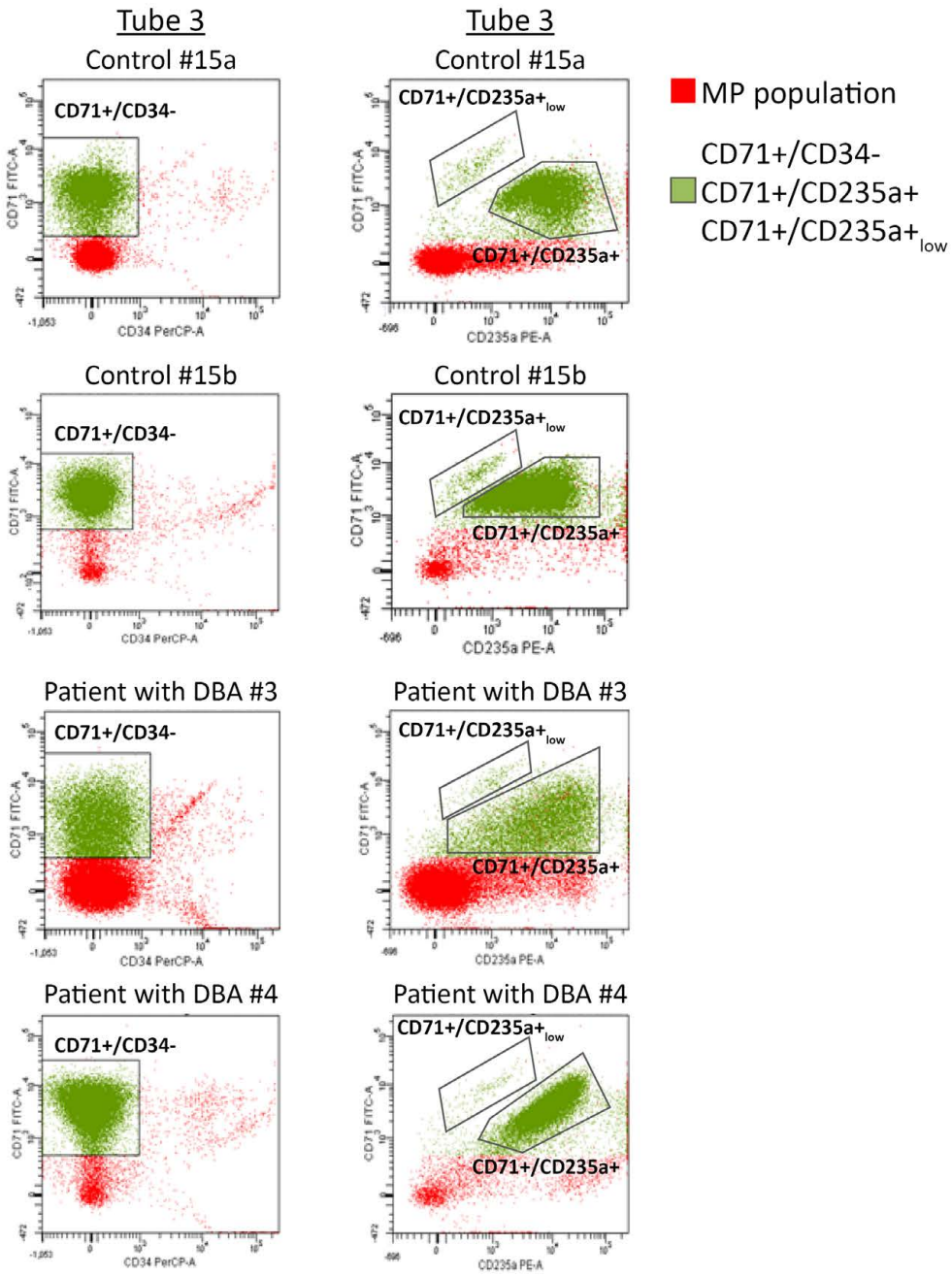

Fig. 25: Qualitative analysis of CD71+/CD34- population. *Dot plot* CD71-FITC *vs* CD34-PerCP (tube 3) is shown on the left panel, whereas *dot plot* CD71-FITC *vs* CD235a-PE (tube 3) is on the right.

Analysis of different MP populations showed that flow cytometry is a useful system to identify MP shed from cells at different stages of erythropoiesis. However the flow cytometry results can be hampered by an artefact due to technical compensation issue. We think that marker profiling analysis need

to be repeated by using the same antibodies conjugated with different fluorochromes.

We also focused on phosphatidylserine (PS) positivity. PS expression on MP surface is debated. Certain authors consider PS a marker that is not expressed by all types of MPs (Connor DE, 2010), (Gelderman MP, 2008). To verify PS expression, we re-analysed all MP populations. We compared all MP populations (Fig. 26A - in red) with a *dot blot* showing only MP PS+ (Fig. 26B – in blue). We observed that CD71+/CD34- cluster was PS- whereas CD34+/CD71$_{low}$ cluster was PS+ (Fig. 25 A-B).

The same observations have been done on CD235a+ populations. The CD71+/CD235a+$_{low}$ population was PS- whereas CD71-/CD235a+ was PS+. Because the graphic representation was not completely exhaustive about CD71-/CD235a+, we quantified the MP CD71-/CD235a+ in the whole MP range and the in MP PS+ range in one representative sample. Applying the same formula used to calculate the number of MP CD71+/CD34- and CD34-/CD71$_{low}$, we observed that 59% of MP CD71-/CD235a+ was also PS+ in agreement with previous papers (Willekens FL, 2008).

In conclusion CD71-/CD235a+ population includes two subpopulations, one PS- and the other one PS+. We can assume that PS+ population derived from erythrocytes undergoing apoptosis (Lang E, 2012), (Ghashghaeinia M, 2012) whereas MP CD235a+ PS- was shed from reticulocytes and erythrocytes.

Our analysis on PS expression in MPs shed from erythroid progenitors/precursors supports the hypothesis that PS expression depends on MP origin.

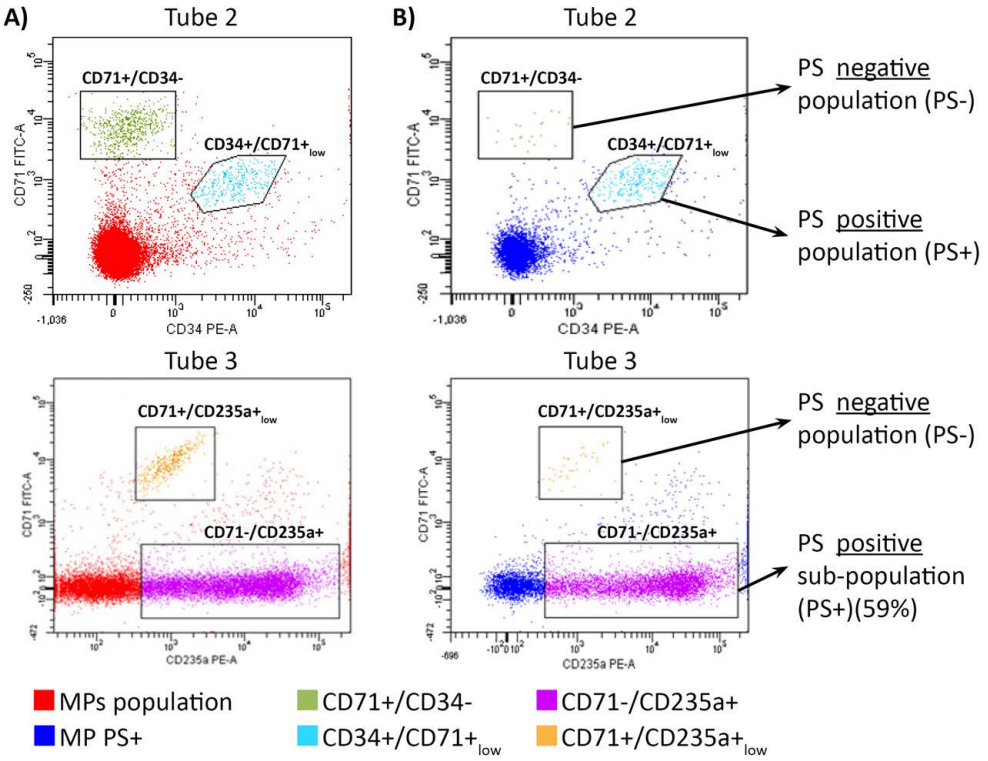

Fig. 26: Phosphatidylserine analysis of MP populations CD71+/CD34-, CD34+CD71$_{low}$, CD71+/CD235a+$_{low}$ and CD71-/CD235a+. *Dot plot* showing the MP populations in whole MP range (red) is on the left panel (A), whereas *dot plot* showing MP population in the MP PS+ range is on the right (B). A quantification analysis has been performed on population CD71-/CD235a+. The number of MP CD71-/CD235a+ PS+ is indicated (59%). The *dot plots* are representative of all samples analysed.

In conclusion, since MP analysis using flow cytometry is reproducible, sensitive and rapid, we feel that it could be used in diagnostic routine. We show that it can identify MPs released from erythroid progenitors and can possibly distinguish DBA patients from controls. Since the DBA research limit is the inability to study erythroid progenitors in the bone marrow, analysis of MPs from erythroid progenitors in peripheral blood could also be useful to improve the knowledge about DBA pathophysiology.

4. Conclusions and future perspectives

Extracellular vesicles (EVs) are phospholipid membrane fragments shed from most cells in physiological and pathophysiological conditions (Théry C., 2009) (Mathivanan S J. H., 2010) (Ratajczak J., 2006) (Cocucci E, 2009) (Johnstone RM, 2006). They exhibit pleiotropic biological functions (Mathivanan S J. H., 2010). In the last years there has been a growing interest because of their potential use for clinical applications (van der Pol E B. A., 2012).

EVs include a mixture of different vesicle types generally classified in three classes: apoptotic bodies (ABs), microvesicles (MVs) and exosomes (EXOs) (György B S. T., 2011).

The classification is based on their size and molecular characteristics, but numerous similarities exist among the different EVs (György B S. T., 2011) (Choi DS, 2012) (Simpson RJ., 2012). Consequently, EV preparations are a mixture of different vesicle types. For these reasons there is a need of nomenclature clarification and of a standardized method able to distinguish EV types (Mathivanan S J. H., 2010).

Applying previously published differential centrifugation-based protocols we demonstrated that the centrifugation method is useful to separate ABs, MVs and EXOs. Vesicles have been isolated from supernatant of three different cell lines (HMC-1, TF-1 and BV2) and EV types analysed looking at their RNA profile, morphology and surface marker expression. Our results show that ABs, MVs and EXOs have clearly different RNA profiles that allow to distinguish them focusing on rRNA. Specifically, rRNA was detectable in ABs from all the studied cell lines, whereas MVs contained little or no rRNA except for those shed from TF-1 cells. In EXOs from all cell lines, rRNA was absent and only small RNAs have been observed according with previous reports (Valadi H, 2007), (Lässer C, 2013).

The RNA profiles for EV types were maintained also when apoptosis was induced. The RNA concentration increased.

Characterization by electron microscopy revealed a morphology compatible with ABs, MVs and EXOs, demonstrating that the centrifugation based protocol is able to separate EV subpopulations.

On the other hand, flow cytometry analysis using anti-CD63-coated beads appeared to not be a system able to distinguish each EV subpopulation. ABs, MVs and EXOs from both HMC-1 and TF-1 cells showed positivity for CD63, CD81 and CD9, except for CD9 that was absent in the TF1-derived vesicles since TF-1 cells do not express this tetraspanin. We can conclude that these markers are not specific for EXOs, as previously thought (Mathivanan S J. H., 2010), (Théry C A. S., 2006).

We also demonstrated that two populations of exosome-like vesicles could be identified. In particular, we showed that when the filtration step was eliminated (filter 0.22 μm pore size) two populations were collected (”EXO w/o filter” and “additional pellet”). Only EXO pellet was obtained using the filtration (”EXO w filter”).

The EXO pellet from the sample that has been filtered (”EXO w filter”) contained mostly short RNAs and just small rRNA peaks, whereas the samples that were not filtered (“EXO w/o filter”) showed more evident rRNA peaks. Interestingly, the “additional pellet” contained large peaks of rRNA. Our result showed that using 0.22 μm filtration step, rRNA content is lost whereas the “additional pellet”, obtained without filtration, contains rRNA. The small rRNA peaks that we observed in the EXO pellet without filtration (“EXO w filter”) indicate a probable contamination from “additional pellet”. It could be interesting to investigate the effect of filtration using filters with different sizes because, the differences shown in exosome studies could be due not only to a different EXO origin but simply to a different filter used.

More attention should be given to the centrifugation rotor used. “EXO w/o filter” and “additional pellet” cannot be separated using a swinging bucket rotor.

A further purification of EXOs isolated using filter (“EXOs w filter”) and of the “additional pellet” was obtained loading these pellets on sucrose gradient. The procedure showed that “additional pellet” was composed by two subpopulations: one was rRNA-negative but included small RNA in lower fractions (1.24-1.31 g/cm^3); the other was rRNA-positive and was

found in the higher fractions (1.09-1.21 g/cm^3). Just one EV population, rRNA negative and enriched with small RNA was present in "EXO w filter". These results demonstrated that sucrose gradient can be useful to further separate and purify vesicles.

Moreover, loading ABs, MVs and EXOs on sucrose gradient we demonstrated that MV pellet is composed of two subpopulations (rRNA positive and rRNA negative vesicles) similar to what was observed in the "additional pellet". These results emphasize that the nomenclature problem is still an open challenge. This finding, together with the dissimilar RNA profiles between of 0.22 μm filtered EXOs and unfiltered EXOs, could explain some of the differences seen for RNA profiles in different exosomal studies. However, it is important to keep in mind that EV characteristics (size, RNA profiles, markers, etc.) could be different between EVs shed from different cell types and in different conditions. We suggest that every research group should perform a study to characterize which vesicles are obtained in the specific system investigated.

After the development of a new isolation protocol to avoid a contamination between different subpopulations of extracellular vesicles, we applied our knowledge to analyse the EV role in a cellular process: ribosomal stress. Although EVs have been studied in many stress types and their roles documented, nobody studied their involvement in ribosomal stress. This is a cellular stress due to an abnormal ribosome biogenesis followed by activation of cell proliferation arrest and apoptosis (Donati G M. L., 2012). Defects in the ribosome biogenesis machinery induce diseases called ribosomopathies. Diamond Blackfan Anemia (DBA) is the first ribosomal disease that was shown to be due to ribosomal stress. Moreover, DBA research is limited by the inability to study erythroid progenitors because they undergo apoptosis induced by abnormal ribosome biogenesis. The EV study performed in this thesis has been useful to overcome this limitation and it represents the first EV analysis in ribosomal stress.

We performed EV analysis *in vitro* using a cell model of DBA and *in vivo* using peripheral blood from patients with DBA.

We first analysed miRNAs included in MVs and EXOs shed during ribosomal stress in $CD34^+$ cells downregulated for RPS19. We decided to focus our attention on miRNA EV content because they are the most studied EV component and their involvement in disease has been well documented (Corrado C, 2013). Moreover, any perturbations in the homeostasis result in alterations of the miRNA expression profile (Mathivanan S J. H., 2010), (Théry C Z. L., 2002). Analysis of miRNA content altered by ribosomal stress is useful to overcome the limit in DBA research due by the lack of erythroid progenitors and to improve the knowledge in DBA pathogenesis.

To analyze vesicular miRNAs a methods based on filter isolation of vesicles has been used. This method is based on size only and filters with different pore sizes are used. We captured particles with a size between 700-200 nm indicated as microvesicles (MVs) and particles with that ranged between 200-20 nm indicated as exosomes (EXOs). The method used to silence $CD34^+$ cells for RPS19 does not yield a sufficient amount of cells to perform more thorough EV separation methods, such as those detailed in the first part of this thesis.

This study represents the first research focused on EVs shed from $CD34^+$ cells and in condition of absence or presence of ribosomal stress. We compared MVs and EXOs from control cells and cells that were silenced for RPS19 and observed a list of miRNAs that were differently represented in the two experimental conditions. The first observation is that none of these miRNAs were in common between MVs and EXOs. This result underlines that different processes are used to produce EV subpopulations and to load their cargo.

Many of the abnormally represented miRNAs have a role in human disease. Several miRNAs are involved in erythropoiesis and thus could have a role in DBA pathogenesis, i.e. miR-412, miR-148a and miR-153. miRNA-148 has a role in and DNA methylation of $CD34^+$ hematopoietic stem cells (Merkerova M, 2010). miR-412 and miRNA-153 are involved in cell death processes (Melamed Z, 2013), (Wu Z, 2013). miR-153 shows an anti-apoptotic function in breast cancer cell cultures (Anaya-Ruiz M, 2013). In

particular, miR-153 accumulation leads to cyclin D overexpression and p21 (Cip1) decrement through regulation of its target gene PTEN (Wu Z, 2013). The miR-153 decrement in MVs shed from $CD34^+$ under ribosomal stress could explain the pro-apoptotic phenotype of cells undergoing ribosomal stress including DBA erythroid progenitors. Moreover, PTEN could have an important role in ribosomal stress because of its ability to repress RNA polymerase I transcription. Thus it regulates indirectly rRNA (Zhang C, 2005). miR-153 involvement in stretch stress (Song L, 2012) could support its role in another cellular stress type, i.e. ribosomal stress.

These results are just preliminary and need to be validated. Validation is feasible because short RNAs are stable in body fluids when surrounded by double phospholipid strand and the levels can be easily assessed by various methods such as RealTime PCR. Consequently, before performing the array analysis we verified the miRNA presence in our samples using RealTime PCR amplification (TaqMan Gene Expression Assays-Applied Biosystems). We analysed some common miRNAs (miR-223, miR-221 and miR-150) and we obtained a good amplification for all of them (data not shown).

We will focus on the two miRNAs showing a role in cell death process (miR-412 and miR-153). We will investigate if their behaviour in MVs silenced for RPS19 in cells releasing them. In particular, miR-153 showed an anti-apoptotic role (Wu Z, 2013), so it is conceivable that it is down-regulated also in cells. This behaviour could explain the pro-apoptotic phenotype showed by erythroid progenitors in DBA.

To investigate its involvement in cell death induction in DBA disease, functional assays are mandatory. We generally use a DBA cell model in erythroleukemia cells (TF1) where RPS19 expression is downregulated by a doxycycline-inducible siRNA against the RPS19 mRNA (TF1 C), or a siRNA against a scramble sequence, (TF1-S) (Miyake K1, 2005).

To validate miR-153 role in DBA we will transduce miR-153 and mir-153 inhibitor (as control) in TF-1 C and S and we will examine the miRNA effect on cell proliferation. For this purpose, useful assays are MTT (3-(4,5-dimethylthiazol-2-yl)-2,5-diphenyltetrazolium bromide) to evaluate cell

viability, colony formation assay to asses cell proliferation and BrdUrd incorporation assay (Bromodeoxyuridine) to analyse the effect on cell cycle progression at G1/S transition.
If the miR-153 role in DBA cell models is demonstrated, assays (as luciferase assay, specific protein level analysis and RealTime-PCR) will be performed to validate its predicted target genes.
These analyses should be useful to investigate miRNA roles in pathways involved in ribosomal stress and in DBA pathogenesis.

The EV *in vivo* analysis has been performed directly on EVs from erythroid progenitors obtained from blood of patients with DBA. In this project, we tried to overcome the limiting factor in DBA research represented by the inability to study erythroid progenitors because of their pro-apoptotic phenotype. Typical erythroid markers (CD34, CD71 and CD235a) a well as phosphatydilserine, were analysed using flow cytometry. In particular, we identified and quantified an EV subpopulation (CD34+/$CD71_{low}$) able to distinguish DBA anemic patient from controls. This subpopulation is well expressed in controls and patients without DBA, but it is absent in patients with DBA.
We observed other EV subpopulations that expressed a variable positivity to different makers. Their analysis has been useful to investigate the EV populations shed from hematopoietic cells at different developmental stages. In particular, a well represented EV subpopulation CD235a+ has been observed in controls and in one patient. CD235a+ is a marker expressed reticulocytes and erythrocytes. On the other hand, we assume that the CD71+/$CD235a+_{low}$ subpopulation derives from a small amount of erythroid progenitors released in circulation.
We showed that flow cytometry is able to investigate EVs shed from erythroid cells at different developmental stages. We plan to analyse their content focusing on miRNA pattern. In particular we will look at miR-412 and miR-153 if their roles in the DBA cell model are validated.

One of the EV research limit is the lack of methods able to separate EV populations positive for specific markers. For this purpose, companies are developing a system based on magnetic beads coated by antibodies. Thus it will soon be possible to isolate specifically EVs from erythroid progenitors to analyse their content.

Furthermore, phosphatidylserine analysis showed that the EV subpopulations are variably positive for this marker. We conclude that phosphatidylserine positivity depends on EV origin and not from a release system common for all cell types. Our conclusion is in agreement with previous reports (Connor DE, 2010) (György B S. T., 2011).

We demonstrated that the four markers analyzed, are able to identify EVs from erythroid progenitors. We would like to continue this work and investigate peripheral blood cells. The limiting factor is the low numbers of these cells.

MPs analysis using flow cytometry resulted to be reproducible, sensitive and rapid and we consider this method suitable for routine testing.

DBA diagnosis is not easy and depends on exclusion of the other bone marrow failure syndromes, eADA activity determination and sequencing of responsible genes. The finding of a low number of erythroid progenitors (i.e. BFU-e and CFU-e) in bone marrow samples is another useful method. This procedure requires two working weeks, MP subpopulation investigation, on the other hand, is done using peripheral blood, requires two working days and can be done on transfused patients.

References

Akers JC, G. D. (2013). Biogenesis of extracellular vesicles (EV): exosomes, microvesicles, retrovirus-like vesicles, and apoptotic bodies. *J Neurooncol.* (1), 1-11.

Ali SY, G. S. (1983). Formation of calcium phosphate crystals in normal and osteoarthritic cartilage. *Ann Rheum Dis.* (Suppl 1), 45-8.

Al-Nedawi K, M. B. (2009). Endothelial expression of autocrine VEGF upon the uptake of tumor-derived microvesicles containing oncogenic EGFR. *Proc Natl Acad Sci U S A.* (10), 3794-9.

Al-Nedawi K, M. B. (2008). Intercellular transfer of the oncogenic receptor EGFRvIII by microvesicles derived from tumour cells. *Nat Cell Biol.* (5), 619-24.

Anaya-Ruiz M, C. J.-L.-V.-S. (2013). miR-153 silencing induces apoptosis in the MDA-MB-231 breast cancer cell line. *Asian Pac J Cancer Prev.* (5), 2983-6.

Anderson HC, M. D. (2010). Role of extracellular membrane vesicles in the pathogenesis of various diseases, including cancer, renal diseases, atherosclerosis, and arthritis. *Lab Invest.* (11), 1549-57.

Anderson HC. (1969). Vesicles associated with calcification in the matrix of epiphyseal cartilage. *J Cell Biol.* (1), 59-72.

Andre C, H. A. (1997). Sequence analysis of two genomic regions containing the KIT and the FMS receptor tyrosine kinase genes. *Genomics.* (2), 216-26.

Antonyak MA, L. B. (2011). Cancer cell-derived microvesicles induce transformation by transferring tissue transglutaminase and fibronectin to recipient cells. *Proc Natl Acad Sci U S A.* (12), 4852-7.

Ardoin SP, S. J. (2007). The role of microparticles in inflammation and thrombosis. *Scand J Immunol.* (2-3), 159-65.

Ball S. (2011). Diamond Blackfan anemia. *Hematology Am Soc Hematol Educ Program.* 487-91.

Baroni M, P. C. (2007). Stimulation of P2 (P2X7) receptors in human dendritic cells induces the release of tissue factor-bearing microparticles. *FASEB J.* (8), 1926-33.

Bellingham SA, C. B. (2012). Small RNA deep sequencing reveals a distinct miRNA signature released in exosomes from prion-infected neuronal cells. *Nucleic Acids Res.* (21), 10937-49.

Bellone M, I. G. (1997). Processing of engulfed apoptotic bodies yields T cell epitopes. *J Immunol.* (11), 5391-9.

Bergsmedh A, S. A. (2001). Horizontal transfer of oncogenes by uptake of apoptotic bodies. *Proc Natl Acad Sci U S A.* (11), 6407-11.

Beyer C, P. D. (2010). The role of microparticles in the pathogenesis of rheumatic diseases. *Nat Rev Rheumatol.* (1), 21-9.

Bhat KP, I. K. (2004). Essential role of ribosomal protein L11 in mediating growth inhibition-induced p53 activation. *EMBO J.* (12), 2402-12.

Bhatnagar S, S. K. (2007). Exosomes released from macrophages infected with intracellular pathogens stimulate a proinflammatory response in vitro and in vivo. *Blood.* (9), 3234-44.

Bilyy RO, S. T. (2012). Macrophages discriminate glycosylation patterns of apoptotic cell-derived microparticles. *J Biol Chem.* (1), 496-503.

Blanc L, D. G.-B. (2005). Exosome release by reticulocytes--an integral part of the red blood cell differentiation system. *Blood Cells Mol Dis.* (1), 21-6.

Blanc L, V. M. (2010). Reticulocyte membrane remodeling: contribution of the exosome pathway. *Curr Opin Hematol.* (3), 177-83.

Bobrie A, C. M. (2012). Diverse subpopulations of vesicles secreted by different intracellular mechanisms are present in exosome preparations obtained by differential ultracentrifugation. *J Extracell Vesicles.* 1.

Bobrie A, C. M. (2011). Exosome secretion: molecular mechanisms and roles in immune responses. *Traffic.* (12), 1659-68.

Bode AP, O. S. (1991). Vesiculation of platelets during in vitro aging. *Blood.* (4), 887-95.

Boilard E, N. P.-O. (2010). Platelets amplify inflammation in arthritis via collagen-dependent microparticle production. *Science.* (5965), 580-3.

Borges FT, R. L. (2013). Extracellular vesicles: structure, function, and potential clinical uses in renal diseases. *Braz J Med Biol Res.* (10), 824-30.

Brown VK, O. E. (1994). Multiple components of the B cell antigen receptor complex associate with the protein tyrosine phosphatase, CD45. *J Biol Chem.* (24), 17238-44.

Caby MP, L. D.-S. (2005). Exosomal-like vesicles are present in human blood plasma. *Int Immunol.* (7), 879-87.

Campagnoli MF, G. E. (2004). Molecular basis of Diamond-Blackfan anemia: new findings from the Italian registry and a review of the literature. *Haematologica.* (4), 480-9.

Campagnoli MF, R. U. (2008). RPS19 mutations in patients with Diamond-Blackfan anemia. *Hum Mutat.* (7), 911-20.

Chaput N, T. C. (2011). Exosomes: immune properties and potential clinical implementations. *Semin Immunopathol.* (5), 419-40.

Chargaff E, W. R. (1946). The biological significance of the thromboplastic protein of blood. *J Biol Chem.* (1), 189-97.

Chen D, Z. Z. (2007). Ribosomal protein S7 as a novel modulator of p53-MDM2 interaction: binding to MDM2, stabilization of p53 protein, and activation of p53 function. *Oncogene.* (35), 5029-37.

Chen T, G. J. (2011). Chemokine-containing exosomes are released from heat-stressed tumor cells via lipid raft-dependent pathway and act as efficient tumor vaccine. *J Immunol.* (4), 2219-28.

Cheruvanky A, Z. H. (2007). Rapid isolation of urinary exosomal biomarkers using a nanomembrane ultrafiltration concentrator. *Am J Physiol Renal Physiol.* (5), F1657-61.

Chironi GN, B. C.-G. (2009). Endothelial microparticles in diseases. *Cell Tissue Res.* (1), 143-51.

Chiu LY, K. P. (2013). Identification of differentially expressed microRNAs in human hepatocellular adenoma associated with type I glycogen storage disease: a potential utility as biomarkers. *J Gastroenterol.* [Epub ahead of print].

Choi DS, C. D. (2012). Quantitative proteomics of extracellular vesicles derived from human primary and metastatic colorectal cancer cells. *J Extracell Vesicles.* (eCollection 2012), 1.

Choong ML, Y. H. (2007). MicroRNA expression profiling during human cord blood-derived CD34 cell erythropoiesis. *Exp Hematol.* (4), 551-64.

Ciravolo V, H. V. (2012). Potential role of HER2-overexpressing exosomes in countering trastuzumab-based therapy. *J Cell Physiol.* (2), 658-67.

Clayton A, C. J. (2001). Analysis of antigen presenting cell derived exosomes, based on immuno-magnetic isolation and flow cytometry. *J Immunol Methods.* (1-2), 163-74.

Clayton A, T. A. (2005). Induction of heat shock proteins in B-cell exosomes. *J Cell Sci.* (Pt 16), 3631-8.

Cmejla R, C. J. (2007). Ribosomal protein S17 gene (RPS17) is mutated in Diamond-Blackfan anemia. *Hum Mutat.* (12), 1178-82.

Cocucci E, R. G. (2009). Shedding microvesicles: artefacts no more. *Trends Cell Biol.* (2), 43-51.

Conde-Vancells J, R.-S. E.-P. (2008). Characterization and comprehensive proteome profiling of exosomes secreted by hepatocytes. *J Proteome Res.* (12), 5157-66.

Connor DE, E. T. (2010). The majority of circulating platelet-derived microparticles fail to bind annexin V, lack phospholipid-dependent procoagulant activity and demonstrate greater expression of glycoprotein Ib. *Thromb Haemost.* (5), 1044-52.

Corrado C, R. S. (2013). Exosomes as intercellular signaling organelles involved in health and disease: basic science and clinical applications. *Int J Mol Sci.* (3), 5338-66.

Crescitelli R, L. C. (2013). Distinct RNA profiles in subpopulations of extracellular vesicles: apoptotic bodies, microvesicles and exosomes. *J Extracell Vesicles.* (eCollection 2013), 2.

Dai MS, L. H. (2004). Inhibition of MDM2-mediated p53 ubiquitination and degradation by ribosomal protein L5. *J Biol Chem.* (43), 44475-82.

Dai MS, Z. S. (2004). Ribosomal protein L23 activates p53 by inhibiting MDM2 function in response to ribosomal perturbation but not to translation inhibition. *Mol Cell Biol.* (17), 7654-68.

Dalton AJ. (1975). Microvesicles and vesicles of multivesicular bodies versus "virus-like" particles. *J Natl Cancer Inst.* (5), 1137-48.

Daniel L, D. L.-H.-G. (2008). Circulating microparticles in renal diseases. *Nephrol Dial Transplant.* (7), 2129-32.

Danilova N, S. K. (2008). Ribosomal protein S19 deficiency in zebrafish leads to developmental abnormalities and defective erythropoiesis through activation of p53 protein family. *Blood.* (13), 5228-37.

de Gassart A, G. C. (2003). Lipid raft-associated protein sorting in exosomes. *Blood.* (13), 4336-44.

Deisenroth C, Z. Y. (2010). Ribosome biogenesis surveillance: probing the ribosomal protein-Mdm2-p53 pathway. *Oncogene.* (30), 4253-60.

Del Conde I, S. C. (2005). Tissue-factor-bearing microvesicles arise from lipid rafts and fuse with activated platelets to initiate coagulation. *Blood.* (5), 604-11.

Dianzani I, G. E. (1997). Diamond-Blackfan anemia: expansion of erythroid progenitors in vitro by IL-9, but exclusion of a significant pathogenetic role for the IL-9 gene and the hematopoietic gene cluster on chromosome 5q. *Exp Hematol.* (12), 1270-7.

Dignat-George F, B. C. (2011). The many faces of endothelial microparticles. *Arterioscler Thromb Vasc Biol.* (1), 27-33.

Distler JH, P. D. (2005). Microparticles as regulators of inflammation: novel players of cellular crosstalk in the rheumatic diseases. *Arthritis Rheum.* (11), 3337-48.

Doherty L, S. M. (2010). Ribosomal protein genes RPS10 and RPS26 are commonly mutated in Diamond-Blackfan anemia. *Am J Hum Genet.* (2), 222-8.

Dolo V, G. A. (1998). Selective localization of matrix metalloproteinase 9, beta1 integrins, and human lymphocyte antigen class I molecules on membrane vesicles shed by 8701-BC breast carcinoma cells. *Cancer Res.* (19), 4468-74.

Donati G, B. E. (2011). Selective inhibition of rRNA transcription downregulates E2F-1: a new p53-independent mechanism linking cell growth to cell proliferation. *J Cell Sci.* (Pt 17), 3017-28.

Donati G, M. L. (2012). Ribosome biogenesis and control of cell proliferation: p53 is not alone. *Cancer Res.* (7), 1602-7.

Draptchinskaia N, G. P. (1999). The gene encoding ribosomal protein S19 is mutated in Diamond-Blackfan anaemia. *Nat Genet.* (2), 169-75.

Dvorak HF, Q. S. (1981). Tumor shedding and coagulation. *Science.* (4497), 923-4.

Eken C, G. O. (2008). Polymorphonuclear neutrophil-derived ectosomes interfere with the maturation of monocyte-derived dendritic cells. *J Immunol.* (2), 817-24.

Eldh M, E. K. (2010). Exosomes communicate protective messages during oxidative stress; possible role of exosomal shuttle RNA. *PLoS One.* (12), e15353.

Escola JM, K. M. (1998). Selective enrichment of tetraspan proteins on the internal vesicles of multivesicular endosomes and on exosomes secreted by human B-lymphocytes. *J Biol Chem.* (32), 20121-7.

Escudier B, D. T. (2005). Vaccination of metastatic melanoma patients with autologous dendritic cell (DC) derived-exosomes: results of thefirst phase I clinical trial. *J Transl Med.* (1), 10.

Fabbri M, P. A.-S. (2012). MicroRNAs bind to Toll-like receptors to induce prometastatic inflammatory response. *Proc Natl Acad Sci U S A* (31), E2110-6.

Fajtova M, K. A. (2011). Immunophenotypic profile of nucleated erythroid progenitors during maturation in regenerating bone marrow. *Leuk Lymphoma.* (11), 2523-30.

Farrar JE, N. M. (2008). Abnormalities of the large ribosomal subunit protein, Rpl35a, in Diamond-Blackfan anemia. *Blood.* (5), 1582-92.

Faure V, D. L.-G. (2006). Elevation of circulating endothelial microparticles in patients with chronic renal failure. *J Thromb Haemost.* (4), 566-73.

Filipe V, H. A. (2010). Critical evaluation of Nanoparticle Tracking Analysis (NTA) by NanoSight for the measurement of nanoparticles and protein aggregates. *Pharm Res.* (5), 796-810.

Fischer von Mollard G, M. G. (1990). rab3 is a small GTP-binding protein exclusively localized to synaptic vesicles. *Proc Natl Acad Sci U S A.* (5), 1988-92.

Fixsen W, S. P. (1985). Genes that affect cell fates during the development of Caenorhabditis elegans. *Cold Spring Harb Symp Quant Biol.* 99-104.

Follenzi A, A. L. (2000). Gene transfer by lentiviral vectors is limited by nuclear translocation and rescued by HIV-1 pol sequences. *Nat Genet.* (2), 217-22.

Freyssinet JM, T. F. (2010). Membrane microparticle determination: at least seeing what's being sized! *J Thromb Haemost.* (2), 311-4.

Freyssinet LM. (2003). Cellular microparticles: what are they bad or good for? *J Thromb Haemost.* (7), 1655-62.

Furness SG, M. K. (2006). Beyond mere markers: functions for CD34 family of sialomucins in hematopoiesis. *Immunol Res.* (1), 13-32.

Galli M, G. A. (1996). Platelet-derived microvesicles in thrombotic thrombocytopenic purpura and hemolytic uremic syndrome. *Thromb Haemost.* (3), 427-31.

Gao W, S. H. (2011). MiR-21 overexpression in human primary squamous cell lung carcinoma is associated with poor patient prognosis. *J Cancer Res Clin Oncol.* (4), 557-6.

Gasser O, H. C. (2003). Characterisation and properties of ectosomes released by human polymorphonuclear neutrophils. *Exp Cell Res.* (2), 243-57.

Gazda HT, G. A.-L. (2006). Gazda HT, Grabowska A, Merida-Long LB, Latawiec E, Schneider HE, Lipton JM, Vlachos A, Atsidaftos E, Ball SE, Orfali KA, Niewiadomska E, Da Costa L, Tchernia G, Niemeyer C, Meerpohl JJ, Stahl J, Schratt G, Glader B, Backer K, Wong C, Nathan DG, Beggs AH, Sieff CA. *Am J Hum Genet.* (6), 1110-8.

Gazda HT, G. A.-L. (2006). Ribosomal protein S24 gene is mutated in Diamond-Blackfan anemia. *Am J Hum Genet.* (6), 1110-8.

Gazda HT, S. M. (2008). Ribosomal protein L5 and L11 mutations are associated with cleft palate and abnormal thumbs in Diamond-Blackfan anemia patients. *Am J Hum Genet.* (6), 769-80.

Geiss GK, B. R. (2008). Direct multiplexed measurement of gene expression with color-coded probe pairs. *Nat Biotechnol.* (3), 317-25.

Gelderman MP, S. J. (2008). Flow cytometric analysis of cell membrane microparticles. *Methods Mol Biol.* 79-93.

Géminard C, D. G. (2004). Degradation of AP2 during reticulocyte maturation enhances binding of hsc70 and Alix to a common site on TFR for sorting into exosomes. *Traffic.* (3), 181-93.

Géminard C, d. G. (2002). Reticulocyte maturation: mitoptosis and exosome release. *Biocell.* (2), 205-15.

Georgantas RW 3rd, H. R. (2007). CD34+ hematopoietic stem-progenitor cell microRNA expression and function: a circuit diagram of differentiation control. *Proc Natl Acad Sci U S A.* (8), 2750-5.

Ghashghaeinia M, C. J. (2012). The impact of erythrocyte age on eryptosis. *Br J Haematol.* (5), 606-14.

Ginestra A, L. P. (1998). The amount and proteolytic content of vesicles shed by human cancer cell lines correlates with their in vitro invasiveness. *Anticancer Res.* (5A), 3433-7.

Giusti I, D. S. (2008). Cathepsin B mediates the pH-dependent proinvasive activity of tumor-shed microvesicles. *Neoplasia* (5), 481-8.

Grange C, T. M. (2011). Microvesicles released from human renal cancer stem cells stimulate angiogenesis and formation of lung premetastatic niche. *Cancer Res.* (15), 5346-56.

Grewal SS, E. J. (2007). Drosophila TIF-IA is required for ribosome synthesis and cell growth and is regulated by the TOR pathway. *J Cell Biol.* (6), 1105-13.

Griffiths RE, K. S. (2012). Maturing reticulocytes internalize plasma membrane in glycophorin A-containing vesicles that fuse with autophagosomes before exocytosis. *Blood.* (26), 6296-306.

Gutwein P, M. S. (2003). ADAM10-mediated cleavage of L1 adhesion molecule at the cell surface and in released membrane vesicles. *FASEB J.* (12), 292-4.

György B, M. K. (2011). Detection and isolation of cell-derived microparticles are compromised by protein complexes resulting from shared biophysical parameters. *Blood* (4), e39-48.

György B, S. T. (2011). Membrane vesicles, current state-of-the-art: emerging role of extracellular vesicles. *Cell Mol Life Sci.* (16), 2667-88.

Hölzel M, B. K. (2010). The tumor suppressor p53 connects ribosome biogenesis to cell cycle control: a double-edged sword. *Oncotarget.* (1), 43-7.

Hamilton KK, H. R. (1990). Complement proteins C5b-9 induce vesiculation of the endothelial plasma membrane and expose catalytic surface for assembly of the prothrombinase enzyme complex. *J Biol Chem.* (7), 3809-14.

Harding C, H. J. (1983). Receptor-mediated endocytosis of transferrin and recycling of the transferrin receptor in rat reticulocytes. *J Cell Biol.* (2), 329-39.

Hargett LA, B. N. (2013). On the origin of microparticles: From "platelet dust" to mediators of intercellular communication. *Pulm Circ.* (2), 329-340.

Hedlund M, N. O.-N. (2011). Thermal- and oxidative stress causes enhanced release of NKG2D ligand-bearing immunosuppressive exosomes in leukemia/lymphoma T and B cells. *PLoS One.* (2), e16899.

Holmgren L, S. A. (1999). Horizontal transfer of DNA by the uptake of apoptotic bodies. *Blood.* (1), 3956-63.

Hood JL, P. H., & (C-TRAIN)., C. f. (2009). Paracrine induction of endothelium by tumor exosomes. *Lab Invest.* (11), 1317-28.

Horn HF, V. K. (2007). Coping with stress: multiple ways to activate p53. *Oncogene.* (9), 1306-16.

Hristov M, E. W. (2004). Apoptotic bodies from endothelial cells enhance the number and initiate the differentiation of human endothelial progenitor cells in vitro. *Blood.* (9), 2761-6.

Hsu HH, C. N. (1999). Isolation of calcifiable vesicles from human atherosclerotic aortas. *Atherosclerosis.* (2), 353-62.

Huebers HA, B. Y. (1990). Intact transferrin receptors in human plasma and their relation to erythropoiesis. *Blood.* (1), 102-7.

Hunter MP, I. N.-S. (2008). Detection of microRNA expression in human peripheral blood microvesicles. *PLoS One.* (11), e3694.

Huotari J, H. A. (2011). Endosome maturation. *EMBO J.* (17), 3481-500.
Iadevaia V, C. S. (2010). PIM1 kinase is destabilized by ribosomal stress causing inhibition of cell cycle progression. *Oncogene.* (40), 5490-9.

Ismail S, H. M. (2003). Helicobacter pylori outer membrane vesicles modulate proliferation and interleukin-8 production by gastric epithelial cells. *Infect Immun.* (10), 5670-5.

Izquierdo-Useros N, N.-G. M.-F.-P. (2009). Capture and transfer of HIV-1 particles by mature dendritic cells converges with the exosome-dissemination pathway. *Blood* (12), 2732-41.

JA., S. (1988). Measuring the accuracy of diagnostic systems. *Science.* (4857), 1285-93.

Jackson DG, B. J. (1990). Isolation of a cDNA encoding the human CD38 (T10) molecule, a cell surface glycoprotein with an unusual discontinuous pattern of expression during lymphocyte differentiation. *J Immunol.* (7), 2811-5.

Jayachandran M, L. R. (2009). Circulating microparticles and endogenous estrogen in newly menopausal women. *Climacteric.* (2), 177-84.

Jenjaroenpun P, K. Y. (2013). Characterization of RNA in exosomes secreted by human breast cancer cell lines using next-generation sequencing. *PeerJ.* (eCollection 2013), 201.

Jin A, I. K. (2004). Inhibition of HDM2 and activation of p53 by ribosomal protein L23. *Mol Cell Biol.* (17), 7669-80.

Johnstone RM. (2006). Exosomes biological significance: A concise review. *Blood Cells Mol Dis.* (2), 315-21.

Johnstone RM, A. M. (1987). Vesicle formation during reticulocyte maturation. Association of plasma membrane activities with released vesicles (exosomes). *J Biol Chem.* (19), 9412-20.

Johnstone RM, M. A. (1991). Exosome formation during maturation of mammalian and avian reticulocytes: evidence that exosome release is a major route for externalization of obsolete membrane proteins. *J Cell Physiol.* (1), 27-36.

Kahner BN, D. R. (2008). Role of P2Y receptor subtypes in platelet-derived microparticle generation. *Front Biosci.* (1), 433-9.

Kalra H, S. R.-P.-A.-N.-'.-M.-M. (2012). Vesiclepedia: a compendium for extracellular vesicles with continuous community annotation. *PLoS Biol.* (12), e1001450.

Keller S, S. M. (2006). Exosomes: from biogenesis and secretion to biological function. *Immunol Lett.* (2), 102-8.

Kerr JF, W. A. (1972). Apoptosis: a basic biological phenomenon with wide-ranging implications in tissue kinetics. *Br J Cancer.* (4), 239-57.

King HW, M. M. (2012). Hypoxic enhancement of exosome release by breast cancer cells. *BMC Cancer.* 421.

Kongsuwan K, Y. Q. (1985). A Drosophila Minute gene encodes a ribosomal protein. *Nature.* (6037), 555-8.

Kotlabova K, D. J. (2011). Placental-specific microRNA in maternal circulation--identification of appropriate pregnancy-associated microRNAs with diagnostic potential. *J Reprod Immunol.* (2), 185-91.

Kucharzewska P, B. M. (2013). Emerging roles of extracellular vesicles in the adaptive response of tumour cells to microenvironmental stress. *J Extracell Vesicles.* (eCollection 2013), 2.

Kuehn MJ, K. N. (2005). Bacterial outer membrane vesicles and the host-pathogen interaction. *Genes Dev.* (22), 2645-55.

Lässer C. (2013). Identification and analysis of circulating exosomal microRNA in human body fluids. *Methods Mol Biol.* 109-28.

Lässer C, A. V. (2011). Human saliva, plasma and breast milk exosomes contain RNA: uptake by macrophages. *J Transl Med.* (9), 9.

Lässer C, E. M. (2012). Isolation and characterization of RNA-containing exosomes. *J Vis Exp.* (59), e3037.

Lacroix R, R. S.-G., & Workshop., I. S. (2010). Standardization of platelet-derived microparticle enumeration by flow cytometry with calibrated beads: results of the International Society on Thrombosis and Haemostasis SSC Collaborative workshop. *J Thromb Haemost.* (11), 2571-4.

Lai RC, Y. R. (2013). Exosomes for drug delivery - a novel application for the mesenchymal stem cell. *Biotechnol Adv.* (5), 543-51.

Lang E, Q. S. (2012). Killing me softly - suicidal erythrocyte death. *Int J Biochem Cell Biol.* (8), 1236-43.

Le Pecq JB. (2005). Dexosomes as a therapeutic cancer vaccine: from bench to bedside. . *Blood Cells Mol Dis.* (2), 129-35.

Le Roy C, W. J. (2005). Clathrin- and non-clathrin-mediated endocytic regulation of cell signalling. *Nat Rev Mol Cell Biol.* (2), 112-26.

Lempiäinen H, S. D. (2009). Growth control and ribosome biogenesis. *Curr Opin Cell Biol.* (6), 855-63.

Lentz BR. (2003). Exposure of platelet membrane phosphatidylserine regulates blood coagulation. *Prog Lipid Res.* (5), 423-38.

Leroyer AS, T. A. (2008). Role of microparticles in atherothrombosis. *J Intern Med.* (5), 528-37.

Lespagnol A, D. D. (2008). Exosome secretion, including the DNA damage-induced p53-dependent secretory pathway, is severely compromised in TSAP6/Steap3-null mice. *Cell Death Differ.* (11), 723-33.

Levine AJ. (1997). p53, the cellular gatekeeper for growth and division. *Cell.* (3), 323-31.

Li J, S.-B. C.-T. (2009). Claudin-containing exosomes in the peripheral circulation of women with ovarian cancer. *BMC Cancer.* (9), 244.

Li J, Y. L. (2009). Down-regulation of pescadillo inhibits proliferation and tumorigenicity of breast cancer cells. *Cancer Sci.* (12), 2255-60.

Liao JM, Z. X. (2013). Ribosomal proteins L5 and L11 co-operatively inactivate c-Myc via RNA-induced silencing complex. *Oncogene.* [Epub ahead of print].

Lipton JM, E. S. (2009). Diamond-Blackfan anemia: diagnosis, treatment, and molecular pathogenesis. *Hematol Oncol Clin North Am.* (2), 261-82.

Lohrum MA, L. R. (2003). Regulation of HDM2 activity by the ribosomal protein L11. *Cancer Cell.* (6), 577-87.

Lv LH, W. Y. (2012). Anticancer drugs cause release of exosomes with heat shock proteins from human hepatocellular carcinoma cells that elicit effective natural killer cell antitumor responses in vitro. *J Biol Chem.* (19), 15874-85.

Mahaweni NM, K.-L. M. (2013). Tumour-derived exosomes as antigen delivery carriers in dendritic cell-based immunotherapy for malignant mesothelioma. *J Extracell Vesicles.* (2), eCollection 2013.

Martínez-Lorenzo MJ, A. A. (2004). The human melanoma cell line MelJuSo secretes bioactive FasL and APO2L/TRAIL on the surface of microvesicles. Possible contribution to tumor counterattack. *Exp Cell Res.* (2), 315-29.

Martin-Jaular L, N. E. (2011). Exosomes from Plasmodium yoelii-infected reticulocytes protect mice from lethal infections. *PLoS One.* (10), e26588.

Mathivanan S, J. H. (2010). Exosomes: extracellular organelles important in intercellular communication. *J Proteomics.* (10), 1907-20.

Mathivanan S, L. J. (2010). Proteomics analysis of A33 immunoaffinity-purified exosomes released from the human colon tumor cell line LIM1215 reveals a tissue-specific protein signature. *Mol Cell Proteomics.* (9), 197-208.

Mathivanan S, S. R. (2009). ExoCarta: A compendium of exosomal proteins and RNA. *Proteomics.* (21).

McGowan KA, L. J. (2008). Ribosomal mutations cause p53-mediated dark skin and pleiotropic effects. *Nat Genet.* (8), 963-70.

Melamed Z, L. A.-F.-M. (2013). Alternative splicing regulates biogenesis of miRNAs located across exon-intron junctions. *Mol Cell.* (6), 869-81.

Merkerova M, V. A. (2010). MicroRNA expression profiles in umbilical cord blood cell lineages. *Stem Cells Dev.* (1), 17-26.

Miller L, G. J. (1970). Mutations affecting the size of the nucleolus in Xenopus laevis. *Nature.* (5263), 1108-10.

Miranda KC, B. D. (2010). Nucleic acids within urinary exosomes/microvesicles are potential biomarkers for renal disease. *Kidney Int.* (2), 191-9.

Miyake K, F. J. (2005). Development of cellular models for ribosomal protein S19 (RPS19)-deficient diamond-blackfan anemia using inducible expression of siRNA against RPS19. *Mol Ther.* (4), 627-37.

Miyake K1, F. J. (2005). Development of cellular models for ribosomal protein S19 (RPS19)-deficient diamond-blackfan anemia using inducible expression of siRNA against RPS19. *Mol Ther.* (4), 627-37.

Miyazaki Y, N. S. (1996). High shear stress can initiate both platelet aggregation and shedding of procoagulant containing microparticles. *Blood.* (9), 3456-64.

Mladenovic J, A. J. (1982). Characteristics of circulating erythroid colony-forming cells in normal and polycythaemic man. *Br J Haematol.* (3), 377-84.

Morse MA, G. J. (2005). A phase I study of dexosome immunotherapy in patients with advanced non-small cell lung cancer. *J Transl Med.* (1), 9.

Myatt SS, W. J.-M. (2010). Definition of microRNAs that repress expression of the tumor suppressor gene FOXO1 in endometrial cancer. *Cancer Res.* (1), 367-77.

Namløs HM, M.-Z. L.-J. (2012). Modulation of the osteosarcoma expression phenotype by microRNAs. *PLoS One.* (10), e48086.

Nanjundappa RH, W. R. (2011). GP120-specific exosome-targeted T cell-based vaccine capable of stimulating DC- and CD4(+) T-independent CTL responses. *Vaccine.* (19), 3538-47.

Nantakomol D, C. P. (2008). Quantitation of cell-derived microparticles in plasma using flow rate based calibration. *Southeast Asian J Trop Med Public Health.* (1), 146-53.

Nielsen MH, B.-N. H. (2014). A flow cytometric method for characterization of circulating cell-derived microparticles in plasma. *J Extracell Vesicles.* (3), eCollection 2014.

Nikolova-Karakashian MN, R. K. (2010). Ceramide in stress response. *Adv Exp Med Biol.* , 86-108.

Noerholm M, B. L. (2012). RNA expression patterns in serum microvesicles from patients with glioblastoma multiforme and controls. *BMC Cancer.* (12), 22.

Nolte-'t Hoen EN, B. H. (2012). Deep sequencing of RNA from immune cell-derived vesicles uncovers the selective incorporation of small non-coding RNA biotypes with potential regulatory functions. *Nucleic Acids Res.* (18), 9272-85.

Nowotny A, B. U. (1982). Release of toxic microvesicles by Actinobacillus actinomycetemcomitans. *Infect Immun.* (1), 151-4.

Ohno S, T. M. (2013). Systemically injected exosomes targeted to EGFR deliver antitumor microRNA to breast cancer cells. *Mol Ther.* (1), 185-91.

Olausson KH, N. L. (2012). p53 -Dependent and -Independent Nucleolar Stress Responses. *Cell* (14), 774-798.

Onodera T, S. T. (2010). Btbd7 regulates epithelial cell dynamics and branching morphogenesis. *Science.* (5991), 562-5.

Orfali KA, O.-A. Y. (2004). Diamond Blackfan anaemia in the UK: clinical and genetic heterogeneity. *Br J Haematol.* (2), 243-52.

Orozco AF, L. E. (2010). Flow cytometric analysis of circulating micro-particles in plasma. *Cytometry A.* (6), 502-514.

Osterud B. (2003). The role of platelets in decrypting monocyte tissue factor. *Dis Mon.* (1), 7-13.

Pásztói M, N. G. (2009). Gene expression and activity of cartilage degrading glycosidases in human rheumatoid arthritis and osteoarthritis synovial fibroblasts. *Arthritis Res Ther.* (3), R68.

Pan BT, J. R. (1983). Fate of the transferrin receptor during maturation of sheep reticulocytes in vitro: selective externalization of the receptor. *Cell.* (3), 967-78.

Pan BT, T. K. (1985). Electron microscopic evidence for externalization of the transferrin receptor in vesicular form in sheep reticulocytes. *J Cell Biol.* (3), 942-8.

Panganiban RP, P. M. (2012). Differential microRNA epression in asthma and the role of miR-1248 in regulation of IL-5. *Am J Clin Exp Immunol.* (2), 154-65.

Pap E, P. E. (2008). T lymphocytes are targets for platelet- and trophoblast-derived microvesicles during pregnancy. *Placenta.* (9), 826-32.

Park JE, T. H. (2010). Hypoxic tumor cell modulates its microenvironment to enhance angiogenic and metastatic potential by secretion of proteins and exosomes. *Mol Cell Proteomics.* (6), 1085-99.

Parolini I, F. C. (2009). Microenvironmental pH is a key factor for exosome traffic in tumor cells. *J Biol Chem.* (49), 34211-22.

Parrella S, A. A. (2014). Loss of GATA-1 full length as a cause of Diamond-Blackfan anemia phenotype. *Pediatr Blood Cancer.* [Epub ahead of print].

Peinado H, A. M.-S.-B.-R.-S.-H. (2012). Melanoma exosomes educate bone marrow progenitor cells toward a pro-metastatic phenotype through MET. *Nat Med.* (6), 883-91.

Pestov DG, S. Z. (2001). Evidence of p53-dependent cross-talk between ribosome biogenesis and the cell cycle: effects of nucleolar protein Bop1 on G(1)/S transition. *Mol Cell Biol.* (13), 4246-55.

Pignot G, C.-C. G.-O. (2013). microRNA expression profile in a large series of bladder tumors: identification of a 3-miRNA signature associated with aggressiveness of muscle-invasive bladder cancer. *Int J Cancer.* (11), 2479-91.

Pisitkun T, S. R. (2004). Identification and proteomic profiling of exosomes in human urine. *Proc Natl Acad Sci U S A.* (36), 3368-73.

Pluskota E, W. N. (2008). Expression, activation, and function of integrin alphaMbeta2 (Mac-1) on neutrophil-derived microparticles. *Blood.* (6), 2327-35.

Polgar J, M. J. (2005). The P-selectin, tissue factor, coagulation triad. *J Thromb Haemost.* (8), 1590-6.

Ponka P, L. C. (1999). The transferrin receptor: role in health and disease. *Int J Biochem Cell Biol.* (10), 1111-37.

Quarello P, G. E. (2010). Diamond-Blackfan anemia: genotype-phenotype correlations in Italian patients with RPL5 and RPL11 mutations. *Haematologica.* (2), 206-13.

Ragusa M, C. R. (2013). MicroRNAs in vitreus humor from patients with ocular diseases. *Mol Vis.* 430-40.

Raiser DM, N. A. (2013). The emerging importance of ribosomal dysfunction in the pathogenesis of hematologic disorders. *Leuk Lymphoma.* [Epub ahead of print].

Raposo G, N. H. (1996). B lymphocytes secrete antigen-presenting vesicles. *J Exp Med.* (3), 1161-72.

Raposo G, S. W. (2013). Extracellular vesicles: exosomes, microvesicles, and friends. . *J Cell Biol.* (4), 373-83.

Ratajczak J., W. M.-W. (2006). Membrane-derived microvesicles: important and underappreciated mediators of cell-to-cell communication. *Leukemia.* (9), 1487-95.

Rautou PE, L. A. (2011). Microparticles from human atherosclerotic plaques promote endothelial ICAM-1-dependent monocyte adhesion and transendothelial migration. *Circ Res* (3), 335-43.

Record M, S. C.-P. (2011). Exosomes as intercellular signalosomes and pharmacological effectors. *Biochem Pharmacol.* (10), 1171-82.

Robert S, P. P.-G. (2009). Standardization of platelet-derived microparticle counting using calibrated beads and a Cytomics FC500 routine flow cytometer: a first step towards multicenter studies? *J Thromb Haemost.* (1), 190-7.

Roizin L, N. K. (1967). The fine structure of the multivesicular body and their relationship to the ultracellular constituents of the central nervous system. *J Neuropathol Exp Neurol.* (2), 223-49.

Roperch JP, A. V. (1998). Inhibition of presenilin 1 expression is promoted by p53 and p21WAF-1 and results in apoptosis and tumor suppression. *Nat Med.* (7), 835-8.

Rubbi CP, M. J. (2003). Disruption of the nucleolus mediates stabilization of p53 in response to DNA damage and other stresses. *EMBO J.* (22), 6068-77.

Rubin O, C. D. (2010). Pre-analytical and methodological challenges in red blood cell microparticle proteomics. *Talanta* (1), 1-8.

Sankaran VG, G. R. (2012). Exome sequencing identifies GATA1 mutations resulting in Diamond-Blackfan anemia. *J Clin Invest.* (7), 2439-43.

Santos PM, B. L. (2011). Molecular resolution of the B cell landscape. *Curr Opin Immunol.* (2), 163-70.

Sanz-Rodriguez F, G.-E. M. (2004). Endoglin regulates cytoskeletal organization through binding to ZRP-1, a member of the Lim family of proteins. *J Biol Chem.* (31), 32858-68.

Sayed AS, X. K. (2013). Circulating microRNAs: a potential role in diagnosis and prognosis of acute myocardial infarction. *Dis Markers.* (5), 561-6.

Seelig LL. (1972). Surface multivesicular structures associated with maturing erythrocytes in rats. *Z Zellforsch Mikrosk Anat.* (2), 81-6.

Sellam J, P. V. (2009). Increased levels of circulating microparticles in primary Sjögren's syndrome, systemic lupus erythematosus and rheumatoid arthritis and relation with disease activity. *Arthritis Res Ther.* (5), R156.

Shah MD, B. A. (2008). Flow cytometric measurement of microparticles: pitfalls and protocol modifications. *Platelets.* (5), 365-72.

Shet AS, A. O. (2003). Sickle blood contains tissue factor-positive microparticles derived from endothelial cells and monocytes. *Blood.* (7), 2678-83.

Simak J, G. M. (2006). Cell membrane microparticles in blood and blood products: potentially pathogenic agents and diagnostic markers. *Transfus Med Rev.* (1), 1-26.

Simons M, R. G. (2009). Exosomes--vesicular carriers for intercellular communication. *Curr Opin Cell Biol.* (4), 575-81.

Simpson CF, K. J. (1968). The mechanism of mitochondrial extrusion from phenylhydrazine-induced reticulocytes in the circulating blood. *J Cell Biol.* (1), 103-9.

Simpson RJ, L. J. (2009). Exosomes: proteomic insights and diagnostic potential. *Expert Rev Proteomics.* (3), 267-83.

Simpson RJ., M. S. (2012). Extracellular microvesicles: the need for internationally recognised nomenclature and stringent purification criteria. *J Proteomics Bioinform* (5), ii-ii.

Skog J, W. T.-E. (2008). Glioblastoma microvesicles transport RNA and proteins that promote tumour growth and provide diagnostic biomarkers. *Nat Cell Biol.* (12), 1470-6.

Sokolova V, L. A. (2011). Characterisation of exosomes derived from human cells by nanoparticle tracking analysis and scanning electron microscopy. *Colloids Surf B Biointerfaces.* (1), 146-50.

Song L, D. P. (2012). Downregulation of miR-223 and miR-153 mediates mechanical stretch-stimulated proliferation of venous smooth muscle cells via

activation of the insulin-like growth factor-1 receptor. *Arch Biochem Biophys.* (2), 204-11.

Stegmayr B, R. G. (1982). Promotive effect on human sperm progressive motility by prostasomes. *Urol Res.* (5), 253-7.

Stephen J. Gould, G. R. (2013). As we wait: coping with an imperfect nomenclature for extracellular vesicles. *Journal of extracellular vesicles* (2), 20389.

Sulston JE, H. H. (1977). Post-embryonic cell lineages of the nematode, Caenorhabditis elegans. *Dev Biol.* (1), 110-56.

Sun D, Z. X. (2010). A novel nanoparticle drug delivery system: the anti-inflammatory activity of curcumin is enhanced when encapsulated in exosomes. *Mol Ther.* (9), 1606-14.

Tanimura A, M. D. (1983). Matrix vesicles in atherosclerotic calcification. *Proc Soc Exp Biol Med.* (2), 173-7.

Tao YM, H. J. (2013). BTB/POZ domain-containing protein 7: epithelial-mesenchymal transition promoter and prognostic biomarker of hepatocellular carcinoma. *Hepatology.* (6), 2326-37.

Taraboletti G, D. S. (2006). Bioavailability of VEGF in tumor-shed vesicles depends on vesicle burst induced by acidic pH. *Neoplasia.* (2), 96-103.

Tatischeff I, L. E.-P. (2012). Fast characterisation of cell-derived extracellular vesicles by nanoparticles tracking analysis, cryo-electron microscopy, and Raman tweezers microspectroscopy. *J Extracell Vesicles.* (eCollection 2012), 1.

Tauro BJ, G. D. (2012). Comparison of ultracentrifugation, density gradient separation, and immunoaffinity capture methods for isolating human colon cancer cell line LIM1863-derived exosomes. *Methods.* (2), 293-304.

Taverna S, F. A. (2012). Role of exosomes released by chronic myelogenous leukemia cells in angiogenesis. *Int J Cancer.* (9), 2033-43.

Taylor DD, G.-T. C. (2011). Exosomes/microvesicles: mediators of cancer-associated immunosuppressive microenvironments. *Semin Immunopathol.* (5), 441-54.

Taylor DD, Z. W.-T. (2011). Exosome isolation for proteomic analyses and RNA profiling. *Methods Mol Biol.* , 235-46.

Testa U. (2004). Apoptotic mechanisms in the control of erythropoiesis. *Leukemia.* (7), 1176-99.

Théry C, A. S. (2006). Isolation and characterization of exosomes from cell culture supernatants and biological fluids. *Curr Protoc Cell Biol.* (Chapter 3), Unit 3.22.

Théry C, B. M.-C. (2001). Proteomic analysis of dendritic cell-derived exosomes: a secreted subcellular compartment distinct from apoptotic vesicles. *J Immunol.* (12), 7309-18.

Théry C, O. M. (2009). Membrane vesicles as conveyors of immune responses. *Nat Rev Immunol.* (8), 581-93.

Théry C, R. A.-C. (1999). Molecular characterization of dendritic cell-derived exosomes. Selective accumulation of the heat shock protein hsc73. *J Cell Biol.* (3), 599-610.

Théry C, Z. L. (2002). Exosomes: composition, biogenesis and function. *Nat Rev Immunol.* (8), 569-79.

Théry C., O. M. (2009). Membrane vesicles as conveyors of immune responses. *Nat Rev Immunol.* (9), 581-93.

Trajkovic K, H. C. (2008). Ceramide triggers budding of exosome vesicles into multivesicular endosomes. *Science.* (5867), 1244-7.

Trams EG, L. C. (1981). Exfoliation of membrane ecto-enzymes in the form of micro-vesicles. *Biochim Biophys Acta.* (1), 63-70.

Turiák L, M. P. (2011). Proteomic characterization of thymocyte-derived microvesicles and apoptotic bodies in BALB/c mice. *J Proteomics.* (10), 2025-33.

Umezu T, O. K. (2013). Leukemia cell to endothelial cell communication via exosomal miRNAs. *Oncogene.* (22), 2747-55.

Valadi H, E. K. (2007). Exosome-mediated transfer of mRNAs and microRNAs is a novel mechanism of genetic exchange between cells. *Nat Cell Biol.* (6), 654-9.

Valenti R, H. V. (2007). Tumor-released microvesicles as vehicles of immunosuppression. *Cancer Res.* (7), 2912-5.

van den Goor JM, N. R. (2007). Retransfusion of pericardial blood does not trigger systemic coagulation during cardiopulmonary bypass. *Eur J Cardiothorac Surg.* (3), 1029-36.

van der Pol E, B. A. (2012). Classification, functions, and clinical relevance of extracellular vesicles. *Pharmacol Rev.* (3), 676-705.

van der Pol E, H. A. (2010). Optical and non-optical methods for detection and characterization of microparticles and exosomes. *J Thromb Haemost.* (12), 2596-607.

van der Vlist EJ, N.-'. H. (2012). Fluorescent labeling of nano-sized vesicles released by cells and subsequent quantitative and qualitative analysis by high-resolution flow cytometry. *Nat Protoc.* (7), 1311-26.

van Niel G, P.-C. I. (2006). Exosomes: a common pathway for a specialized function. *J Biochem.* (1), 13-21.

van Schooneveld E, W. M. (2012). Expression profiling of cancerous and normal breast tissues identifies microRNAs that are differentially expressed in serum from patients with (metastatic) breast cancer and healthy volunteers. *Breast Cancer Res.* (1), R34.

Vella LJ, G. D. (2008). Enrichment of prion protein in exosomes derived from ovine cerebral spinal fluid. *Vet Immunol Immunopathol.* (3-4), 385-93.

Videl M. (2010). Exosomes in erythropoiesis. *Transfus Clin Biol.* (3), 131-7.

Vlachos A, B. S. (2008). Diagnosing and treating Diamond Blackfan anaemia: results of an international clinical consensus conference. *Br J Haematol.* (6), 859-76.

Vlachos A, M. E. (2010). How I treat Diamond-Blackfan anemia. *Blood.* (19), 3715-23.

von Schwedler UK, S. M. (2003). The protein network of HIV budding. *Cell.* (6), 701-13.

Wang W, C.-C. M. (2012). MicroRNA profiling of follicular lymphoma identifies microRNAs related to cell proliferation and tumor response. *Haematologica.* (4), 586-9.

Ware RE, R. W. (1995). Immunophenotypic analysis of reticulocytes in paroxysmal nocturnal hemoglobinuria. *Blood.* (4), 1586-9.

Wolf P. (1967). The nature and significance of platelet products in human plasma. *Br J Haematol.* (3), 269-88.

Wollert T, H. J. (2010). Molecular mechanism of multivesicular body biogenesis by ESCRT complexes. *Nature.* (7290), 864-9.

Wu Z, H. B. (2013). Upregulation of miR-153 promotes cell proliferation via downregulation of the PTEN tumor suppressor gene in human prostate cancer. *Prostate.* (6), 596-604.

Wubbolts R, L. R. (2003). Proteomic and biochemical analyses of human B cell-derived exosomes. Potential implications for their function and multivesicular body formation. *J Biol Chem.* (13), 10963-72.

Wysoczynski M, R. M. (2009). Lung cancer secreted microvesicles: underappreciated modulators of microenvironment in expanding tumors. *Int J Cancer.* (7), 1595-603.

Xu J, L. X. (2011). Chromatin-modifying drugs induce miRNA-153 expression to suppress Irs-2 in glioblastoma cell lines. *Int J Cancer.* (10), 2527-31.

Yamada T, I. Y. (2012). Comparison of methods for isolating exosomes from bovine milk. *J Vet Med Sci.* (11), 1523-5.

Yu X, H. S. (2006). The regulation of exosome secretion: a novel function of the p53 protein. *Cancer Res.* (9), 4795-801.

Yu X, R. T. (2009). The regulation of the endosomal compartment by p53 the tumor suppressor gene. *FEBS J.* (8), 2201-12.

Yuana Y, B. R. (2011). Pre-analytical and analytical issues in the analysis of blood microparticles. *Thromb Haemost.* (105), 396–408.

Zang W, W. Y. (2013). Differential expression profiling of microRNAs and their potential involvement in esophageal squamous cell carcinoma. *Tumour Biol.* [Epub ahead of print].

Zernecke A, B. K. (2009). Delivery of microRNA-126 by apoptotic bodies induces CXCL12-dependent vascular protection. *Sci Signal.* (100), ra81.

Zhan R, L. X. (2009). Heat shock protein 70 is secreted from endothelial cells by a non-classical pathway involving exosomes. *Biochem Biophys Res Commun.* (2), 229-33.

Zhang C, C. L. (2005). PTEN represses RNA Polymerase I transcription by disrupting the SL1 complex. *Mol Cell Biol.* (16), 6899-911.

Zhang HC, L. X. (2012). Microvesicles derived from human umbilical cord mesenchymal stem cells stimulated by hypoxia promote angiogenesis both in vitro and in vivo. *Stem Cells Dev.* (18), 3289-97.

Zhang Y, L. H. (2009). Signaling to p53: ribosomal proteins find their way. *Cancer Cell.* (5), 369-77.

Zhang Y, W. G. (2003). Ribosomal protein L11 negatively regulates oncoprotein MDM2 and mediates a p53-dependent ribosomal-stress checkpoint pathway. *Mol Cell Biol.* (23), 8902-12.

Zhang Y, X. Y. (2001). Control of p53 ubiquitination and nuclear export by MDM2 and ARF. *Cell Growth Differ.* (4), 175-86.

Zhu W, H. L. (2012). Exosomes derived from human bone marrow mesenchymal stem cells promote tumor growth in vivo. *Cancer Lett.* (1), 28-37.

Zhu W, X. W. (2006). Mesenchymal stem cells derived from bone marrow favor tumor cell growth in vivo. *Exp Mol Pathol.* (3), 267-74.

Acknowledgments

I would like to express my gratitude to all people who, in different ways, helped me to make this thesis possible. I wish to thank:

My supervisor **Prof. Irma Dianziani** to have chosen me among many other students providing me the opportunity to attempt this project. Thanks to have felt me free to explore my ideas giving me the possibility to spend a year and half abroad.

My co-supervisor **Prof. Jan Lötvall** to have made me an *"exosomist, vesicologist, confusologist"* ☺ in few words to have explained to me how much amazing the exosomic field is, for believing in my abilities and to have looked at my results always smiling. Thank you to have encouraged me to present my results at conferences, to have understood when I was sad knowing the exact word that I would like to hear in that moment.

Prof. Steve Ellis to have had the idea to study vesicles in Diamond Blackfan Anemia, to have believed in this project supporting me when I needed.

Dr. Patrizia Notari and **Dr. Claudia Vizziello** for their hard work with flow cytometry; **Dr. Yong Song Gho** and his collaborator **Dr. Dae-Kyum Kim** for array analysis. Thank you so much for your technical support.

All **members of Istituto Piemontese per la ricerca sulla Anemia di Diamond-Blackfan**, my research would not be possible without you, I really hope to have done something for you. Research is slow but something very important has been discovered and much more can be done, all together.

My colleagues in Novara, **Elisa, Marta, Anna, Serena, Sara**, all people in **Santoro's lab, Andrea, Beppe** and **Rossana** to have been there for me to help, encourage and support when I was sad.

A special “thanks” to **Elisa** and **Serena** to have continued the lab work after my leaving, this thesis would not be the same without you.

All people at Krefting Research Centre: **Eva-Marie** to have always been there ready to help me; **Linda, Carina, Serena, Margareta, Madeleine, Malin, Apostolos** and **all nurses** to have been a scientific support and for making the KRC such as friendly work place! A special thanks to the exosome group: **Ganesh, Taral, Maria, Alexander, Lilit, Roxana, Gabriela** for the support and many laughs at work, for nice evenings, to have repeated to me: “Don’t worry, you will come back here”, it has been a pleasure to work with you. A special thanks to **Cecilia** to have been a great tutor at KRC, to have guided me around *exosomal stuff* but, mostly, to have taught me that bad results do not exist, a result is a result and it is always important: this is science! My first first-author paper is now published thanks to you and this thesis, of course, would not be the same without you!

Stefania per avermi fatto ricredere sui siciliani, per avermi fatto capire che non lasciare in mezzo a una strada una persona può tornare davvero utile ☺, perché non credevo, prima di conoscerla, che potesse esistere una persona speciale sia come collega che come amica. Grazie per esserci stata e per continuare a supportarmi nei miei momenti di sconforto. Dai, ritorna su per formare il “dream lab”! ☺

Solo “grazie” è riduttivo, per tutti gli amici conosciuti a Göteborg, per essere stati la mia famiglia all’estero: **Carlo, Gabriel, Stefania, Paolo, Matteo, Giovanna, Sepehr, Lioba, Alessandro, Rocco, Elena, Francesco, Cristina, Fabio, Gerardo, Andrea, Lisa, Pier Paolo, Silvia, Federico.** Un “grazie” particolare va a **Roberto** per aver dato quel pizzico di “anomalia” ai miei giorni a Göteborg, per non essere mai banale ma sicuramente non facile da capire, che pur esprimendo poco, ha sopportato i miei monologhi senza scappare. Io non ti ho ancora ammazzato e tu non sei ancora fuggito, chissà cosa vorrà dire… ☺

Un “grazie” speciale va alla mia amica e “mamma” **Livia**, per avermi adottata dal mio primo giorno a Göteborg, per non avermi mai lasciata un attimo sola, per avermi introdotta, fatto conoscere tutti ed aiutata materialmente e moralmente.

Ai miei amici di sempre che, nonostante la distanza e la mancanza di tempo, sono sempre con me: **Alessandra**, per essere stata più di un’amica, quasi una sorella, durante il periodo universitario e per esserlo ancor di più a distanza di chilometri; **Emanuele,** che con il suo prendermi in giro e dirmene di tutto e di più, trova il modo più efficace e sincero per dimostrarmi il suo affetto.

Agli amici di Avellino, in particolare **Roberta, Adele, Claudio, Julia, Gaetano, Gaeton, Vincenzo, Mario e Carmine** semplicemente per esserci.
Se c’è una cosa che più di tutto ho imparato in questi tre anni è che la distanza serve a far capire quali sono le amicizie vere e se sono tali, la distanza non ha alcuna importanza.

A tutti i **cugini**, agli **zii** e alle **nonne** che, pur non comprendendo a fondo le mie scelte, non hanno smesso un attimo di starmi vicini.

A **mio fratello Marco**, per essere forse più amico che fratello, per avermi difeso, supportato e mai lasciata sola facendomi capire che Avellino è e sarà sempre la mia “casa” con o senza le persone “di un tempo”.

… e infine un enorme “grazie” ai **miei genitori**.
Newton nel dire “sono arrivato più lontano degli altri perché ho camminato sulle spalle dei giganti”, si riferiva ai luminari della scienza e della filosofia.
Io lo dico di due persone senza le quali non avrei mosso un passo fuori di casa; ho “camminato” sui loro insegnamenti e sui loro esempi affrontando a testa alta tutte le esperienze che hanno fatto di me una persona migliore.

Grazie! Thank you! Tack!